

Alma Mater Studiorum – Università di Bologna

DOTTORATO DI RICERCA IN
SCIENZE BIOMEDICHE E NEUROMOTORIE

Ciclo XXX

Settore Concorsuale: 06/B1

Settore Scientifico Disciplinare: MED/09

**EXPLORING THE ROLE OF LDH IN CANCER CELLS
THROUGH THE USE OF SMALL-MOLECULE
INHIBITORS**

Presentata da: Dott.ssa Lorenza Di Ianni

Coordinatore Dottorato:

Prof. Lucio Cocco

Supervisore:

Prof.ssa Giuseppina Di Stefano

Esame finale anno 2018

THESIS ABSTRACT

Metabolic reprogramming represents a potential therapeutic target in cancer. The studies of this thesis work lead to assume the enzyme lactate dehydrogenase (LDH) as key element coordinating neoplastic proliferation and invasive growth, suggesting for LDH inhibitor compounds a wider potential in anticancer treatment.

The increased LDH-A expression has been observed in many tumor forms. In neoplastic cells, LDH commonly reduce pyruvate to lactate even in the presence of adequate oxygen supply (aerobic glycolysis). The rationale for targeting LDH activity in anticancer strategies is because LDH activity is not needed for pyruvate metabolism through the TCA cycle, thus, LDH inhibitors should spare glucose metabolism of normal cells.

The objective of this work, simultaneously with the ongoing search for new LDH inhibitors, is the study of the role of LDH in cancer cells by pharmaceutical approach, through the use of inhibitors in different cell lines and conditions, and by genetic approach consisting in the depletion of LDH genes by the innovative CRISPR/Cas9 technology.

By the use of two LDH inhibitors, oxamate and galloflavin, we demonstrated that LDH inhibition can impact on chemo-sensitivity, inflammation and heat shock response in cancer cell lines.

The genetic knock-out of LDH enzyme evidenced that some cells are able to survive by switching their metabolism from glycolysis to OXPHOS, showing limited ability to grow and proliferate. Importantly, this genetic knock-out, used as control allowed us to confirm the specificity of GNE-140 (LDH inhibitor) for the target, representing an important help in the search of LDH inhibitors suitable for clinical use, proved to be, in our studies, an important goal in the anti-cancer treatments.

INDEX

INTRODUCTION.....	3
1.1 Cancer metabolism.....	3
MOLECULAR PATHWAYS IN AEROBIC GLYCOLYSIS	5
TUMOR ACIDITY AND LACTATE/H ⁺ SYMPORTERS	8
1.2 Lactate Dehydrogenase (LDH)	9
LDH-A REGULATION	12
LDH-A AS THERAPEUTIC TARGET	13
LDH INHIBITORS.....	13
AIM OF THE THESIS	16
MATERIALS AND METHODS	17
Laboratory of cell biology, DIMES Department, Bologna - Italy	17
3.1 Cell cultures.....	17
3.2 Compounds.....	18
3.3 Enzymatic assays on purified human LDH-A.....	18
3.4 Viability assays	19
3.5 Lactate assay	20
3.6 LDH assay.....	20
3.7 Glucose uptake assay	21
3.8 NAD/NADH assay.....	21
3.9 ATP production assay	22
3.10 Immunoblotting.....	22
3.11 Gelatin zymography	23
3.12 Real time PCR.....	24
3.13 Flow cytometry	25
3.14 Colony formation assay.....	25
3.15 ATPase activity	26
3.16 Alkaline phosphatase assay.....	26
3.17 2',7'-Dichloro-dihydro-fluorescein diacetate assay	27
3.18 Assay of thiobarbituric acid reactive substances (TBARS).....	27
3.19 Senescence-associated β -galactosidase staining assay	27
3.20 Statistical analyses.....	27

Laboratory of “Hypoxia signalling and cancer metabolism”, IRCAN Institute, Nice – France.....	28
3.21 Cell culture and hypoxic exposure conditions	28
3.22 CRISPR/Cas9 technology	28
3.23 Immunoblotting.....	30
3.24 Real time PCR.....	30
3.25 LDH-A and LDH-B enzymatic assay	31
3.26 Proliferation and cell viability assay	31
3.27 Metabolic flux analysis	32
3.28 Extracellular lactate measure	32
3.29 Clonogenic assay.....	33
3.30 Statistical analyses.....	33
RESULTS.....	34
4.1 Pharmacological approach to inhibit LDH enzyme activity	34
Part A: Study of the role of LDH in cancer cells through the use of known inhibitors ...	35
EXPERIMENTAL PART 1A: Lactate dehydrogenase inhibitors sensitize lymphoma cells to cisplatin without enhancing the drug effects on immortalized normal lymphocytes	35
EXPERIMENTAL PART 2A: Lactate dehydrogenase inhibitors can reverse inflammation induced changes in colon cancer cells	46
EXPERIMENTAL PART 3A: LDH inhibition impacts on heat shock response and induces senescence of hepatocellular carcinoma cells	57
Part B: The research of new LDH inhibitors.....	68
EXPERIMENTAL PART 1B: Identification of N-acylhydrazone derivatives as novel lactate dehydrogenase A inhibitors	68
EXPERIMENTAL PART 2B: Synthesis of natural urolithin M6, a galloflavin mimetic, as a potential inhibitor of lactate dehydrogenase A	74
4.2 Genetic approach to inhibit LDH enzyme activity	77
Gene Knock-Out by CRISPR/Cas9 technology.....	79
Characterization of single and double LDH-A/LDH-B KO clones of LS174T and B16 cell lines	81
Comparison of the effects of the LDH inhibitor compound with the genetic knockout of LDH	88
FINAL DISCUSSION	91
REFERENCES.....	94

Chapter 1

INTRODUCTION

1.1 Cancer metabolism

One of the hallmark of cancer cells consists in the reprogramming of energy metabolism. The activation of oncogenes and loss of tumor suppressors results in enhanced nutrient uptake to supply energetic and biosynthetic pathways, which provide cancer cells not only with essential energy, but also important precursors to support large-scale biosynthesis, rapid proliferation, continuous growth, tissue invasion, metastasis, survival and resistance to anti-cancer therapies.

Indeed, the chronic and often uncontrolled cell proliferation that represents the essence of neoplastic disease involves not only deregulated control of cell proliferation but also corresponding adjustments of energy metabolism in order to fuel cell growth and division.

In normal cells, under aerobic conditions, pyruvate is generated from glucose via glycolysis in the cytosol and enters the citric acid cycle in the mitochondria where it is oxidatively decarboxylated to form acetyl-CoA, which is used to fuel oxidative phosphorylation, theoretically generating 36 net adenosine triphosphate (ATP) per molecule of glucose; under anaerobic conditions, glycolysis is favoured and relatively little pyruvate is dispatched to the oxygen-consuming mitochondria (Hanahan and Weinberg 2011). NAD^+ is usually regenerated through oxidative phosphorylation by the electron transport chain, so when the oxygen supply is restricted, NAD^+ is regenerated from NADH by Lactate Dehydrogenase A (LDH-A) in order to maintain glycolysis, generating lactate as a by-product. One example can be observed in the overworking skeletal muscle. During intense work, glucose uptake and glycolytic flux show a massive increase, often in conditions of saturated respiratory capacity. In this situation, LDH-A isozyme (the form prevalently found in muscle) proves to be much more efficient in NAD^+ regeneration and can ensure the maintenance of the glycolytic flux and of the resulting ATP production.

In cancer metabolism, one of the most well-known phenomena is the Warburg effect.

In 1924, Otto Warburg observed that cancer cells consume much larger quantities of glucose than their normal counterparts and metabolize it predominantly through glycolysis, thus

producing high levels of lactate even in oxygen-rich conditions, hence the term aerobic glycolysis (WARBURG 1956).

Using the glycolysis, the yield of ATP is 18-fold lower than that of oxidative phosphorylation. However, cancer cells increasing the glycolytic flux can exceed the percentage of cellular ATP produced from oxidative phosphorylation. In addition, switch to an aerobic glycolysis metabolic phenotype benefits cancer cells by avoiding generation of oxidative stress by the electron transport chain (Kroemer and Pouyssegur 2008). Moreover, the aerobic glycolysis provides the intermediates of the citric acid cycle for anabolic reactions to synthesize the lipids, fatty acids and nucleotides required for rapid cell proliferation (DeBerardinis et al. 2008, Vander Heiden, Cantley and Thompson 2009). For example:

- glucose-6-phosphate can be oxidized into PPP in order to produce NADPH and ribose-5-phosphate, which in turn are used to synthesize nucleotides for DNA and RNA;
- dihydroxyacetone phosphate is the precursor to glycerol-3-phosphate, that is crucial for the biosynthesis of the phospholipids and triacylglycerols that serve as major structural lipids in cell membranes;
- 3-phosphoglycerate provides the carbons for cysteine, glycine and serine, whereas pyruvate provides the carbons for alanine.

Besides aerobic glycolysis, cancer cells exhibit substantial alterations in several metabolic pathways including tricarboxylic acid (TCA) cycle, glutaminolysis, mitochondrial respiratory chain and PPP. The metabolic changes can be attributed to the activation and/or malfunction of oncogenes, and/or loss of tumor suppressors (Chen and Russo 2012).

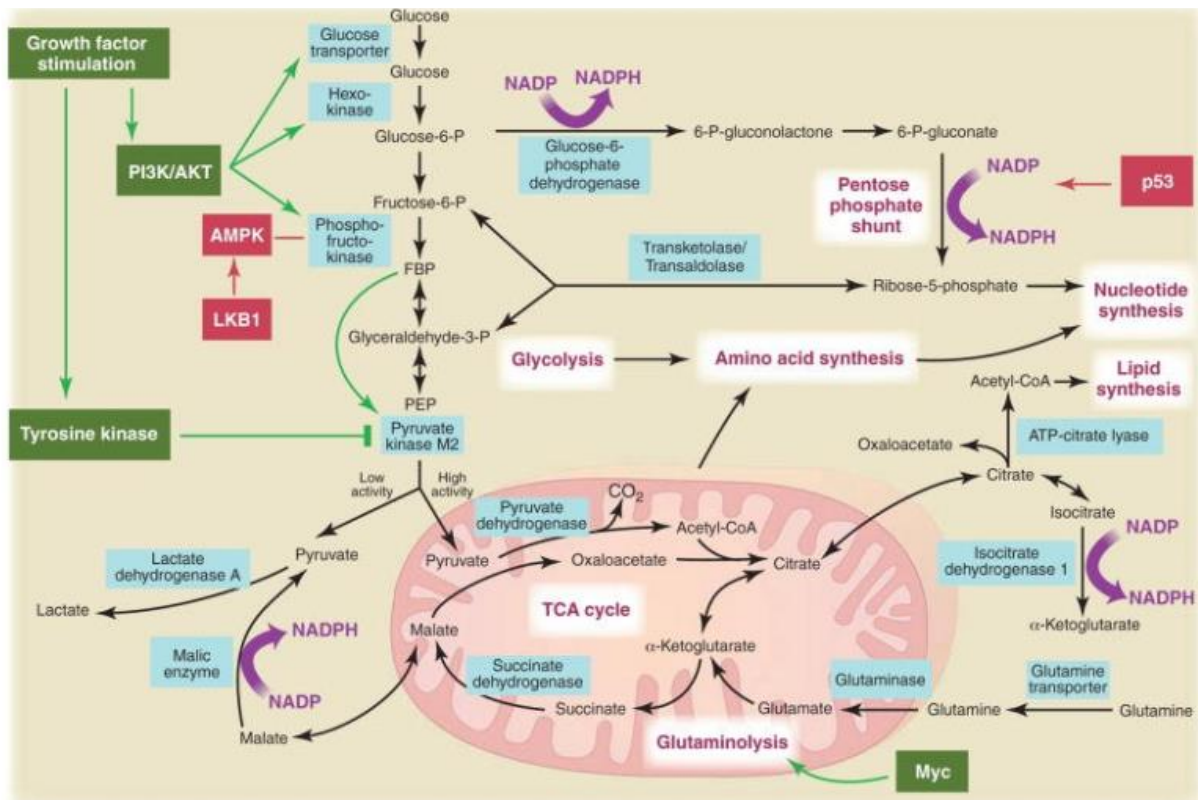


Figure 1.1. Metabolic pathways active in proliferating cells are directly controlled by signalling pathways involving known oncogenes (in green) and tumor suppressor genes (in red). Key metabolic pathways are labeled in purple with white boxes, and the enzymes controlling critical steps in these pathways are shown in blue (Vander Heiden et al. 2009).

MOLECULAR PATHWAYS IN AEROBIC GLYCOLYSIS

The reprogramming of cellular metabolism is driven by growth factor-independent activation of the PI3K/Akt and c-Myc pathways to promote cancer cell growth and proliferation. These pathways facilitate increased rates of glucose uptake and glycolysis. Akt signaling promotes increased surface expression of the glucose transporter Glut1 and enhances the activity of glycolytic enzymes. The TORC1 complex, which contains mTOR and its binding partner Raptor, activated by PI3K/Akt signals, regulates protein translation (Jones and Thompson 2009).

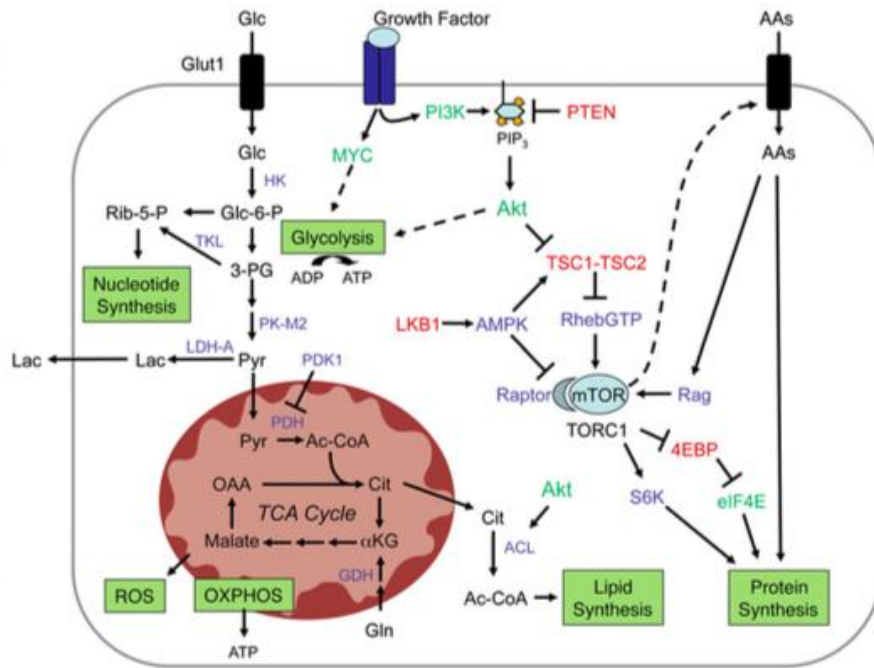


Figure 1.2. Jones, R.G., and Thompson, C.B. (2009). Tumor suppressors and cell metabolism: a recipe for cancer growth. *Genes Dev.* 23, 537–548.

In normal cells, the PI3K pathway is tightly controlled to increase glucose uptake and metabolism in response to growth signals (Cantley 2002). However, in cancer cells, various mutations activate PI3K in the absence of growth signals, which suggests that inappropriate activation of this pathway may be a major driver of aerobic glycolysis in cancer cells (DeBerardinis et al. 2008).

Rapidly proliferating cells require close proximity to blood vessels for access to oxygen and nutrients. As tumors grow, cells may encounter hypoxic conditions that lead to induction of HIF-1 transcription factor. HIF-1 increases the expression of VEGF to facilitate the growth of new blood vessels. HIF-1 also increases the transcription of glucose transporters (GLUT1, GLUT3), many glycolytic enzymes, and LDHA (O'Rourke et al. 1996, Jiang et al. 1997) (Fig. 1.3). During periods of fast growth and rapid biomass synthesis, such as embryogenesis and tumorigenesis, local hypoxic conditions may arise and stimulate HIF-1 to enhance glycolytic gene expression. HIF-1 is required for embryogenesis, as mice homozygous for a loss-of-function mutation in HIF-1 α or HIF-1 β die at mid gestation (Iyer et al. 1998, Maltepe et al. 1997). Loss of HIF-1 α in cancer cells also dramatically slows their growth as xenograft tumors in nude mice (Jiang et al. 1997, Maxwell et al. 1997, Ryan, Lo and Johnson 1998). Even under normoxic conditions, HIF-1 α can be induced by the glycolytic metabolites pyruvate and lactate (McFate et al. 2008), mTOR activation, NAD⁺ levels, reactive oxygen

species, nitric oxide, many TCA cycle metabolites (Semenza 2010b), and oncogene gain of function or tumor suppressor gene loss of function (Semenza 2010a).

Activation of the PI3K pathway appears to be an important way to increase HIF-1 transcription in cancer (DeBerardinis et al. 2008, Majumder and Sellers 2005). Thus, activation of HIF resulting from hypoxia, PI3K activation, or other mechanisms can promote glucose metabolism by aerobic glycolysis.

The transcription factor c-Myc promotes expression of glucose transporters and glycolytic enzymes (Ahuja et al. 2010, Osthus et al. 2000) (Fig. 1.3). c-Myc regulates the expression of LDHA (Shim et al. 1997), and c-Myc-dependent tumors cannot proliferate when LDH-A expression is knocked down (Le et al. 2010). Furthermore, c-Myc regulates enzymes in the nucleotide biosynthesis pathway, including thymidylate synthase, inosine monophosphate dehydrogenase 1 and 2, and phosphoribosyl pyrophosphate synthetase-2 (Tong, Zhao and Thompson 2009). Ras, another oncogene widely implicated in human cancer, also promotes glucose metabolism by enhancing glucose uptake (Yun et al. 2009). Mutation of p53 is another common genetic event in human cancer, and the p53 protein prevents tumor growth by suppressing metabolic pathways conducive to proliferation of stressed or damaged cells. p53 promotes mitochondrial respiration through expression of SCO2 protein (Synthesis of Cytochrome c Oxidase) (Cheung and Vousden 2010, Levine and Puzio-Kuter 2010). Thus, glycolysis can be promoted by loss of p53 function in cancer (Fig. 1.3).

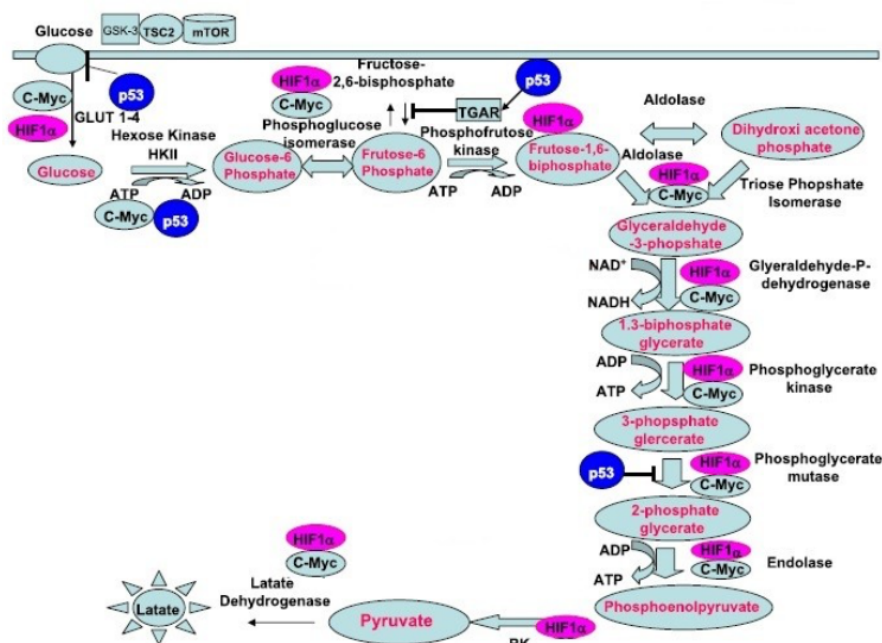


Figure 1.3. (Chen, J. Q. & J. Russo (2012) Dysregulation of glucose transport, glycolysis, TCA cycle and glutaminolysis by oncogenes and tumor suppressors in cancer cells. *Biochim Biophys Acta*, 1826, 370-84).

TUMOR ACIDITY AND LACTATE/H⁺ SYMPORTERS

Acidic extracellular pH (pHe) is a major feature of tumor tissue; it increases not only the activation of some lysosomal enzymes with acidic optimal pH, but also the expression of some genes involved with pro-metastatic factors (Kato et al. 2013). The high conversion rate of pyruvate into lactate, via the enzymatic activity of lactate dehydrogenase A (LDHA), is usually assumed to be the major mechanism responsible for tumour acidity. Indeed, high lactate levels correlate with metastases and tumor recurrence in some cancer patients (Brizel et al. 2001, McFate et al. 2008).

For many years, lactate was thought to be removed from cells merely via transmembrane diffusion of its undissociated form, lactic acid. However, studies from Halestrap's group on human red blood cells established the presence of specific transmembrane lactate transporters, belonging to a family of monocarboxylate transporters (MCTs) (Halestrap 2013, Halestrap and Denton 1974). This transport is mainly controlled by the H⁺ and monocarboxylate concentration gradient across the plasma membrane, which determines the net direction of transport (influx or efflux) (Poole and Halestrap 1993). Four isoforms (MCT1-4) have been functionally validated to transport monocarboxylates, such as L-lactate, pyruvate and ketone bodies (Halestrap 2012, Halestrap 2013).

Up-regulation of MCT1 and MCT4 has been reported in several solid tumours, such as glioblastoma, breast, colon, liver, ovarian and lung cancers (Pinheiro et al. 2012). The distribution pattern of these two MCTs is different, not only between distinct cancer types but also between different intra-tumoral compartments and cell types. MCT4 was reported to be up-regulated in hypoxic tumour cells (Meijer et al. 2012, Rademakers et al. 2011) and tumour associated fibroblasts (Pavlides et al. 2009, Whitaker-Menezes et al. 2011, Witkiewicz et al. 2012) where it supports lactate release; whereas, MCT1 was highly expressed in oxidative tumour cells and angiogenic endothelial cells (Sonveaux et al. 2012, Végran et al. 2011, Bonuccelli et al. 2010) that recapture lactate and convert it into pyruvate to feed the TCA cycle, thereby increasing glucose availability for hypoxic cells (Bonuccelli et al. 2010). Recent work shows that blocking both MCT1 and MCT4 in human colon adenocarcinoma, glioblastomas and non-small cell lung carcinoma cells causes a shift of their metabolism from glycolysis to OXPHOS, which sensitizes them to biguanides, such as metformin and phenformin (Granja et al. 2015, Marchiq et al. 2015).

1.2 Lactate Dehydrogenase (LDH)

The best characterized LDH function is its role in cell metabolism. Lactate Dehydrogenase is an enzyme belonging to the oxydoreductase family. LDH inter-converts pyruvate and lactate using nicotinamide adenine dinucleotide (NAD[H]), an essential cofactor that is required for a wide range of cellular reactions including ATP production.

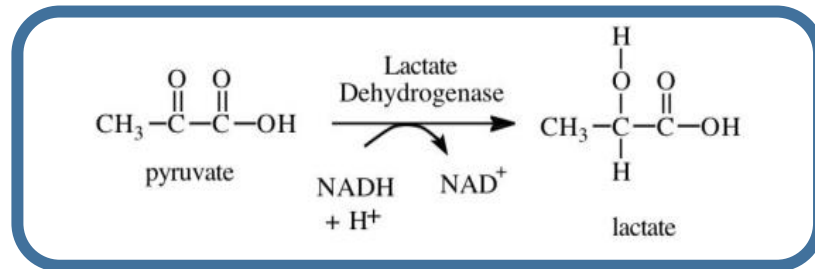


Figure 1.4. Conversion of pyruvate in lactate by Lactate Dehydrogenase enzyme, using NADH as cofactor.

In vertebrates, including humans, three LDH-encoding loci have been identified in DNA: *ldh-a*, *ldh-b* and *ldh-c*, which produce the M (muscle), H (heart) and X subunits, respectively. The three genetic loci show 71–75% sequence identity, indicating wide conservation in amino acid composition of the LDH subunits (Markert, Shaklee and Whitt 1975). The M and H subunits are also commonly called as LDH-A and LDH-B. The LDH forms enriched in A subunits is predominant in skeletal muscle and liver, while those enriched in B subunits are mainly found in heart and brain.

The association of A and B isoforms can produce five isozymes: LDH-1 (A_0B_4), LDH-2 (A_1B_3), LDH-3 (A_2B_2), LDH-4 (A_3B_1) and LDH-5 (A_4B_0).

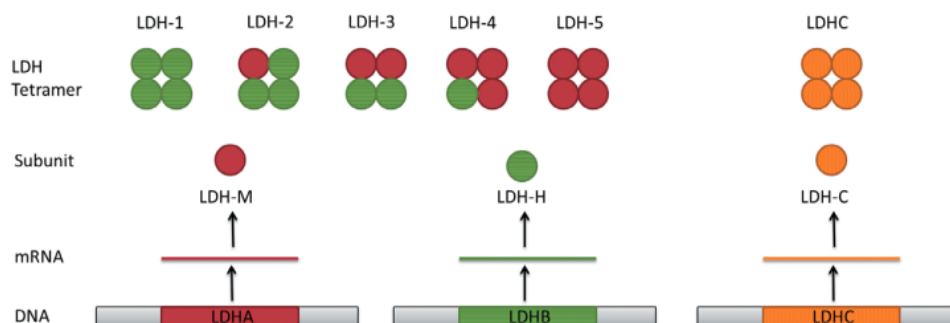


Figure 1.5. Lactate dehydrogenase (LDH) homo- and tetramer formation. The LDH isoenzymes LDH-1, LDH-2, LDH-3, LDH-4 and LDH-5 are made up of different ratios of LDH-M and LDH-H subunits, transcribed from LDHA and LDHB, respectively. The LDHC tetramer is only made up of LDHC subunits (Valvona et al. 2016).

These five isozymes have different electrophoretic mobility, which is dependent on their B subunit content: LDH-1 is the fastest moving form, LDH-5 the slowest. LDH-A and -B also display different kinetic properties (Read et al. 2001). LDH-A requires higher pyruvate concentrations to reach the maximum activity: the **K_m** for pyruvate is 158 μM for LDH-A and 58 μM for LDH-B. Moreover, at substrate concentrations needed for optimal LDH-A activity, the -B isozyme is inhibited: the **K_i** for pyruvate is 770 μM for LDH-B and 3900 μM for LDH-A (Eszes et al. 1996, Hewitt et al. 1999).

(Read et al. 2001), obtained the first crystal structures of the purified human isozymes LDH-1 and LDH-5 at a resolution of $\sim 2 \text{ \AA}$, allowing an in-depth evaluation of the differences between these two major enzyme forms. Two large domains can be identified: the first is formed by residues 20–162 and 248–266 and is characterized by a ‘Rossmann’ fold, a region of the peptide where three parallel β -strands enclose two alpha-helices. In this region, NADH binds in a groove of the central β -sheet with the His195; Asp168, Arg171, Ile250 and Thr246 are essential residues to assemble the geometry of the catalytic site. The second is the substrate binding domain, comprising the residues 163–247 and 267–331. The pyruvate binding cavity is located at the interface between the two domains, where residues 99–110 form the so-called ‘active site loop’. The active site structure, which is outlined in Fig. 1.6, displays high similarity in M and H subunits. The catalytic reaction is an ordered event, starting with the binding of NADH with His195. One of the prominent features of the coenzyme pocket in LDH is the hydrophobic environment, mainly due to the presence of the Ile250 residue (Deng et al. 1994). This explains the preferential bond of the neutral NADH over the charged NAD^+ .

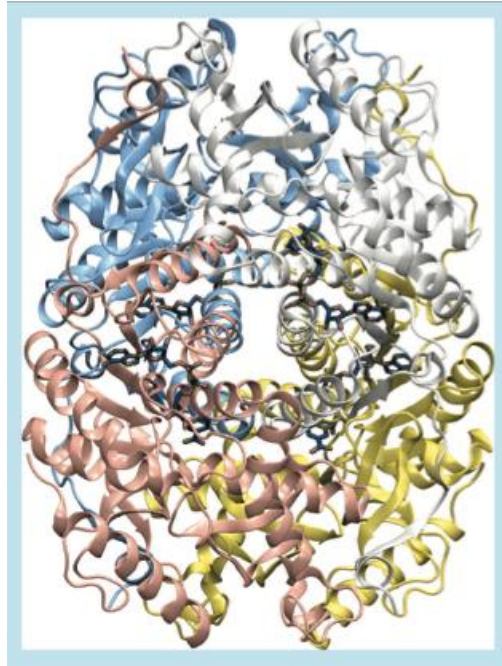


Figure 1.6. Tertiary structure of a LDH subunit. This mode of representation does not allow to show the differences between the A and B subunit. See also (Read et al. 2001).

In medicine, the interest for LDH has been prevalently linked for a long time to its importance as a diagnostic tool in human diseases. A sharp increase of LDH activity in serum is a consequence of massive cell death, which causes the release of the intracellular enzyme into the circulation, and is associated with acute diseases. The determination of serum LDH is widely used for the diagnosis of myocardial infarct and of liver, hematological and skeletal muscle diseases; high levels of LDH in serum are also detected during neoplastic diseases, as a consequence of tissue destruction caused by the neoplastic growth (Fiume et al. 2014).

Currently, the increased LDH-A expression observed in many tumor forms, and the role of this protein in neoplastic change is a matter of extensive research and debate (Fiume et al. 2014, Petrelli et al. 2015, Sugden and Holness 2003, Gillies, Robey and Gatenby 2008, Granchi et al. 2010, Zhao, Butler and Tan 2013c).

Nuclear LDH

Although LDH-A is predominantly found in the cytoplasm, it is also localized in the nucleus of many tumors and binds to ssDNA and mRNA (Pavlidis et al. 2009, Koukourakis et al. 2003a, Koukourakis et al. 2003b, Pioli et al. 2002, Sharief, Wilson and Li 1986).

Zheng, Luo and collaborators demonstrated that the enzyme is an essential component of the transcriptional complex of the histone 2B gene (H2B) (Dai et al. 2008). In this transcriptional complex, LDH-A subunit is in association with glyceraldehyde 3-phosphate dehydrogenase

(GAPDH) and the coordinated activity of the two enzymes maintain the proper NAD⁺/NADH ratio necessary for optimal H2B expression (Dai et al. 2008, He et al. 2013). In contrast with cytoplasmic LDH, for which the minimal functional unit was shown to be a dimer (Wang, Jiang and Zhou 1997), the nuclear enzyme is monomeric and is presumably maintained catalytically active by the supramolecular structure formed with GAPDH and with the other components of the transcriptional complex (Pavrides et al. 2009).

Moreover, LDHA with tyrosine phosphorylation has also been reported as localized to the nucleus, suggesting that tyrosine phosphorylation may play an essential role in LDHA function in the nucleus (Zhong and Howard 1990).

LDH-A REGULATION

LDH-A regulation is complex and is far from being completely understood. The LDH-A promoter region contains the consensus sequences for well-known transcription factors, HIF-1 and c-Myc (Firth, Ebert and Ratcliffe 1995, Lewis et al. 1997, Semenza et al. 1996, Shim et al. 1997), and recently discovered, forkhead box protein M1 (FOXO1) (Cui et al. 2014) and Kruppel-like factor 4 (KLF4) (Shi et al. 2014). LDH-A transcription is also known to be influenced by many factors including lactate (Lu et al. 2005), cyclic adenosine monophosphate (cAMP) (Miles, Hung and Jungmann 1981), estrogen (Burke, Harris and McGuire 1978), ErbB2 and heat shock factor 1 (Zhao et al. 2009) and is likely to be influenced by other unknown factors (Valvona et al. 2016).

LDH-A post-transcriptional activity is regulated, like many enzymes, by phosphorylation and acetylation of amino acid residues. The oncogenic receptor tyrosine kinase FGFR1 has been shown to directly phosphorylate LDH-A at Y10 and Y83 (Fan et al. 2011). Y10 phosphorylation of LDH-A, which is common in many human cancers, promotes active, tetrameric LDH-A formation, whereas phosphorylation of Y83 promotes NADH substrate binding (Fan et al. 2011). Recently, Zhao *et al* have also shown that deacetylation of LDH-A at lysine-5 is regulated by SIRT2 deacetylase in pancreatic cancer (Zhao et al. 2013a). Furthermore, they found that the acetylation of LDH-A at K5 leads to degradation of LDHA (Valvona et al. 2016).

LDH-A AS THERAPEUTIC TARGET

Multiple studies on various cell lines have shown that attenuation of LDH-A increases apoptosis (Fantin, St-Pierre and Leder 2006, Le et al. 2010) and reduces migration and invasion ability (Sheng et al. 2012, Xie et al. 2009) demonstrating its use as a potential therapeutic target.

The rationale for targeting LDH activity in the development of innovative anticancer strategies is because of the enzyme position at the end of glycolytic pathway: LDH inhibitors are not expected to hinder glucose metabolism of normal cells. In fact, because LDH activity is not needed for pyruvate metabolism through the TCA cycle, inhibitors of this enzyme should spare glucose metabolism of normal non-proliferating cells (Fiume et al. 2014).

Patients with homozygous absence of either A or B subunit do not show any symptom under ordinary circumstances. Individuals lacking A subunits only complain of muscle rigidity and sudden myoglobinuria after strenuous exercise (Miyajima et al. 1993, Kanno et al. 1988), when an increase in aerobic glycolysis and in ATP synthesis is required. B subunit is the major enzyme isoform found in red blood cells, which do not have mitochondria and obtain all their ATP by aerobic glycolysis. In spite of a heavily reduced LDH activity in erythrocytes, individuals with genetic deficiency of the B subunit do not suffer from anaemia and only in some cases show signs of mild haemolysis. The lack of significant clinical symptoms in individuals with A or B subunit deficiency can be explained by the presence of NADH re-oxidizing systems other than LDH (Kanno et al. 1983).

Thus, it could be expected that LDH inhibition causes adverse effects only when rapid generation of new cells is needed, such as in tissue repair or during the activation of immune response or in cancer cells.

As observed by Fantin et al., reduction in LDH-A activity resulted in stimulation of mitochondrial respiration and decrease of mitochondrial membrane potential. The ability of these tumor cells to proliferate under hypoxia is also compromised (Fantin et al. 2006).

Moreover, the abrogation of LDH-A results in reprogramming of pyruvate metabolism, with decreased lactic fermentation in vitro, in vivo associated with a severe restriction of tumor growth (Xie et al. 2014).

LDH INHIBITORS

Oxamic acid (PAPACONSTANTINO and COLOWICK 1961) and gossypol (Dodou et al. 2005) are long-known inhibitors, displaying no selectivity between the A and B LDH

isoforms.

Gossypol, a natural phenol derived from the cotton plant, inhibits LDH by competition with NADH, but it is not specific for this enzyme. Moreover, because of its structural characteristics gossypol can interact with different cellular components affecting several biological functions, which causes unspecific toxicity (Dodou et al. 2005, Lee et al. 1982).

FX11 [3-dihydroxy-6-methyl-7-(phenylmethyl)-4-propylnaphthalene-1-carboxylic acid] was a promising new gossypol-derived specific LDH-A small molecule inhibitor, commercially available. However, further studies have challenged the validity of FX-11, giving rise to the suspicion that some of the observed effects could be not specifically ascribed to LDH inhibition, but to the reactive nature of the catechol group of the molecule (Kohlmann et al. 2013, Lee et al. 1982).

Oxamic acid (OXA) is a pyruvate analogue which inhibits LDH by substrate competition. Zhou et al. demonstrated that downregulation of LDHA by using both LDHA-targeted siRNA and oxamate increased the sensitivity of the Taxol-resistant cells to Taxol and promoted apoptosis (Zhou et al. 2010).

One of the problems with oxamate is that it has limited cell penetration; therefore, relatively high doses are required to have any significant effect which are not expected to be reached *in vivo*. However, galloflavin (GF), a synthesized LDH-A and LDH-B inhibitor (Manerba et al. 2012), has high levels of cell penetration even if it is still a higher concentration than commonly used in chemotherapeutics. Furthermore, the highest tested dose of galloflavin (250 μM) caused <30% reduction of ATP and lactate production of normal human lymphocytes and lymphoblasts but had a mild effect on their growth and survival (Farabegoli et al. 2012). As explained in details in the next chapters, we demonstrated that both OXA and GF sensitize lymphoma cells to cisplatin without enhancing the drug effects on immortalized normal lymphocytes (Manerba et al. 2015). These inhibitors can reverse inflammation induced changes in colon cancer cells (Manerba et al. 2017a). In addition, they can impact on heat shock response and induces senescence of hepatocellular carcinoma cells (Manerba et al. 2017b).

Last year the Genentech group, using a high throughput small-molecule screening, found a new LDH inhibitor, GNE-140, that binds LDH-A in the active site near the binding site of NADH molecule. It is actually the only inhibitor with nanomolar potency *in vitro*. They showed that GNE-140 inhibits the biochemical activities of LDH-A and LDH-B with IC_{50} s of 0,003 and 0,005 μM , respectively. In MiaPaCa2 pancreatic cancer cell lines, it reduces in 6 hours the lactate production with an IC_{50} of 0,67 μM and increases the pyruvate production.

GNE-140 also inhibits the proliferation with an IC_{50} of 0,43 μ M. In addition, by assessing a panel of 30 pancreatic cell lines they showed that cell lines which rely more on glycolysis than on oxidative phosphorylation are more sensitive to LDH inhibition. However, GNE-140 showed rapid clearance that not allow to appreciate its effects in studies *in vivo* (Boudreau et al. 2016).

Unfortunately, in spite of extensive studies also involving multinational drug companies (Ward et al. 2012, Billiard et al. 2013, Fauber et al. 2014, Xie et al. 2014) the development of LDH inhibitors suitable for clinical use is proving a very difficult task. Nevertheless, the availability of *in vitro* active compounds can allow at present a better understanding of the potentiality of LDH inhibition in anticancer treatments.

Chapter 2

AIM OF THE THESIS

Lactate Dehydrogenase is an enzyme that inter-converts pyruvate and lactate using nicotinamide adenine dinucleotide (NAD[H]). The increased LDH-A expression has been observed in many tumor forms. In neoplastic cells, this enzyme commonly reduce pyruvate to lactate even in presence of adequate oxygen supply (aerobic glycolysis). The rationale for targeting LDH activity in the development of innovative anticancer strategies is because of the enzyme position at the end of glycolytic pathway. In fact, because LDH activity is not needed for pyruvate metabolism through the TCA cycle, inhibitors of this enzyme should spare glucose metabolism of normal non-proliferating cells.

Unfortunately, in spite of extensive studies also involving multinational drug companies the development of LDH inhibitors suitable for clinical use is proving a very difficult task. Nevertheless, the availability of in vitro active compounds can allow at present a better understanding of the potentiality of LDH inhibition in anticancer treatments.

The objective of this thesis work, simultaneously with the ongoing search for new LDH inhibitors, is the study of the role of LDH in cancer cells by pharmaceutical approach, through the use of known inhibitors in different cell lines and conditions, and by genetic approach, consisting in the depletion of LDH genes. This last approach is important to can study the effects of the LDH activity's absence without taking into account the possible non-specific effects of the small molecule inhibitors.

Chapter 3

MATERIALS AND METHODS

Laboratory of cell biology, DIMES Department, Bologna - Italy

3.1 Cell cultures

All the cell cultures were routinely tested for Mycoplasma contamination and found to be free.

Loukes cells are derived from a sporadic, EBV negative Burkitt's lymphoma (Marchini, Longnecker and Kieff 1992). *GM00130C* is a B lymphocyte cell line immortalized by EBV infection; they were obtained from Coriell Cell Repositories (Coriell Institute for Medical Research, Camden, New Jersey, USA). These cells were grown as a suspension culture in RPMI 1640 containing 10% FBS (20% for GM00130C), 100 U/ml penicillin/streptomycin, 4 mM glutamine and were maintained at a concentration of $1-2 \times 10^5$ viable cells/ml. (Paragraph EXPERIMENTAL PART 1A)

CaCo-2 cells (ATCC) were grown in DMEM containing 10% FBS, 100 U/ml penicillin/streptomycin, 4 mM glutamine. Before each experiment, cells were let to reach the confluence, then harvested and seeded at a density of 50.000 cells/cm². This procedure was adopted for all experiments, since it was found to be important for evaluating the expression of some of the studied proteins. (Paragraph EXPERIMENTAL PART 2A)

PLC/PRF/5 cells were grown in DMEM (1 g/l glucose), supplemented with 10% FBS, 100 U/ml penicillin/streptomycin, 2 mM glutamine and 1 mM sodium pyruvate. (Paragraph EXPERIMENTAL PART 3A)

Raji cells were grown as a suspension culture in RPMI 1640 containing 10% FBS, 100 U/ml penicillin/streptomycin, 4 mM glutamine and were maintained at a concentration of $3,75 \times 10^5$ viable cells/ml. (Paragraph EXPERIMENTAL PART 1B e 2B)

Normal lymphocytes were obtained from peripheral blood and purified by density gradient

centrifugation using Histopaque-1077 (Sigma). They were maintained in RPMI 1640 and used within 48h from the purification. (Paragraph EXPERIMENTAL PART 1B)

3.2 Compounds

Galloflavin (GF) was synthesized according to the procedure described by (Manerba et al. 2012). It was added to the culture media in the presence of 0.6% DMSO for all the experiments. Equivalent amounts of DMSO were also added to the control (untreated) cultures.

OXA, cisplatin (cis-diamminedichloroplatinum(II)) and all other compounds and reagents were purchased from Sigma–Aldrich.

TNF- α and IL-17 were from R&D Systems and were used at a concentration of 25 and 50 ng/ml, respectively.

3.3 Enzymatic assays on purified human LDH-A

Purified LDH-A (from human liver) was obtained from Lee Bio-solutions (St Louis, Missouri, USA). 20 mM stock solutions of the selected 67 hits were prepared in DMSO. They were added in scalar amounts (0 – 200 μ M final concentrations) to a reaction mix containing 100 mM phosphate buffer pH 7.5, 0.015 U LDH / ml, 1 mM pyruvate and 150 μ M NADH. For all the determinations (including those without the compounds), DMSO in the reaction mix was always kept to 0.6%. The enzymatic activity was measured by monitoring NADH oxidation for a period of 5 min. To avoid interference of the compounds with the UV reading of NADH oxidation, we adopted the procedure reported by (Moran and Schnellmann 1996), which measured LDH activity by recording the decrease of NADH fluorescence. The assay was performed in 96-well white body plates, using a Fluoroskan Ascent FL reader (Labsystems). The concentration of compounds causing 50% inhibition of LDH activity (IC_{50}) was calculated from the second order polynomial regression of the experimental data, using the Prism 5 GraphPad software.

In EXPERIMENTAL PART 1B, at the wavelengths used for NADH determinations (λ_{ex} 340 nm, λ_{em} 460 nm) all tested compounds, except compound **4**, did not appear to appreciably interfere with the fluorescence reading. Compound **1** was further characterized in order to

assess its mechanism of inhibition. To this aim, competition assays were performed in the presence of scalar concentrations of pyruvate (0 – 2 mM) or NADH (20 – 150 μ M). In the first case NADH in the reaction mix was maintained to 150 μ M; in the second case pyruvate was 2 mM. The two sets of experimental data were analyzed by applying the mixed model fit, using the Prism 5 GraphPad software (Fig. 4.42).

3.4 Viability assays

Neutral red assay

CaCo2 and PLC/PRF/5 cell viability was measured by using the Neutral Red assay, tested in triplicate. Cells (1.0×10^4 /well) were seeded in 96-multiwell plates, allowed to adhere overnight and treated for 24 h at 37 °C. After incubation, cells were maintained 3 h at 37 °C with the Neutral Red dye dissolved in medium at the final concentration of 30 μ g/ml. Medium was then removed and the cells were solubilized with 200 μ l of 1% acetic acid in 50% ethanol. Absorbance of the solutions was measured at λ 540 using a microplate reader (Multiskan Ascent FL, Labsystems).

Cells counts

To study the effect of the LDH inhibitors on cell proliferation, suspension culture cells (1×10^5) were seeded in 24-multiwell plates and treated for 24 h at 37°C with scalar doses of inhibitors (0-200 μ M, tested in duplicate). After incubation, cells were counted under a light microscope using a Neubauer chamber and their viability was determined by Trypan blue exclusion. The cell growth was calculated from the difference between the number of viable cells counted at 24 h and that at the beginning of experiment. Data were plotted as cell growth vs dose of compound. The dose causing 50% inhibition of cell growth (cell growth IC_{50}) was calculated by applying the second order polynomial regression to the experimental data. (Paragraph EXPERIMENTAL PART 1B e 2B)

When the effects of compound **1** were tested on normal lymphocytes, cells (1×10^5 in 24-multiwell plates) were exposed for 24h to 0-200 μ M inhibitor. At the end of incubation time the number of viable cells was counted and compared to that measured after treatment of Raji cells.

Combination experiments

Cells (1×10^5 in 24-multiwell plates) were incubated for 24h in the presence of LDH inhibitor

(cell growth IC₅₀ dose) and an anticancer agent, given alone or in combination. At the end of incubation, the percentage of living cells was evaluated by Trypan blue exclusion. The interaction between LDH inhibitor and the anticancer agent was assessed by calculating the combination index according to the procedure described by (Dos Santos Ferreira et al. 2012), which applies the following formula:

$$\frac{\text{Surviving cells treated with the association}}{(\text{Surviving cells treated with cisplatin}) \times (\text{Surviving cells treated with OXA(GF)})}$$

According to Dos Santos Ferreira et al. (2012), a result ranging from 0.8 to 1.2 denotes an additive effect. Synergism is indicated by a result < 0.8; antagonism by a result > 1.2.

In EXPERIMENTAL PART 1A, combination experiment of OXA(GF) (LDH IC₅₀ dose) with cisplatin (3 and 6 μM) was performed with Loukes and GM00130C cells.

In EXPERIMENTAL PART 1B, combination experiment of compound 1 with anticancer agents was performed with Raji cells. For each anticancer agent, the lowest dose causing a statistically significant effect on cell viability (previously determined) was used. The doses were: 6 μM cisplatin; 0.1 μM daunomycin; 10 μM sunitinib; 1 μM etoposide.

3.5 Lactate assay

LDH inhibition was evaluated by dosing the produced lactate according to the method of Barker and Summerson (1941) and following the procedure described by (Farabegoli et al. 2012). 5×10⁵ cells in 1 ml of Krebs Ringer buffer were seeded in each well of a 6-well plate. Different amounts of inhibitors (tested in duplicate) were then added to the cultures. Lactate (both intracellular and released in medium) was measured 6 h after incubation at 37 °C. At the end of incubation, cells were lysed by adding 100 μl of 100% trichloroacetic acid (TCA) in the Krebs Ringer medium (TCA final concentration = 10%). After centrifugation to remove the cell debris and acid insoluble material, lactate was measured in the supernatant. The dose of compound causing 50% inhibition of lactate production (LDH IC₅₀) was calculated from the second order polynomial regression of experimental data, using the Prism 5 GraphPad software.

3.6 LDH assay

Control and cytokines treated cells (2×10⁶) were harvested, pelleted and suspended in 100 μl

of PBS. The suspension was lysed by sonication and centrifuged (1600g, 30 min at 4 °C) to discard the cell debris. Protein content of the supernatant was measured according to the method of Bradford. To determine the LDH isoform composition of the cellular extracts (5–10 µl amounts) we utilized the coenzyme analogue ratio method, originally set up by (GOLDMAN, KAPLAN and HALL 1964), which is based on the comparison of the enzyme activity obtained with a reaction mixture containing reduced nicotinamide hypoxanthine dinucleotide (NHXDH) and low pyruvate concentration to that measured in the presence of NADH and high pyruvate concentration.

Two reaction mixtures were prepared: the first containing 0.22 mM NHXDH and 0.33 mM pyruvate and the second containing 0.13 mM NADH and 10 mM pyruvate, both in a final volume of 3 ml of 100 mM phosphate buffer (pH 7.5). The reactions were started by adding the cellular extract to each mixture and the optical density change at λ 340nm between 30 and 120 s was determined. The detailed procedure for calculating the relative amounts of A and B isoforms was described by (GOLDMAN et al. 1964). LDH activity was expressed as mU/mg cell proteins (Table 4.2).

3.7 Glucose uptake assay

CaCo-2 cells were seeded into 96-well black plates at 20,000 cells/well and let to adhere overnight. They were then treated with TNF- α and IL-17 for 24 h, after which they were maintained for 20 min in the presence of 2-[N-(7-Nitrobenz-2-oxa-1,3-diazole-4-yl)amino]-2-deoxy-D-glucose (2-NBDG), 100 µM in glucose free medium. Medium was removed and cells were washed with PBS. Fluorescence (λ_{exc} 485; λ_{em} 530) was measured by using the Fluoroskan Ascent FL reader (Labsystems) (Table 4.2).

3.8 NAD/NADH assay

Cellular levels of NAD⁺ and NADH were estimated on samples of $1,5 \times 10^6$ cells. After 18 h incubation with LDH inhibitor (cell growth IC₅₀ dose) cells were counted, pelleted at 4°C and lysed with ice-cooled extraction buffer (500µL / 6×10^6 cells) containing 20 mM sodium bicarbonate, 100 mM sodium carbonate, 10 mM nicotinamide and 0.1% Triton X-100. The cell lysate was centrifuged at 16000g, 4°C for 5 min to remove the insoluble material. A 50 µl aliquot of the sample was kept at 60°C for 30 min to selectively decompose NAD⁺. A further

50 μ l was mixed with 840 μ l of a buffer containing 100 mM Tris-HCl pH 8, 0.5 mM EDTA, 0.5 mM MTT, 0.2 mg/ml of yeast alcohol dehydrogenase. After addition of 10 μ l of 200 mM phenazine ethosulfate, the solution was incubated for 5 min at 25°C. Then 100 μ l of 6 M ethanol was added, the mixture was centrifuged at 16000g, 25°C for 30s, and the absorbance at 570 nm of the supernatant was measured for 120s with 10s intervals, using an UV/visible spectrophotometer, in the “kinetics” mode. This sample allowed measuring total NAD(H) (NAD⁺ and NADH) content. The same reaction was then repeated on the sample incubated at 60°C, to measure NADH. The measured absorbance change/second is proportional to the amount of the dinucleotide. NAD⁺ and NADH concentrations in the experimental samples were calculated using a calibration curve previously obtained with known amounts of NAD(H) standards.

3.9 ATP production assay

ATP production was measured after 6 h of incubation in the presence of varying amounts of OXA(GF), tested in duplicate. 1×10^4 cells were used for this assay. ATP levels were measured using the CellTiter-Glo Luminescent Cell Viability Assay (Promega, Madison, Wisconsin, USA), following the kit instructions. A second-order polynomial regression was applied to experimental data to calculate the dose of OXA(GF) causing a 50% reduction in levels (IC₅₀). Prism 5 GraphPad software was used for statistical analyses. (Table 4.1).

3.10 Immunoblotting

Cell cultures were exposed to relative treatments. After incubation, they were lysed in RIPA buffer containing protease and phosphatase inhibitors (Sigma Aldrich). The cell homogenates were left 30 min on ice and then centrifuged 15 min at 10.000g. Selected μ g proteins of the supernatants (measured according to Bradford) were loaded into polyacrylamide gel for electrophoresis. The separated proteins were blotted on a low fluorescent PVDF membrane (GE Lifescience) using a standard apparatus for wet transfer with an electrical field of 60-80mA for 4-18h. The blotted membrane was blocked with 5% BSA (or casein) in TBS-Tween and probed with the primary antibody. Binding was revealed by a Cy5-labelled secondary antibody (anti rabbit-IgG, GE Lifescience; anti mouse-IgG, Jackson Immuno-Research). All incubation steps were performed according to the manufacturer’s instructions. Fluorescence

of the blots was assayed with the Pharos FX scanner (BioRad) at a resolution of 100 μm , using the Quantity One software (BioRad).

Loukes cell cultures (1.5×10^6 cells) were exposed to cisplatin (6 μM) and OXA(GF) (LDH IC_{50} dose) by using the schedules reported in the Figure legends. 50 μg proteins of the supernatants were loaded into 12% or 8% polyacrylamide gel for electrophoresis. The used antibodies were: rabbit anti-gammaH2AX [phospho S139] (Abcam), mouse anti-PADPR [H10] (Abcam), rabbit anti-Rad51 (Thermo Fisher), rabbit anti-MYC [Y69] (Abcam), rabbit anti-Actin (Sigma Aldrich). (Experimental Part 1A).

CaCo2 cells were exposed to cytokines treatment (4 or 24 h). 40 or 100 μg proteins of the supernatants were loaded into 10% or 8% polyacrylamide gels for electrophoresis. The used antibodies were: mouse anti-E-cadherin (R&D Systems), rabbit anti-Snail [C15D3] (Cell Signaling), rabbit anti-Notch1 [D1E11] (Cell Signaling), rabbit anti-MYC [Y69] (Abcam), rabbit anti-Actin (Sigma Aldrich), rabbit anti-LDHA (Cell Signaling), rabbit anti-Oct4 (Cell Signaling). (Experimental Part 2A).

PLC/PRF/5 cell cultures were exposed to 60 mM OXA or 200 μM GF for 24 h. Proteins of the supernatants (40 or 100 μg) were loaded into 4–12% pre-casted polyacrylamide gels (Life Technologies) for electrophoresis. The used antibodies were: rabbit monoclonal anti-AFP (D12C1) (Cell Signaling); mouse monoclonal anti-hsp27 (G31) (Cell Signaling); rabbit anti-phospho-hsp27(Ser78) (Cell Signaling); rabbit anti-hsp90 (Enzo Life Sciences); mouse monoclonal anti-hsp72 (C92F3A-5) (Enzo Life Sciences); rabbit anti-Actin (Sigma Aldrich). (Experimental Part 3A).

Apoptosis was assayed by measuring the differential expression of BAX and BCL2 proteins in treated cells. *Raji cell cultures* (1.5×10^6 cells, seeded in 25 cm^2 flasks) were exposed to compound **1** (cell growth IC_{50} dose) for 18 h. 40 μg proteins of the supernatants were loaded into 10 % polyacrylamide gel for electrophoresis. The used antibodies were: rabbit anti-BCL2 (Abcam), rabbit anti-BAX (Abcam). (Experimental Part 1B).

3.11 Gelatin zymography

Matrix metalloproteinases (MMP) secretion and activity was assessed using gelatin

zymography (Heussen and Dowdle 1980). Cells were grown at density of 5×10^4 cells/cm², treated for 24 h with TNF- α and IL-17 and then maintained in serum-depleted media for 18 h. Conditioned media were collected by spinning each sample at 1700 rpm for 5 min, to pellet cell debris. Supernatants (3 ml) were then concentrated using Amicon Ultra-centrifuge filters (Millipore), according to the manufacturer's directions. Protein concentration was determined using the Lowry method. Equal amounts of samples (30 μ g) were then loaded with sample buffer (1 M Tris-HCl pH 6.8, 2% sodium dodecyl sulfate, 10% glycerol) onto a 10% polyacrylamide gel containing 1 mg/ml gelatin. After electrophoresis, SDS was removed from the gel by washing twice with 2.5% Triton X-100 for 1 h. After a brief rinse, gel was incubated at 37 °C for 18 h in a zymography buffer (100 mM Tris-HCl, 10 mM CaCl₂, 20 mM NaCl, pH 7.6). Gel was stained with 1% Coomassie Brilliant Blue R250 for 30 min and then treated with a de-staining solution (40% methanol, 10% acetic acid, 50% distilled water). The MMP activities, indicated by clear bands of gelatin digestion on a blue background, were quantified by using an image analysis software (Kodak 1D Image Analysis Software).

3.12 Real time PCR

RNA was extracted according to the procedure described by (Chomczynski and Sacchi 1987), and was quantified spectrophotometrically. Retro-transcription to cDNA was performed by using the Revert Aid TM First Strand cDNA Synthesis Kit, in different steps: 5 min denaturation at 65 °C, 5 min annealing at 25 °C, 1 h retro-transcription at 42 °C and 5 min denaturation at 70 °C. Real Time PCR analysis of cDNA was performed using SYBR Green (SSO Advanced, BioRad), with specific Forward and Reverse primers. Annealing temperature was 60 °C. All samples were run in triplicate, in 10 μ l reaction volume containing 100 ng of cDNA. The thermal cycler (CFX96 TM Real Time System, BioRad) was programmed as follows: 30s at 95 °C; 40 cycles of 15s at 95°C; 30s at 60°C.

LDH-A, LDH-B and H2B histone expressions were evaluated by measuring their mRNA levels, using β -tubulin and HPRT as internal controls of the reaction. Primers used in Experimental part 2A:

LDH-A	Forw: 5'- GACCTACGTGGCTTGAAGA-3'	Rev: 5'-TCCATACAGGCACACTGGAA- 3'
LDH-B	Forw: 5'-CCAACCCAGTGGACATTCTT-3'	Rev: 5'- AAACACCTGCCACATTCACA-3'
H2B histone	Forw: 5'-CAGTGCTATG CCAGAGCCAGCGAA-3'	Rev:5'-CTGTTTACTTAGCGCTGGTGTACTTGGTGA-3'

HSPs and alpha-fetoprotein (AFP) expressions were evaluated by measuring their mRNA

levels, using β -tubulin and HPRT as internal controls of the reaction. For each protein, the used primers were obtained from published papers, as follows: hsp27 (Tourtas et al. 2012); hsp72 (Walsh et al. 2001) hsp90A (Lauten et al. 2003); hsp90B (Chhabra et al. 2015); AFP (Zhang, Lie and Wei 2009). (Experimental Part 3A).

3.13 Flow cytometry

Assay of ROS production

Loukes cells (1×10^6 in 25 cm² flasks) were collected after 6 h treatment with LDH inhibitors (LDH IC₅₀ dose) and cisplatin (6 μ M) given alone or in association. After centrifugation and washing with PBS, the cells were maintained for 30 min in the dark in a solution containing 10 μ M 2-7-dichlorofluorescein diacetate (DCF). ROS production was analyzed by flow cytometry using 10.000 cells in the FACSCalibur system (Becton–Dickinson, San Jose, CA, USA).

Assay of cell cycle

Raji cells (1×10^6 in 25 cm² flasks) were collected 18 h after treatment with compound **1** (cell growth IC₅₀ dose), fixed with 70% ethanol and stored overnight at 4°C. After centrifugation and washing with PBS twice, the fixed cells were maintained for 30 min in the dark in 500 μ l of a staining solution containing 10 μ g/ml propidium iodide, 200 μ g/ml RNase (DNase free) and 0.1 % Triton in PBS. Cell cycle distribution was analyzed by flow cytometry using 10.000 cells in the FACSCalibur system (Becton-Dickinson, San Jose, CA, USA). The experiment was repeated twice

3.14 Colony formation assay

Suspension culture

Loukes cells were treated with cisplatin (3 μ M, 1 h) and LDH inhibitors (15 mM OXA or 30 μ M GF, 6 h) given alone or in combination. In the cultures treated with the drug combination, cisplatin was added during the last hour of OXA/GF treatment. Each dose was tested in triplicate. These short exposure times were chosen since the heavy toxicity of longer treatments were previously found to completely abolish cell clonogenicity, impeding the quantification of effects. After the treatment, cells were centrifuged to remove the drug

containing medium and were seeded in 24 well plates (1000 cells/well) in 1 ml complete RPMI 1640 containing 1% methylcellulose and incubated at 37 °C in humidified atmosphere for 15 days. Colonies of more than 50 cells were scored visually under an inverted microscope by two independent observers.

Adhesion cultures

PLC7PRF/5 cells were plated into 6-well plates, at the density of 500 cells/well. They were treated with 60 mM OXA or 200 μ M GF (tested in triplicate) for 24 h. Compounds were then removed and cultures were maintained for additional 15 days. Cells were stained with 0.5% crystal violet (dissolved in 6% glutaraldehyde). The colonies were photographed and counted to generate a histogram.

3.15 ATPase activity

ATPase activity was measured in a 96-well plate, by using a commercially available kit (Sigma-Aldrich). In each well, 500 ng recombinant protein was added to 30 μ l assay buffer and incubated 3h at 37°C with 1mM GF. 1mM ATP was then added and the plate was maintained at 37 °C for further 3 h. Reaction was stopped by adding to each well 200 μ l of the kit included reagent which, after 20 min incubation at room temperature generates the colorimetric product. Absorbance was read at λ 620 by using a microplate reader (Multiskan Ascent FL, Labsystems).

Recombinant, functionally active hsp72 and hsp90 from Enzo Life Science were used. They were diluted 1:4 to limit interference from their medium (PBS buffer) in the detection of phosphate released by ATPase activity.

3.16 Alkaline phosphatase assay

Alkaline phosphatase (ALP) activity was measured on cell homogenate using p-nitrophenyl phosphate (p-NPP) as substrate and measuring the release of p-nitrophenol (p-NP), detected at 405 nm in a microplate multifunctional reader. The procedure described by (Ferruzza et al. 2012) was followed. ALP activity in each sample was calculated from a p-NP standard curve.

3.17 2',7'-Dichloro-dihydro-fluorescein diacetate assay

Cells were grown on cover slips (5×10^5 /well) in 6-well plates and they were treated for 4 h with 200 μ M GF or 60 mM OXA. After washing with PBS, the cells were incubated at room temperature in the dark for 20 min with 10 μ M 2',7'-dichloro-dihydro-fluorescein diacetate (DCFH-DA) dissolved in PBS. After incubation, the cells were rinsed three times with PBS and mounted with a solution of DAPI (300 nM) and DABCO. The samples were observed at a Nikon epifluorescence microscope equipped with filters for DAPI and FITC. At least 3 fields for sample were analysed and ≥ 200 cells for sample were counted.

3.18 Assay of thiobarbituric acid reactive substances (TBARS)

PLC/PRF/5 cells (6×10^6) were seeded in a T75 flask and let to adhere overnight. They were then exposed for 18 h to 60 mM OXA or 200 μ M GF, dissolved in serum free medium. After treatment, they were pelleted and lysed by sonication in 100 μ l H₂O. Samples were then added with 66 μ l 8.1% SDS, 500 μ l 20% acetic acid pH 3.5, 500 μ l 0.8% thiobarbituric acid and heated at 95 °C for 1 h. After chilling at room temperature, TBARS were extracted with 700 μ l of 15:1 N-butanol/ pyridine. Samples were then centrifuged at 4000 rpm for 10 min and the absorbance of their organic layer was measured at $\lambda 532$ nm. The amount of TBARS was normalized to the protein content of the cell pellet.

3.19 Senescence-associated β -galactosidase staining assay

Cells were plated at a density of 3×10^4 in 6-well plates. After incubation with 60 mM OXA or 200 μ M GF for 48 h, they were fixed in 2% formaldehyde/0.2% glutaraldehyde in phosphate-buffered saline for 5 min and incubated at 37 °C for 12 to 18 h with fresh β -galactosidase staining solution containing 1.0 mg/ml 5-bromo-4-chloro-3-indolyl- β -D-galactopyranoside (X-gal). The procedure described by (Debacq-Chainiaux et al. 2009) was used.

3.20 Statistical analyses

All analyses were performed using the software GraphPad Prism 5. Each experiment was repeated twice with at least triplicate samples per treatment group. Results are expressed as mean \pm SE of replicate values. Analysis was performed by ANOVA corrected by Dunnet's

test or Student's t test. All tests of statistical significance were two-sided and p values < 0.05 were considered statistically significant.

**Laboratory of “Hypoxia signalling and cancer metabolism”, IRCAN Institute,
Nice – France**

3.21 Cell culture and hypoxic exposure conditions

Human glioblastoma U87 cells and human colon adenocarcinoma LS174T cells (provided by Dr. Van de Wetering, NL), unless otherwise specified, in Dulbecco's modified eagle medium (DMEM, Gibco by Life Technologies Corporation, Paisley, UK). Mouse B16 F10 (provided by Pr. Marina Kreutz, Regensburg, Germany) were grown Roswell Park Memorial Institute (RPMI) medium, supplemented with fetal bovine serum (10%), penicillin (10 U/mL) and streptomycin (10 µg/mL). In normoxic conditions, cells were incubated in a humidified atmosphere with 5% CO₂/21% O₂ at 37 °C. In hypoxic conditions the cells were maintained in 1% O₂ in a sealed anaerobic workstation (INVIVO₂ 400, Ruskinn Technology Ltd, Bridgend, South Wales) where the air was replaced by N₂ and CO₂ was maintained at 5%.

3.22 CRISPR/Cas9 technology

In order to get *LDHA* and *LDHB* single-knockouts, human LS174T cells and mouse B16 F10 cells were respectively transfected with CRISPR/Cas9 using pSpCas9(BB)-2A-GFP (PX458). This plasmid was a gift from Feng Zhang (Addgene plasmid #48138) (Ran et al. 2013) bearing GFP-encoding region designed by J. Durivault (Centre Scientifique de Monaco). The guide RNA was designed using the CRISPR Design Tool (<http://crispr.mit.edu>).

Transfection procedure

One day before transfection, the cells were plated in 10-cm dish with growth medium so, that they will be 90-95% confluent at the time of transfection (ex. for LS174T: 2-2.5×10⁶ cells).

One hour before transfection, the growth medium was replaced with 10 ml of growth medium without antibiotics (to avoid the increase of cell mortality). Meantime, 10 µg of DNA (5 µg of LDH-A CRISPR/Cas9 plasmid + 5 µg of LDH-B CRISPR/Cas9 plasmid) were diluted in 1.5

ml of Opti-MEM 1 Reduced Serum Medium without serum, and also 60 µl of Lipofectamine 2000 (Polyplus transfection, Illkirch, France) were diluted in 1.5 ml of Opti-MEM 1 (the Lipofectamine amount varies in proportion to the surface area), incubating them for 5 min at room temperature. After incubation, it is possible to combine the diluted DNA with the diluted Lipofectamine 2000, incubating for other 20 min at room temperature to allow the DNA-Lipofectamine 2000 complexes to form. At this point, the mix was added to the plate and the cells were incubated at 37°C in a CO₂ incubator for 6 to 7 hours. After that, it is possible to replace the medium by new growth medium (in this case the medium can contain antibiotics in).

Sorting of transfected cells

The day after the transfection it is possible to verify the transfection efficiency by visualising the GFP protein at the microscope and to proceed to the sorting of the transfected cells by FACS (Fluorescence-activated cell sorting) procedure.

The cells were trypsinized and counted to not exceed 5×10^6 /ml, washed twice with 10 ml of cold PBS + 1% serum, re-suspended in an appropriate volume of PBS + 3% serum + 1mM EDTA + antibiotics and filtered with specific filter for FACS, transferring the cells in the FACS tubes.

In addition it is necessary to prepare one FACS tube with 1ml DMEM (+10% FCS + antibiotics) for collecting the cells after sorting. Everything is kept in ice during transport to the FACS platform.

The sorting has been done by using the BD FACSaria sorter machine. It allows to select the area of interest by using control cells (not transfected cells) as blank; in this way, only the GFP positive cells, located in the selected area, are sorted (see the Step 2 of Fig. 4.44).

This sorter is also able to seed single cells in 96-well plate. To get single colonies also in 10 cm plates, the rest of the sorted cells have been seeded at very low concentration (5000, 1000 and 300 cells).

Once obtained the single colonies, they were picked up and expanded to can proceed at the selection of the right KO cells by screening.

3.23 Immunoblotting

Cell cultures were lysed in LAEMMLI buffer 1.5 X (containing SDS 20%, glycerol and Tris HCL 1M pH 6.8), scraping the plate to collect the cell homogenates, and put at -20°C. Selected µg proteins of the supernatants (measured according to BCA assay (Interchim, Montluçon, France)) were loaded into polyacrylamide gel for electrophoresis (BioRad gel system). The separated proteins were blotted on a PVDF membrane (Immobilon, Merck Millipore Ltd, Tullagreen, Carrigtwohill, Co. Cork, Ireland) using a standard apparatus for wet transfer (Hoefer TE42 transfer unit) with an electrical field of 100 mA over-night at 4°C. After the transfer is completed, it is possible to check the efficiency of the transfer by Amido Black coloration.

After the re-activation of the membrane in ethanol, the blotted membrane was blocked with 5% of non-fat dry milk in TN buffer (50 mM Tris-HCl pH 7.4, 150 mM NaCl) and probed with the primary antibody.

The used antibodies were: rabbit anti-HIF-1 α (anti-human/mouse polyclonal antibody, produced in the Dr. Pouyssegur's laboratory), mouse anti-LDHA [AT1A4] (Abcam), mouse anti-LDHB [60H11] (Abcam). Antibody against Actin, Tubulin and HSP60 were used as loading control.

Binding was revealed by incubation with a secondary anti-mouse or anti-rabbit antibody (Promega) and develop by ECL working reagents (Millipore Corporation, Billerica, MA, USA). All incubation steps were performed according to the manufacturer's instructions. Chemiluminescence of the blots was assayed with the Pxi machine, using the GeneSys software (Syngene, United Kingdom).

3.24 Real time PCR

RNA was extracted by "AllPrepDNA/RNA/Protein Mini Kit" (Qiagen) according to the procedure described, and was quantified spectrophotometrically. Retro-transcription to cDNA was performed by using the QuantiTect Reverse Transcription kit (Qiagen). Real Time PCR analysis of cDNA was performed using Takyon Rox SYBR MasteMix dTTP Blue (Eurogenetec), with specific LDH-A and LDH-B primers using RPLPO as internal controls of the reaction. Annealing temperature was 60 °C. All samples were run in triplicate, in 20 µl reaction volume. The thermal cycler (Applied StepOne Plus, Life Technologies) was programmed as follows: 3min at 95 °C; 40 cycles of 10s at 95°C; 50s at 60°C.

3.25 LDH-A and LDH-B enzymatic assay

All the clones kept in normoxia or hypoxia 24 h (1×10^5) were washed once with 2 ml of cold PBS and once with 2 ml of cold H₂O. H₂O (100 μ l) of were added in each well and the plates were left at -80°C for at least 10 min. After incubation, the cells were collected into Eppendorf tubes by scratching, centrifuged at 4°C (8000g for 10 min) to discard the cell debris and the supernatant corresponding to the cell extract was transferred to new tubes and stored at -80 °C if not analysed immediately.

Protein content of the supernatant was measured according to the method of BCA assay.

To determine **Pyruvate > Lactate conversion activity** of the cellular extracts (6-12 μ l amounts) were added to a reaction mix containing 200 mM Tris HCL pH 7.4, 1 mM pyruvate and 500 μ M NADH. The enzymatic activity was measured by recording, for a period of 20 min, the decrease of NADH fluorescence, corresponding to the NADH oxidation, coupled to pyruvate reduction to lactate.

To determine **Lactate > Pyruvate conversion activity** of the cellular extracts (2-10 μ l amounts) were added to a reaction mix containing Buffer (0.5 M glycine + 2.5 mM EDTA) pH 9.5, 1.2 mM NAD⁺, 5 mM Lactate, 216.7 mM Hydrazine (to avoid the pyruvate reconversion). Coupled NAD⁺ reduction, the enzymatic activity was measured by recording the increase of NADH fluorescence for a period of 20 min.

The assays were performed in 96-well plates by spectrophotometric determination (Glomax, Promega BioSystems Inc., Sunnyvale, CA, USA). The reactions were started by adding the cellular extract to each mixture and the optical density change at λ 340 nm was determined.

In both reactions, all the components were added in excess, so that the LDHA or LDHB enzyme activity would be the only rate-limiting step and the activity of the enzyme is therefore proportional to the initial rate of the reaction. Five independent experiments were performed per sample and enzyme, and the values normalized to μ g of protein are presented.

3.26 Proliferation and cell viability assay

Cells (5×10^4 for LS174T and 2×10^4 for B16) were seeded in 6-well plates in triplicate per cell line and condition. On days 0 (24h after seeding), 3, 4 and 5 cells were detached by trypsinization and counted with an automatic cell counter (ADAM-MC™, Digital Bio, NanoEnTek Inc., Seoul, Korea). Cell proliferation index was calculated by dividing the cell number obtained for each day by the one obtained 24 hours after seeding (day 0).

For determining cell viability, the supernatant taken 24h after adhesion was collected and cells were washed with PBS, trypsinized, centrifuged (5min, 1000 rpm), added to the supernatant taken previously and resuspended in propidium iodide solution in order to discriminate between live and dead cells. Three independent experiments were performed in duplicate.

3.27 Metabolic flux analysis

Oxygen consumption rates (OCR) and extracellular acidification rates (ECAR) of cells were analysed by Seahorse XF24 extracellular flux analyser (Seahorse Bioscience, MA, USA). Cells were seeded on Seahorse plates in order to reach confluency in 24h. One hour prior to measurement, cell media was replaced by the assay medium (D5030, without glucose, pyruvate, serum and buffer, Sigma) and the plates were incubated in a non-CO₂ incubator at 37 °C. Basal levels of OCR and ECAR were recorded for 24 min, followed by a mitochondrial stress test (1 µM oligomycin, 3 µM FCCP or 100 µM DNP, 1 µM rotenone/1 µM antimycin A). Normalization to protein content was performed after each experiment and data were presented as mpH/min/µg protein for ECAR and as pMolesO₂/min/µg protein for OCR.

3.28 Extracellular lactate measure

Cells (1×10^6) were seeded in 10cm dishes and incubated for 24h in normoxia and in hypoxia, after which 500 µl of supernatant is taken, centrifuged at 8000×g, 4 °C, for 5 minutes and lactate and glucose were analysed in the same samples with Cobass c701 instrument (Roche Diagnostics), in collaboration with the Biochemistry laboratory of the Nice University Hospital. The method used is based on enzymatic conversion of lactate into pyruvate by the lactate oxidase, coupled with the colorimetric reaction of hydrogen-peroxide formed in the first reaction with the hydrogen donor, resulting in a formation of coloured compound, the intensity of which is measured spectrophotometrically and is directly proportional to the concentration of lactate. Three independent experiments were performed in duplicate, and the results were normalized to the quantity of the protein and expressed as mM lactate/µg protein.

3.29 Clonogenic assay

Cells were plated into 60 mm² Ø dishes or 12-well plates. The day after were added the respective treatments. Cultures were maintained for additional 6-8 days. Cells were stained with 5% Giemsa solution (Sigma-Aldrich, Hannover, Germany) for colony visualization.

3.30 Statistical analyses

All analyses were performed using the software GraphPad Prism 5. Each experiment was repeated twice with at least triplicate samples per treatment group. Results are expressed as mean ± SE of replicate values. Analysis was performed by ANOVA corrected by Dunnet's test or Student's t test. All tests of statistical significance were two-sided and p values < 0.05 were considered statistically significant.

Chapter 4

RESULTS

4.1 Pharmacological approach to inhibit LDH enzyme activity

BACKGROUND

The study about the research of new inhibitors is part of a PRIN (Research Projects of National Interest) project started few years before I joined the laboratory of cell biology (DIMES Department, Bologna). It is in collaboration with researchers of the Department of Pharmacy and Biotechnology of Bologna, who have experience in computer assisted drug design and in the synthesis of small organic molecules.

To identify novel LDH inhibitors, a structure-based Virtual Screening protocol was developed. They chose the 2.3 crystal structure of human muscle form (LDH-A, PDB ID: 1I10 (Read et al. 2001)) among the LDH structures found in the RCSB Protein Data Bank (PDB), which was the only LDH-A isoform structure available at the time. The GOLD software package, implementing a genetic algorithm, was used for the VS procedure.

The second phase is the chemical synthesis of the identified compounds and the third part is the one that involves our laboratory (Department of Specialist, Diagnostic and Experimental Medicine): the biological evaluation of the inhibitor activity of the selected compounds.

Initially, we analysed the inhibitory activity on purified human LDH-A by an enzymatic assay. The enzymatic activity is measured by monitoring NADH oxidation for a period of 5 minutes at the wavelength of 340 nm (see paragraph 3.3 for procedure's details). The compounds that showed an inhibitor activity at micromolar level, were also investigated for their activity on lactic acid production and cell proliferation on cancer cell lines.

Galloflavin (GF) is the best compound found by this approach. GF was found to inhibit both the enzymatic activity of purified LDH and lactate production in cultured cells in the micromolar range, thereby proving good cell permeability. Moreover, it was shown to be not harmful for mitochondrial respiration, suggesting tolerability during normal cell metabolism (Manerba et al. 2012). Due to its poor solubility, GF did not prove to be a practical starting point for structural modifications, but it has been considered as a reference compound for potential anticancer glycolytic inhibitors and is now produced and sold by several suppliers for *in vitro* and *in vivo* studies.

Part A: Study of the role of LDH in cancer cells through the use of known inhibitors

EXPERIMENTAL PART 1A: Lactate dehydrogenase inhibitors sensitize lymphoma cells to cisplatin without enhancing the drug effects on immortalized normal lymphocytes

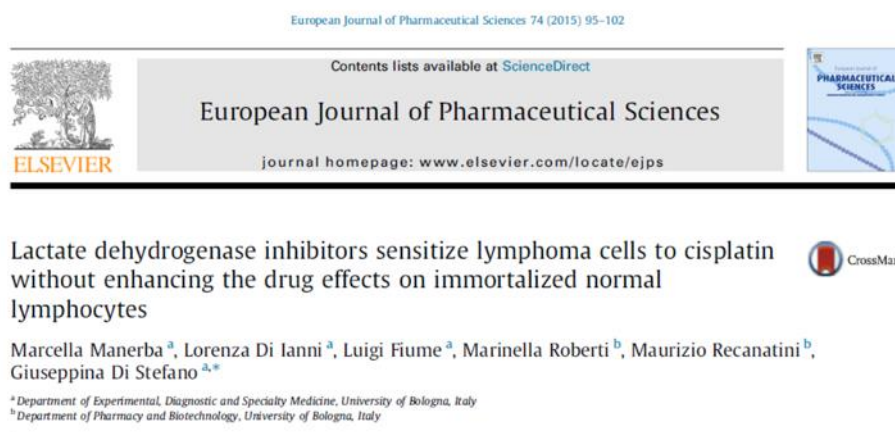


Figure 4.1. (Manerba et al. 2015)

AIM OF THE STUDY

Despite the advances achieved with the introduction of the new generation, “biological” therapeutics, chemotherapy based on DNA damaging agents still maintains a central role in non-surgical cancer treatment.

One of the major problem that limits the effectiveness of chemotherapies used to treat cancer is drug resistance. Tumours may be intrinsically resistant to chemotherapy prior to treatment, or drug resistance can also be acquired during treatment. There are many factors that can affect drug sensitivity. One of these is the *DNA damage repair* (Longley and Johnston 2005). Indeed, an elevated DNA-repair capacity in tumor cells leads to drug or radiation resistance and severely limits the efficacy of these agents. Consequently, interference with DNA repair has emerged as an important approach in combination therapy against cancer (Ding et al. 2006).

However, as DNA-repair inhibitors might also affect repair mechanisms in normal tissues, must be paid special attention to the possibility that enhanced therapeutic efficacy might be accompanied by increased off-target effects. Moreover, another high risk has to be considered: the inhibition of DNA repair with these agents of potential mutagenesis and carcinogenesis can causes the occurrence of secondary malignancies (Ding et al. 2006, Fiume et al. 2014).

Song et al. evidenced that cisplatin-resistant cells showed upregulated glucose metabolism and EGFR signalling pathway. As this, also other studies aimed at understanding the molecular features associated with drug resistance have shown that up-regulation of glycolysis can be predictive of poor chemotherapy response (Dorward and Singh 1996, Song et al. 2014). Moreover, has been already proven in several cancer cells that the inhibition of glucose metabolism can sensitize cancer cells to different commonly used chemotherapeutic agents (Ihrlund et al. 2008, Hernlund et al. 2008, Zhang and Aft 2009, Loar et al. 2010, Xie et al. 2011, Zhao, Ren and Tang 2014, Leung et al. 2014, Sullivan et al. 2014).

In this work, we studied a way to increase the efficacy of a chemotherapeutic agent in cancer cells hindering glucose metabolism without affect normal cells, through the LDH inhibition. As already discussed in previous chapters, aerobic glycolysis is a hallmark of cancer (Hanahan and Weinberg 2011) and the A isoform of LDH is constantly up-regulated in cancer cells, in addition, as LDH activity is not needed for pyruvate metabolism through the TCA cycle, inhibitors of this enzyme should spare glucose metabolism of normal non-proliferating cells (Fiume et al. 2014).

As LDH inhibitor, we used oxamate (OXA) (PAPACONSTANTINO and COLOWICK 1961) and galloflavin (GF) (Manerba et al. 2012) to verify whether hindering LDH activity can sensitize cancer cells to chemotherapeutic effects.

The genotoxic agent used in this study is cisplatin, which, although introduced in the clinics more than forty years ago, is currently administered to treat a multitude of cancers.

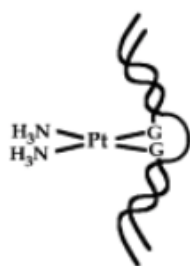


Figure 4.2.
Cisplatin bounds to
DNA.

Cisplatin, as intercalant of DNA, interacts with nucleophilic N7 sites of purine bases forming DNA intra- and inter-strand crosslinking that can cause DNA damage in cancer cells, blocking cell division and resulting in apoptotic cell death. However, its use is often limited by acquired or intrinsic resistance of the cancer cells (Kartalou and Essigmann 2001).

The ability of cells to modulate cisplatin toxicity through repair mechanisms indicated that this function might be important in the cellular processing of platinated DNA (Jamieson and Lippard 1999) and, thus, repair mechanisms can play an important role in the resistance of cancer cells to cisplatin effects.

For our experiments, we used a cell line (Loukes) derived from a Burkitt's lymphoma, which is a tumor form highly responsive to LDH inhibition (Vettraino et al. 2013), and non-neoplastic lymphoblastoid cells, immortalized by Epstein Barr virus infection (GM00130C).

RESULTS

We started characterizing the effects of the two LDH inhibitors (OXA and GF) on Loukes cells, in order to determine the doses of both inhibitors that not affect heavily cell viability and at the same time, hinder sufficiently enzymatic activity. For this purpose, we selected the doses causing 50% inhibition of LDH activity (IC_{50}), evaluated through the reduction of lactate produced after 6 hours of treatment with scalar doses of either compound.

As reported in the Table 4.1, the calculated LDH IC_{50} doses are 15 mM for OXA and 30 μ M for GF.

% Reduction caused on:	OXA 15 mM	GF 30 μ M
Lactate levels	50 ^a	50 ^a
NAD/NADH ratio	43 \pm 3	46 \pm 2
ATP	21 \pm 4	25 \pm 3
Cell viability	42 \pm 7	35 \pm 5

Table 4.1. Effects of the selected doses of inhibitors on Loukes cells. Effects on lactate and ATP levels and on NAD/NADH ratio were assayed at 6 h; cell viability was measured at 24 h.

^a Calculated from the second order linear regression of experimental data obtained by exposing Loukes cells to scalar doses of inhibitors.

Table 4.1 shows the effects caused by these doses of inhibitors on ATP production and NAD/NADH ratio, measured after 6 h of incubation and on cell viability, assayed at 24 h.

LDH IC_{50} doses were used for all the reported experiments with cisplatin association.

Therefore, we proceeded evaluating the effects of two doses (3 and 6 μ M) of cisplatin on these cells in combination experiments with OXA and GF, proving the increase of the efficacy of cisplatin in viability assays after 24 h.

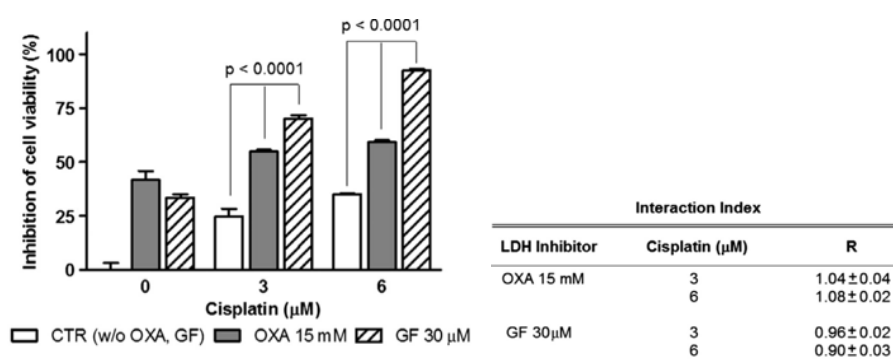


Figure 4.3. Combination experiments of LDH inhibitors (OXA and GF) with cisplatin. OXA and GF were given at their LDH IC_{50} dose (15 mM OXA and 30 μ M GF). After 24 h incubation the viability of Loukes cells was determined by Trypan blue exclusion. The Table shows the Interaction Index (R) of the two LDH inhibitors with cisplatin, calculated according to Dos Santos Ferreira et al. (2012) and using the formula reported in Section 2. “R” values are indicative of additive effects.

The statistical evaluations reported on the graph were performed by ANOVA and compared the results obtained with cisplatin with those caused by its association with either LDH inhibitor. A similar evaluation (for the sake of brevity not shown on the graph) was performed by comparing the effect of either LDH inhibitor with its combination with the two cisplatin doses and also gave indications of statistically significant differences ($p < 0.05$).

One of the most commonly followed methods for analysing the effects of the interaction between pharmacologically active compounds requires the development of the so-called isobologram, which reports the proper compounds' combinations that produce an iso-effective curve (Breitinger, 2012). The need to maintain reliable levels of LDH inhibition in cells exposed to cisplatin did not allow the application of the isobole method. For this reason, to analyse the effect of the interaction between cisplatin and LDH inhibitors we followed the method described by (Dos Santos Ferreira et al. 2012), which is based on the calculation of an Interaction Index (R), obtained through the equation reported in Materials and methods chapter. This equation was applied to the results of three independent experiments. The results are reported in the Table shown in Fig. 4.3 and clearly indicate for both OXA and GF the capacity of causing additive effects on cisplatin toxicity.

Once confirmed the increased cisplatin toxicity, we tried to understand the mechanisms involved.

As known, the major function of LDH is the regeneration of oxidized NAD^+ , required to sustain the glycolytic flux (Fiume et al. 2014). NAD^+ , working as electron acceptor for cellular dehydrogenases, is also the substrate of poly-ADP-ribose polymerases (PARPs) (Di Stefano, Manerba and Vettraiño 2013). PARPs are crucial enzymes in DNA repair and their catalytic activity is strongly induced by binding to single strand DNA breaks, one of the evidenced lesions after cisplatin treatment. Since DNA repair by PARPs requires high NAD^+ amounts, needed to build up the poly-ADP-ribose moieties (Di Stefano et al. 2013), we hypothesized that, by hindering NAD^+ regeneration, LDH inhibitors could affect the repair of cisplatin induced lesions.

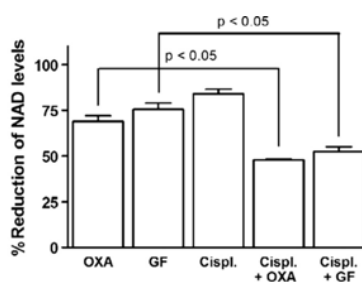


Figure 4.4. Reduction of NAD^+ levels measured in Loukes cells 16 h after incubation with 15 mM OXA and 30 μM GF (LDH IC_{50} dose), given alone or in association with 6 μM cisplatin.

Fig. 4.4 shows that NAD^+ content of the Loukes cells was reduced after 16 h exposure to the IC_{50} dose of OXA(GF), compared to control cells (NAD^+ levels =100%). A slight reduction was caused by cisplatin, which is known to activate PARP mediated response repair

(Olaussen et al. 2013). Whereas, NAD⁺ levels appeared more severely affected in cultures treated with the association of the LDH inhibitor and cisplatin.

Measuring the poly-ADP-ribosylation of the cellular proteins by Western Blot (Fig. 4.4), we found markedly increased signals of poly-ADP-ribosylation in cells treated with the association of cisplatin and OXA(GF).

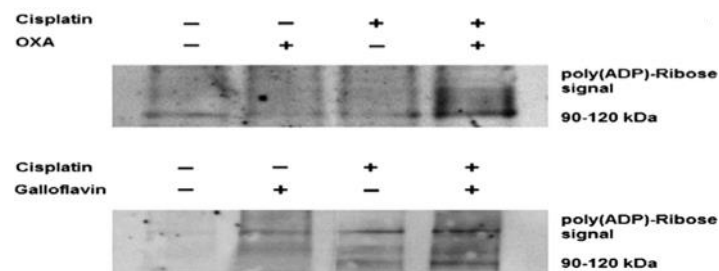


Figure 4.5. Poly-ADP-ribosylation level of cellular proteins measured in Loukes cells 16 h after incubation with 15 mM OXA or 30 μ M GF, given alone or in association with 6 μ M cisplatin.

This result suggested that, differently from our initial hypothesis, the increased anti-neoplastic effect caused by the compounds' association might not be due to a compromised repair, but to an increased DNA damage.

Consequently, we measured in treated cells the levels of phosphorylated histone H2AX and of Rad51. Serine 139 phosphorylation of H2AX is one of the earliest markers of DNA damage (single and double strand breaks) (Sharma, Singh and Almasan 2012). Phospho-H2AX was found to increase linearly with the severity of the damage and to mediate the formation of clusters of proteins involved in DNA repair. The recombinase Rad51 is one the recruited proteins in the Homology Recombination (HR) process and its increased expression indicate the induction of the DNA damage response (Klein 2008). To obtain better evidence of the effects caused by LDH inhibition on the cisplatin induced damage, the following experiment was performed in two steps: A) Loukes cells were exposed to cisplatin (1 h); B) after a 24 h delay, treated and control (untreated) cultures received a further 16h treatment with OXA(GF).

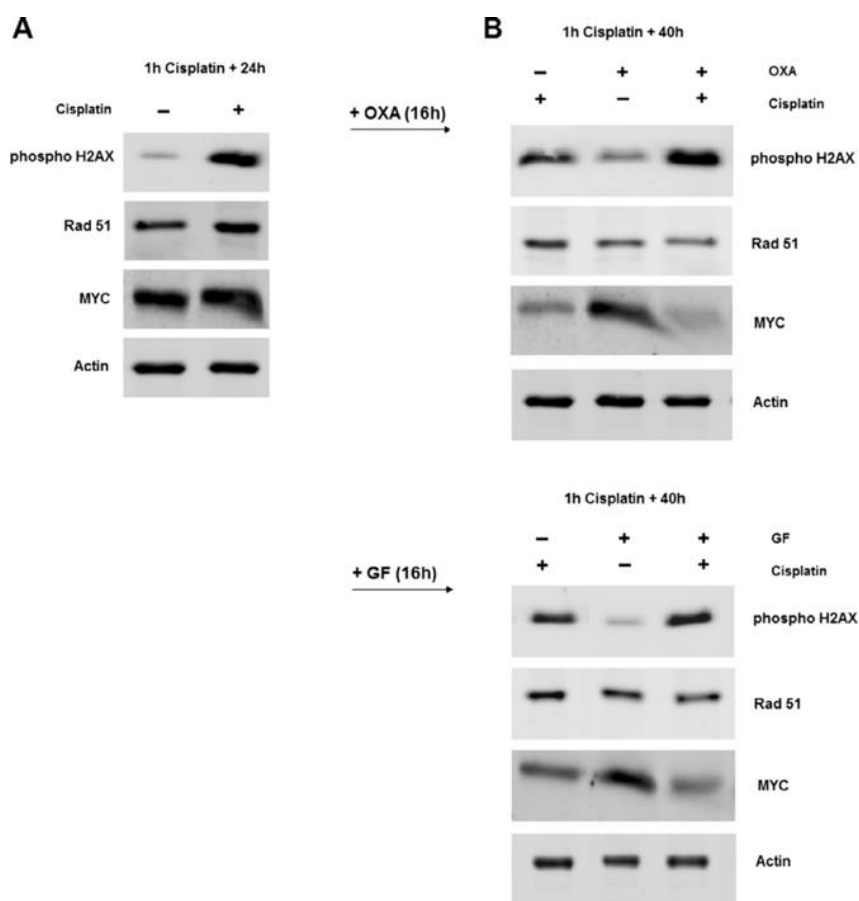


Figure 4.6. Association of LDH inhibitors (OXA and GF) with cisplatin increases DNA damage. (A) Loukes cells were exposed for 1 h to 6 μ M cisplatin. After 24 h increased levels of phospho-H2AX and Rad51 indicated the induction of a DNA damage response. (B) Loukes cells were subsequently exposed for 16 h to OXA (15 mM) or GF (30 μ M). A further increase of phospho-H2AX level was evidenced. The simultaneous heavy reduction of MYC concentration suggests a compromised cell survival.

The western blot images in Fig. 4.5 showed that treating 1 h with 6 μ M cisplatin was sufficient to induce in Loukes cells a DNA damage response, as evidenced by increased phospho-H2AX and Rad51 levels (Fig. 4.5A). After the second step (Fig. 4.5B), in cisplatin treated cells phospho-H2AX signal is slightly reduced. Cells treated with the LDH inhibitor alone show signs of DNA damage, whereas cells receiving the association cisplatin/OXA(GF) showed a markedly enhanced phospho-H2AX level which, however, was not joined with a concurrent increase in Rad51 protein. On the contrary, these cultures showed evidences of Rad51 signal reduction, suggesting that the severity of DNA damage might have caused the failing of the response repair. This is in agreement with the increased antineoplastic effect produced by the compounds' association (Fig. 4.2). A further confirmation came from the heavily reduced levels of MYC protein observed in these cells (Fig. 4.5B), which is expected to deprive Loukes cultures of survival-needed signalling (Brady, Macarthur and Farrell 2008, Zhao et al. 2013b). The above described effects were observed by using both LDH inhibitors, although they seemed best evidenced in OXA treated cells.

The slightly increased H2AX phosphorylation observed in cells treated only with OXA(GF) indicated that signs of DNA damage can also be observed after LDH inhibition. In cells consuming high glucose amounts, such as cancer cells, high amounts of pyruvate can be produced, which can lead to saturation of the mitochondrial electron transport chain and ROS generation (Lu, Tan and Cai 2015), especially in cells with a less efficient respiratory function. ROS generation after LDH inhibition was already evidenced in some cultured cancer cells (Le et al. 2010, Farabegoli et al. 2012).

As consequence of these evidences, in the following experiment we measured by cytometry the levels of ROS produced in Loukes cells exposed for 6 h to the LDH IC₅₀ dose of each inhibitor.

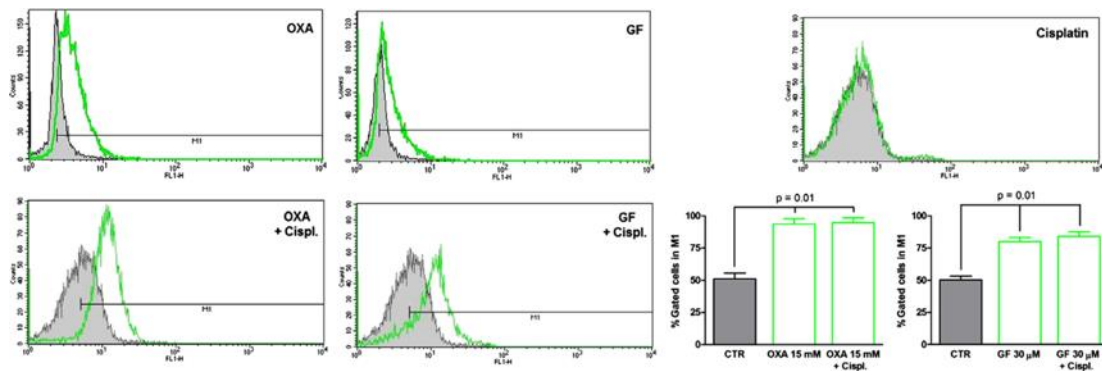


Figure 4.7. ROS levels measured by DCF in Loukes cells after 6 h exposure to 15 mM OXA, 30 μ M GF and 6 μ M cisplatin, given alone or in association. The bar graphs indicate the percentage of gated cells showing a fluorescence signal higher than the median value measured in untreated cells.

Treating cells with OXA, it induces an increase of ROS generation by 40%, compared to control (untreated cultures); GF was found to cause a less marked increase: 30%, compared to control cells. The lower level of ROS in cells treated with GF can be explained considering that the polyphenolic structure of GF molecule can contribute to a partial scavenging of ROS (Di Meo et al. 2013); this could also justify the less marked effects caused by the combination cisplatin/GF on the DNA damage markers shown in Fig. 4.5B.

Moreover, in Fig. 4.6 is also showed that, in agreement with published data (Marullo et al. 2013), ROS generation is not evidenced within the first 6 h of cisplatin exposure, and that the ROS levels measured at this time in Loukes cells treated with the association of cisplatin and OXA/GF can be ascribed to LDH inhibition.

DNA damage is considered an inevitable consequence of ROS derived metabolism (Cooke et al. 2003). The occurrence of oxidative DNA lesions, added to those caused by cisplatin, can

give an explanation of the increased antineoplastic effect observed in the cells treated with the association cisplatin/OXA(GF).

In the western blot experiments of Fig. 4.5, we have seen also heavily reduced levels of MYC protein in cells treated with the association cisplatin/OXA(GF). In MYC over-expressing BL cells, LDH silencing was found to reduce cloning efficiency (Shim et al. 1997) and suppression of MYC activity was related with reduced cell survival (Zhao et al. 2013b). On the basis of these findings, we evaluated the clonogenic growth of Loukes cells, treated with cisplatin given alone or in combination with OXA/GF.

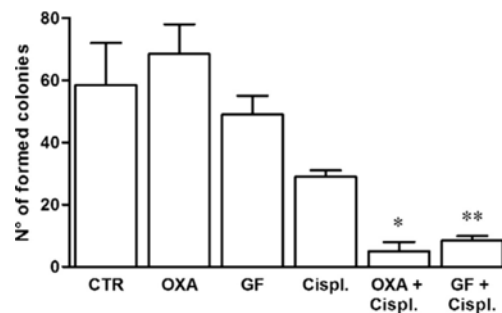


Figure 4.8. Colony formation assay performed on Loukes cells. Cispl., cisplatin. * Statistically significant difference ($p < 0.05$) from cultures treated with OXA and with cisplatin. ** Statistically significant difference ($p < 0.05$) from cultures treated with GF and with cisplatin.

The results of this assay, reported in the histogram in Fig. 4.7, were in agreement with the effects observed on cell viability. A 6 h exposure to LDH inhibitors did not significantly affect the clonogenic survival of Loukes cells. However, combining the LDH inhibitors treatment with 1 h exposure to cisplatin, cell clonogenicity was severely impaired.

As non-neoplastic, control cells for our experiments, we chose the GM00130C lymphoblastoid line. GM00130C cells have been obtained by immortalizing B lymphocytes by Epstein Barr virus infection. They are actively dividing cells, but do not proliferate indefinitely. Therefore, Loukes and GM00130C derive from the same cell type and their substantial difference lies in the neoplastic nature of the Loukes cells. Compared to Loukes cells, GM00130C have reduced levels of LDH and produce lower amounts of lactate (Vettraino et al. 2013). GM00130C cells were treated with the same doses of cisplatin and LDH inhibitors already used on Loukes cells, replicating the experiments reported on Fig. 4.2.

% Inhibition caused on:	OXA 15 mM	GF 30 μ M
Lactate levels	11.6 \pm 0.3	10.4 \pm 1.6
ATP	13.3 \pm 2.1	10.5 \pm 0.8
Cell Viability	15.6 \pm 2.2	14.3 \pm 3.6

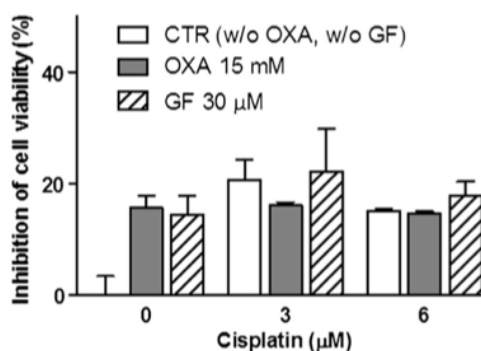


Figure 4.9. The table shows the effects caused by LDH inhibitors (6 h incubation) on lactate and ATP production. The bar graph shows the effects caused on cell viability by cisplatin given alone or in combination with OXA (15 mM) or GF (30 μ M).

The results obtained on GM00130C cells are reported on Fig. 4.8. In agreement with previous results, GM00130C were found less responsive to LDH inhibitors, when cisplatin was given in combination with either OXA or GF, no statistically significant difference was observed in comparison with cells treated with cisplatin alone.

Also in cytometry experiments, treating GM00130C cells with either LDH inhibitor, no significant production of ROS was detected.

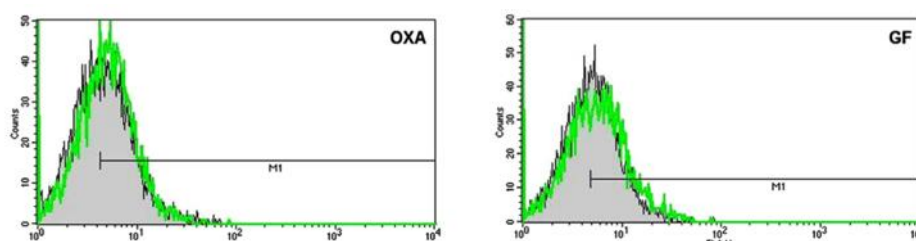


Figure 4.10. ROS detection after 6 h exposure to 15 mM OXA and 30 μ M GF.

According to this result, the postulated mechanism underlying the increase of cisplatin toxicity observed in Loukes cells did not seem to take place in normal lymphoblasts, thus explaining the unchanged cisplatin toxicity.

DISCUSSION

Cisplatin is one of the most potent anticancer agents and has been used in chemotherapy for more than 40 years. However, its use is often limited by acquired or intrinsic resistance of the cancer cells (Kartalou and Essigmann 2001).

The molecular mechanisms that underlie cisplatin resistance are poorly understood; however, the finding of an up-regulated glucose metabolism in resistant cells suggested the attempt of

increasing cisplatin efficacy by glycolysis inhibition (Dorward and Singh 1996, Song et al. 2014).

Increased glucose uptake and metabolism is a widely accepted hallmark of neoplastic change (Gillies et al. 2008). In this context, LDH-A is the most promising target to develop glycolysis inhibitors with selective activity on cancer cells. Since, this enzyme is not active in normal cells with sufficient oxygen levels, the inhibition of LDH-A is considered as a possible way to hinder cancer cell metabolism and growth without causing damage to normal tissues (see Chapter1).

In this work, we verified this hypothesis in a Burkitt's lymphoma cell line (Loukes cells) treated with the association of cisplatin with OXA or GF, and compared the results obtained in these neoplastic cells with those produced by the same treatment in non-neoplastic lymphoblastoid cells, GM00130C.

Only in lymphoma cells we found a sensitizing effect on cisplatin activity. Since proliferating lymphocytes are one of the most susceptible cell populations to the toxic effects of cisplatin-like chemotherapeutics, this result is a further confirm of the tolerability of LDH inhibition for normal cells.

LDH inhibition could be expected to increase the efficacy of genotoxic agents by different mechanisms. LDH-A converts pyruvate into lactate regenerating NAD^+ , an essential cofactor that is required for a wide range of cellular reactions including ATP production. Therefore, LDH inhibition by reducing ATP supply and NAD^+ regeneration, it could primarily be responsible of an inadequate response to DNA damage. In fact, ATP is required for the chromatin remodelling necessary to the recruitment of proteins involved in DNA repair (Swygert and Peterson 2014), and NAD^+ is the substrate of PARP enzymes (Di Stefano et al., 2013), which restore DNA structure. Contrary to our hypothesis, in cell cultures treated with the association of cisplatin with LDH inhibitors we obtained evidence of increased levels of PARP enzyme and also of DNA damage, which was presumably ROS mediated. ROS generation after LDH inhibition was already evidenced in some cultured cancer cells (Le et al. 2010, Farabegoli et al. 2012) and it was already found to lower the apoptotic threshold for cytotoxicity and, through this mechanism, to increase the efficacy of cytostatic treatments (Trachootham, Alexandre and Huang 2009).

In cells under cisplatin treatment, which also activates the PARP mediated repair response (Olaussen et al. 2013), ROS produced by LDH inhibition could be expected to cause relevant effects, since poly-ADP-ribosylation of histones opens chromatin structure, rendering it more accessible to other potentially harmful factors.

Our data show that LDH inhibition led to ROS generation only in neoplastic cells, which differ from their normal counterpart in both high glucose uptake and less efficient mitochondrial function (Gillies et al. 2008). They are also in agreement with data obtained by using dichloroacetate, a non-toxic compound hindering pyruvate dehydrogenase kinase (Xie et al. 2011). Dichloroacetate causes a metabolic shift from aerobic glycolysis to glucose oxidation and was similarly found to cause ROS generation in neoplastic cells and to increase cisplatin efficacy.

Unfortunately, in spite of extensive studies also involving multinational drug companies (Ward et al. 2012, Billiard et al. 2013, Fauber et al. 2014, Xie et al. 2014) the development of LDH inhibitors suitable for clinical use is proving a very difficult task. The results obtained by combining OXA/GF with cisplatin, which is administered intravenously at weeks intervals, could also have the advantage of facilitating the access to clinical trials of new molecules effective on LDH inhibition but showing low oral availability, which is a major reason for drug candidates failing to reach the market.

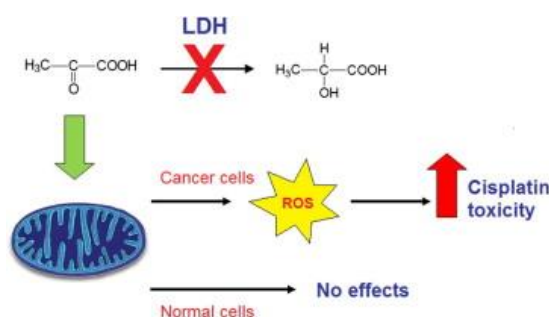


Figure 4.11. Summary scheme: LDH inhibition as a way to sensitize cancer cells to cisplatin without enhancing the drug effects on normal cells.

EXPERIMENTAL PART 2A: Lactate dehydrogenase inhibitors can reverse inflammation induced changes in colon cancer cells



Figure 4.12. (Manerba et al. 2017a)

AIM OF THE STUDY

The connection between inflammation and tumorigenesis is well-established and in the last decade has received a great deal of supporting evidence from genetic, pharmacological, and epidemiological data. Inflammation was found to impact on several steps of tumorigenesis including initiation, promotion, malignant conversion, invasion, and metastasis (Grivennikov, Greten and Karin 2010).

Colon cancer, which is one of the major worldwide health concern, can be considered a model disease to examine the links between chronic inflammation and neoplasia. It often arises in areas of inflamed mucosa and even when it can be mainly imputed to the influence of life-style factors, it is commonly characterized by active inflammation and immune cell infiltration (Terzić et al. 2010).

Because of infiltrating immune-inflammatory cells capacity to activate extracellular matrix breakdown and tissue remodelling, instead of help tumor clearance, they paradoxically facilitate tumor progression (Grivennikov et al. 2010). The most frequent tumor infiltrating immune cells are macrophages and T lymphocytes. About the latter, a critical role seems to be played by the Th17 cell subset, which was found to be associated with poor prognosis of colorectal cancer patients (De Simone et al. 2013). The tumor-promoting effect of both macrophages and Th17 cells are mediated by NF- κ B induced cytokine production (Grivennikov et al. 2010), mainly TNF- α and IL-17.

TNF- α is one of the most important inflammatory factors in the pathogenesis of inflammatory bowel disease and in colitis-associated cancer (Terzić et al. 2010). IL-17 is frequently present

in acute and chronic inflammation and was found to be relevantly linked to colon cancer (De Simone et al. 2013).

Tumor associated inflammatory states were also found to be characterized by a feed-forward loop: cytokines released by macrophages and lymphocytes activate NF- κ B in cancer cells, leading to chemokine production and recruitment of additional inflammatory cells (Grivennikov et al. 2010). In cancer cells, NF- κ B signalling cascade also activates the program of epithelial-mesenchymal transition (EMT) and facilitates tumor invasion and metastasis by up-regulation of Snail and repression of E-cadherin synthesis (Min et al. 2008). As well known, NF- κ B is also a key regulator of energy homeostasis; it increases glucose metabolism and induces aerobic glycolysis (Moretti et al. 2012, Ben-Neriah and Karin 2011). As already discussed in previous chapters, aerobic glycolysis is a hallmark of cancer (Hanahan and Weinberg 2011). Several reports evidenced increased glycolysis and lactate production in cancer cells exposed to inflammatory cytokines (Kumar et al. 2014, Straus 2013, Vaughan et al. 2013), and the inhibition of inflammatory cascade was found to reduce the Warburg effect (Leidgens et al. 2015, Vaughan et al. 2013). However, to our knowledge these studies did not consider the role played by lactate dehydrogenase (LDH) in inflammation-induced metabolic changes. LDH is a key enzyme in glucose metabolism and is the master regulator of the Warburg effect (Fiume et al. 2014). Probably, in these previous studies the involvement of LDH in inflammation-induced metabolic changes could be disguised since none of the Authors considered the differences between the two enzymatic isoforms, LDH-A and LDH-B. These two enzyme isoforms, with different kinetic properties, catalyse the same reaction, the conversion of pyruvate to lactate at the end of glycolysis. LDH-A is constantly up-regulated in cancer cells, while the role of LDH-B is still controversial (Fiume et al. 2014).

In this work, we adopted CaCo-2 cell line as model. This well-studied colon carcinoma is able to reversibly express differentiation markers (morphological and functional characteristics of the mature enterocyte) according to the time-course of culture (Sambuy et al. 2005). We treated the cultured colon cancer cells with TNF- α and IL-17 and studied the effect of these inflammatory signals on LDH-A and -B gene transcription, on LDH enzymatic activity and on the develop of the features of EMT. Furthermore, on the basis of the above described connections between inflammation, tumor progression and cell metabolism, we study the effects of LDH inhibitors on the cell alterations induced by TNF- α and IL-17. Since inhibition of LDH-A is considered as a possible way to hinder cancer cell metabolism and growth

without causing damage to normal tissues, being LDH not active in normal cells under sufficient oxygen supply (Fiume et al. 2014).

RESULTS

To evaluate the effect of the inflammatory cytokines on Lactate Dehydrogenase, we started to evaluate the LDHA and LDHB mRNAs in actively growing CaCo2 cells treated for 4-72 h with the two cytokines, TNF- α and IL-17.

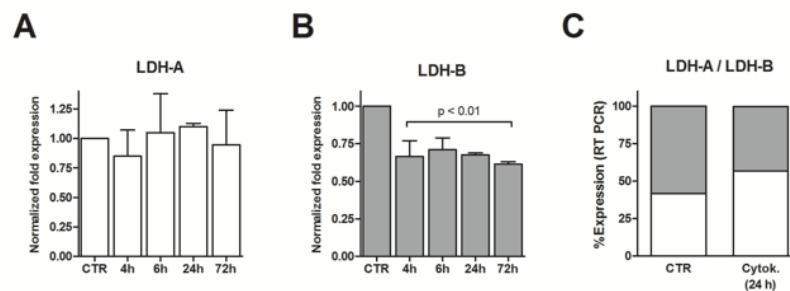


Figure 4.13. Real Time PCR evaluating mRNA expression of LDH-A (A), LDH-B (B) at different times after exposure to TNF- α and IL-17. (C) The relative ratio between LDH-A and -B mRNAs after 24 h of treatment with the two cytokines.

The results show that there are no significant changes for LDH-A mRNA (Fig. 4.13A), whereas a constant reduction of 30% was measured for LDH-B mRNA from 4 h (Fig. 4.13B). These data indicate that cytokines treatment induces the switch of the predominant LDH isoform from LDH-B to -A, as summed up in Fig. 4.13C showing the relative ratio between LDH-A and -B mRNAs after 24 h of cytokines treatment.

In fact, using an anti-inflammatory drug (dexamethasone), it increases both LDH isoforms in CaCo2 cells and, in combination with the two cytokines, it restores LDH-B as the prevalent enzyme isoform, abolishing the cytokines induced effect.

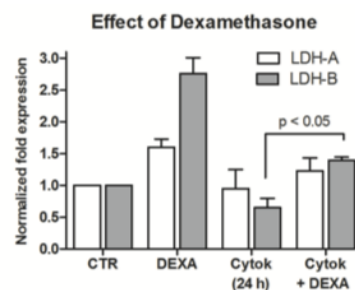


Figure 4.14. Dexamethasone restores LDH-B as the prevalent mRNA in cytokines treated cells (24 h). A statistically significant difference in LDH-B expression was observed between cells exposed to DEXA + cytokines and those treated with cytokines alone. Data were analyzed by ANOVA followed by Dunnet's post-test.

Below, in Table 4.2 is shown that treatment of 24 h with TNF- α and IL-17 caused a moderate (about 30%), but statistically significant increase of total LDH activity in cell cytoplasm, as already observed by PCR. In spite of the observed reduction of LDH-B mRNA, the enhanced enzymatic activity measured in the treated cells could be explained by the kinetic properties of the A isoform, which has a higher Vmax compared to LDH-B. A further explanation could also be hypothesized from the data reported in Fig. 4.15.

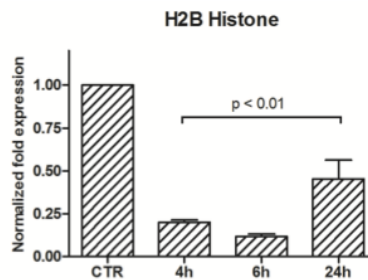


Figure 4.15. Real Time PCR evaluating mRNA expression of H2B histone at different times after exposure to TNF- α and IL-17. Data were analysed by ANOVA followed by Dunnet's post-test.

Besides participating in glycolysis, LDH-A is a nuclear protein and was found to be necessary for H2B histone gene transcription (Dai et al. 2008). Treatment with TNF- α and IL-17 markedly reduced the expression of H2B histone, suggesting that inflammation can preferentially direct LDH-A function to cell cytoplasm.

Keeping on to characterize the effects of inflammatory cytokines in CaCo2 cells, we evaluated LDH-A/LDH-B % composition, glucose uptake, lactate production and alkaline phosphatase (ALP) activity.

Table 4.2. Effects of inflammatory cytokines on CaCo-2 cells.

	Control CaCo-2 cells	Treated CaCo-2 cells
LDH activity (mU/mg cell proteins)	699 \pm 30	890 \pm 60*
% LDH composition (LDH-A/LDH-B) (assayed by enzyme activity)	42 \pm 12/58 \pm 12	57 \pm 20/43 \pm 20
Glucose uptake (relative to controls)	1.00	1.25 \pm 0.05*
Lactate production (μ g/10 ⁶ cells/1 h)	15.7 \pm 1.1	24.8 \pm 2.0*
ALP activity (nmoles p-NP/min/mg cell proteins)	8.3 \pm 0.9	Undetectable

* p < 0.05, as evaluated by Student's t-test.

Since we found that the commonly available anti-LDH antibodies show cross-reactivity for LDH-A and -B, as observed also by other authors (Allison et al. 2014), evaluation by

immunoblotting was considered inaccurate. To assess LDH protein level in the treated cells, we used the enzymatic assay procedure described by Goldman et al., which allows to discriminate between the two enzyme forms (GOLDMAN et al. 1964) (Table 4.2). In addition, indicative evaluation of LDH-A level was also performed by immunoblot (Fig. 4.17) and the densitometric analysis of the protein band is in line with the results obtained in the enzymatic assay.

Our experiments confirmed also that inflammatory cytokines enhance glucose uptake in the treated cells, as reported in literature (Kumar et al. 2014, Straus 2013, Vaughan et al. 2013) and, in line with the increase of LDH-A activity, higher production of lactate was measured in CaCo2 cells treated 24 hours with the two cytokines (Table 4.2).

Then, we analysed also the signs of differentiation by ALP activity. ALP is a protein located in the apical membrane of enterocytes, involved in the maintenance of gut homeostasis; it is one of the markers of mature intestinal cells (Ferruzza et al. 2012). In treated CaCo-2 cultures, the ALP activity dropped to undetectable levels, indicating signs of de-differentiation after 24 h exposure to inflammatory cytokines (Table 4.2).

Baumann et al. 2009, observed that increased lactate production by LDH-A can play an active role in tumor progression and was found to increase cancer cell migration (Baumann et al. 2009). Thus, we proceeded evaluating the expression of proteins indicative of increased proliferative or metastatic potential and known markers of EMT, in CaCo-2 cells treated with TNF- α and IL-17. As a first step, we measured the levels of c-Myc and HIF-1 α proteins after 4 h exposure to the inflammatory cytokines. c-Myc was previously found to be markedly induced by TNF- α (Liu et al. 2015); HIF-1 α plays a major role in inflammation and is critical for the maintenance of cancer stem cells (Peng and Liu 2015).

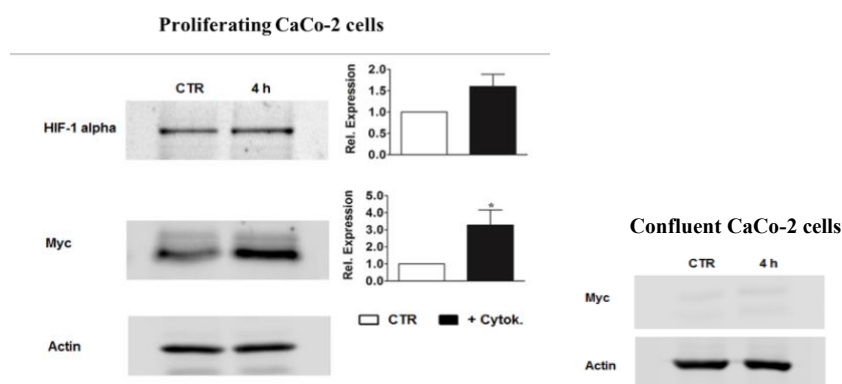


Figure 4.16. Evaluation of the effects of 4 hours cytokines treatment in in both confluent and actively growing (50,000 cells/cm²) cells. Proliferating cells: the treatment causes a statistically significant increase of c-Myc protein. Confluent cultures: no effect was observed; as an example, the immunoblotting evaluation of c-Myc expression after a 4 h treatment is reported. Asterisk indicates a statistically significant difference with untreated cultures, with $p < 0.05$.

In proliferating cells, the 4 h treatment markedly increased the level of c-Myc protein; a 1.6-fold increase in HIF-1 α level was also detected, which, however, did not result statistically significant.

c-Myc levels were measured also in confluent cells (Fig. 4.16). Confluent and proliferating CaCo-2 cultures showed a different response to inflammatory cytokines: in confluent cells, c-Myc is not expressed and was not induced by TNF- α and IL-17 treatment (Fig. 4.16).

This finding suggested that the effects of inflammatory cytokines are dependent on the proliferative status of CaCo-2 cells.

In proliferating cells, the expression of proteins indicative of increased proliferative or metastatic potential and known markers of EMT were evaluated after 24 h cytokines treatment:

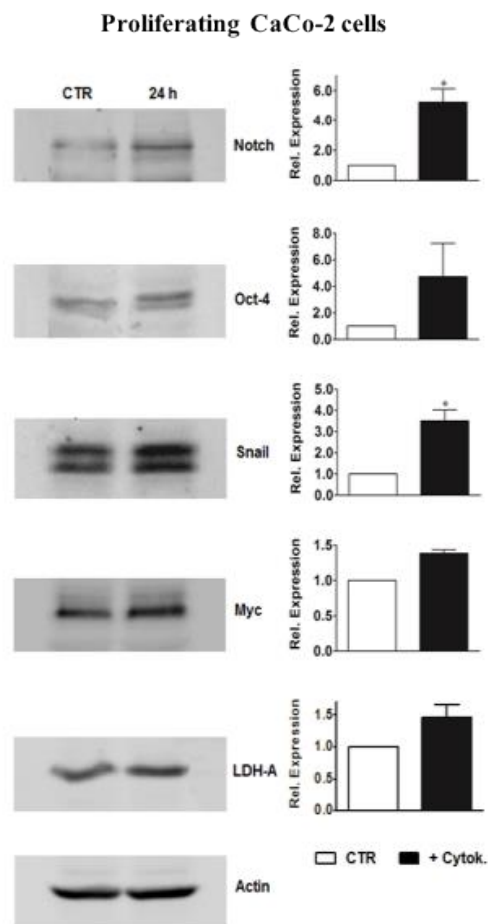


Figure 4.17. Evaluation of the effects of 24 hours cytokines treatment in proliferating (50,000 cells/cm²) cells on the expression of proteins indicative of increased proliferative or metastatic potential and known markers of EMT. Notch and Snail levels appeared significantly raised by TNF- α and IL-17 treatment; the change measured in Oct-4 protein (a mean 4.5-fold increase) was scarcely reproducible in the replicated experiments and did not result statistically significant. Asterisk indicates a statistically significant difference with untreated cultures, with $p < 0.05$.

The effect of TNF- α and IL-17 on c-Myc protein levels appeared in gradual depletion after 24 h, while upregulation of Notch (cleaved form), Oct-4 and Snail was detected.

Notch is a known regulator of cell fate, controlling proliferation and apoptosis; it has recently been implicated in the induction of the glycolytic switch associated with tumor progression (Basak, Roy and Banerjee 2014). Oct-4 protein enhances cell self-renewal ability and inhibit the genes that start differentiation; it was found to be dependent on LDH-A expression (Zhang et al. 2012) and to predict disease recurrence in patients with rectal cancer (Saigusa et al. 2009). Snail is well-known to induce the phenotypic changes associated with EMT (Barrallo-Gimeno and Nieto 2005, Min et al. 2008).

These results prove that inflammation induces EMT signatures in proliferating cells, confirming the notion of the tumor promoting effects exerted by inflammatory cytokines. The development of these effects was previously shown to be controlled by commonly used anti-inflammatory agents (Usman et al. 2015).

Since, as already discussed above, inflammation was found as a direct inducer of aerobic glycolysis (Moretti et al. 2012, Ben-Neriah and Karin 2011), we investigated whether the tumor promoting effects caused by inflammation could also be controlled by a metabolic reprogramming of cancer cells, mediated by LDH inhibition. As LDH inhibitors we used OXA and GF (details in the chapter 1). First of all, we determined the doses of OXA or GF that significantly affect LDH activity, without causing heavy cell death on CaCo-2 cell cultures.

	OXA (40 mM)	GF (200 μ M)
Lactate production (% reduction at 6h)	43 \pm 5 *	48 \pm 7 *
Cell growth (% reduction at 24h)	32 \pm 6 *	46 \pm 5 *

*p <0.05, as evaluated by student's *t*-test.

Table 4.3. Effects of the used LDH inhibitors on CaCo-2 cells. Inhibition of LDH was assessed by measuring the level of lactate in cell cytoplasm and culture medium.

Thus, we tested the effect caused by these OXA and GF doses on the levels of proteins previously found to be significantly modified by TNF- α and IL- 17 treatment. We also evaluated the levels of E-cadherin. Reduction of E-cadherin expression is the major phenotypic change associated with EMT (Farahani et al. 2014). E-cadherin is down-regulated by the transcription factor Snail, moreover, its reduction is very frequently observed during the progression of malignant epithelial tumors, and it is responsible for the loss of

intercellular adhesion during invasion (Perl et al. 1998).

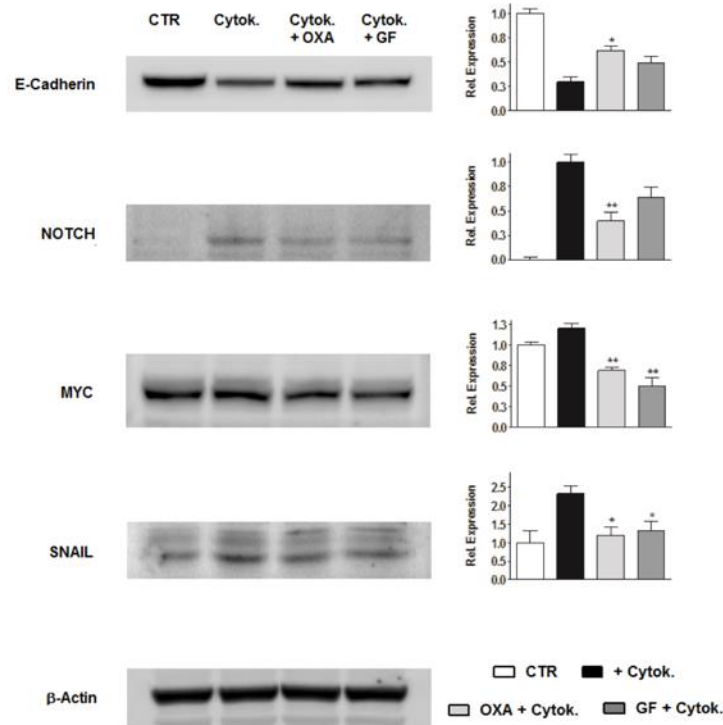


Figure 4.18. LDH inhibitors reverse the inflammation-induced effects. OXA (40 mM) and GF (200 μM) were added to the CaCo-2 culture medium during the 24 h treatment with TNF-α and IL-17. Asterisks indicate a statistically significant difference of protein expression in comparison with cytokines treated cells. *, p <0.05; **, p <0.01.

Snail levels appeared reduced to the levels measured in untreated cells, while c-Myc expression was significantly downregulated, compared to control cultures. This last finding can be explained considering the effect caused by OXA and GF on cell viability (see Table 4.3).

These results show that LDH inhibitors, added to the culture medium of cytokines exposed cells, were found to significantly mitigate all the inflammation induced phenotypic changes; the major effects were observed with OXA, the specific enzyme inhibitor.

The EMT signatures also become evident at the morphological level when the treatment was extended to 72 h.

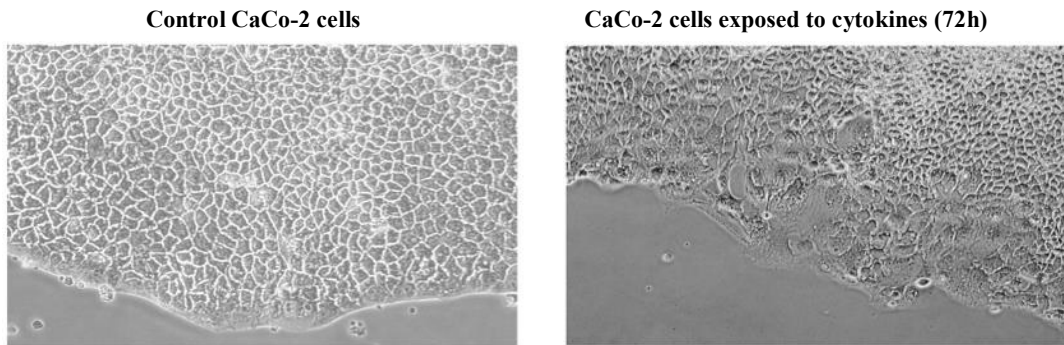


Figure 4.19. Untreated and cytokines-exposed CaCo-2 cells were maintained in culture for 72 h and then photographed under a reverse microscope at a global magnification of 200 \times . The pictures evidence the differences in cell shape and growth pattern.

Morphology of the growth pattern of untreated CaCo-2 cells shows that they are characterized by a regular, polygonal shape and show a growth front with a well-defined rim. On the contrary, TNF- α and IL-17 exposed cells appear irregularly shaped, especially in proximity of the growth front, and form tissue islets with undefined margins. This growth pattern is indicative of increased invasive properties.

The effects caused by both OXA and GF on cell viability did not allow the evaluation of the treated cells at 72 h. However, a further proof of the potential of LDH inhibitors in controlling cell invasive behaviour was obtained by gelatin zymography, which allows a semi-quantitative measure of the matrix metalloproteinases-2 and -9 (MMP-2 and MMP-9) (Heussen and Dowdle 1980) after 24 h treatment.

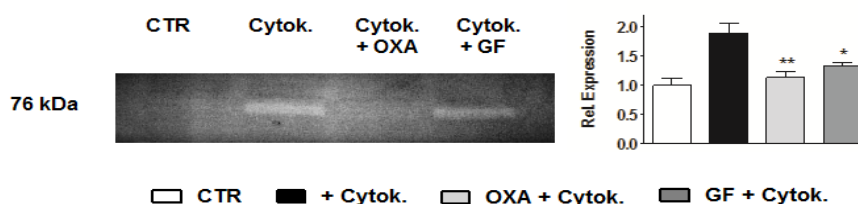


Figure 4.20. Zymography evaluation of MMP secretion in culture medium after a 24 h treatment in the presence of cytokines and LDH inhibitors. In cells exposed to cytokines, a single band of degraded gelatine with a molecular weight of 76 kDa was observed, which appeared reduced by LDH inhibitors. Asterisks indicate a statistically significant difference in comparison with cytokines treated cells. *, $p < 0.05$; **, $p < 0.01$.

In TNF- α and IL-17 treated cells, zymography showed a major band of degraded gelatin with a molecular weight of about 76 kDa, compatible with activated MMP-2. LDH inhibitors were found to significantly reduce gelatin degradation; similar to previous experiments, the best evidenced results were observed with OXA.

DISCUSSION

To sum up, the relationship between cancer and inflammation has long been investigated, most of all with regard to colorectal tumors, representing the highest risk of neoplastic disease in the general population (Kraus and Arber 2009). Among the extracellular signals, diffuse in tissue microenvironment, which orchestrate inflammation-driven effects, cytokines have the widest distribution and can mediate effects on both immune and tissue-resident epithelial cells. In our study, we used the cytokines found to be relevantly linked to colon cancer (IL-17 and TNF- α). Their intracellular signalling is activated by the transcription factor NF- κ B. NF- κ B provides a mechanistic link between inflammation and neoplastic change by increasing the expression of apoptotic inhibitors and of genes promoting cell growth, and can be considered the most important component of the tumor-promoting machinery activated by inflammation. The inflammatory microenvironment was also found to have a direct effect on cancer cell metabolism. As reported, the cytokine TNF- α positively regulates some genes of the glycolytic pathway by increasing the transcription of HIF-1 α and Myc (Straus 2013); and IL-17 was found to co-operate with TNF- α by stabilizing the mRNA of the induced genes (Lee et al. 2008). Moreover, the inflammatory microenvironment also affects the capacity of local invasion, the most critical feature of cancer lesions (Dworak, 1986).

Lactate is the end-product of LDH reaction. Lactate response elements were identified in genes involved in tissue remodelling (Formby and Stern 2003) and this metabolite was found to directly stimulate VEGF production by endothelial cells (Beckert et al. 2006), leading to neo-angiogenesis.

In neoplastic tissues, enhanced lactate levels are basically linked to the increased LDH-A expression. Lactate was found to increase cancer cell migration by promoting TGF- β mediated regulation of matrix metallo-proteinase-2 (MMP-2) (Baumann et al. 2009).

In our experiments, we evidenced features of EMT in CaCo-2 cells treated with the two cytokines, and the mitigation of these effects by treating with OXA and GF, two inhibitors of LDH activity, as summarized in Fig. 4.21.

On the basis of these results, we can assume LDH-A as common elements coordinating neoplastic proliferation, invasive growth and inflammation; highlighting the involvement of LDH protein in crucial signalling pathways for cancer cell survival and spread, and suggest for LDH inhibitors wider potential in anticancer treatment.

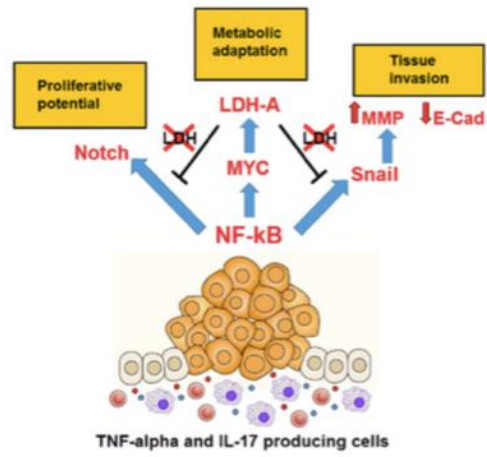


Figure 4.21. Proteins induced in colon cancer cells by TNF- α and IL-17 and their role in tumor progression.

EXPERIMENTAL PART 3A: LDH inhibition impacts on heat shock response and induces senescence of hepatocellular carcinoma cells



Figure 4.22. (Manerba et al. 2017b)

AIM OF THE STUDY

Heat shock proteins (HSPs), also called stress proteins, have an essential role in the synthesis, transport and folding of proteins under stressful conditions (Morimoto 1993).

The first report about the synthesis of a few proteins immediately after a source of stress in cells has been reported for drosophila cells in 1974. Surprisingly, the HSPs result highly conserved among different organisms. For many years, a lot of literature has been accumulated on a variety of events in a cell's response to a heat shock. Whereas, in the last years this field has focused on the function of HSPs and their role as “molecular chaperones” (Schlesinger 1990).

In normal cells, after stress signals the HSPs are up-regulated to restore the protein homeostasis and to allow the cells to survive by refolding the proteins or mediating their disintegration. Many of these "stress proteins" are common to a variety of stresses while others are uniquely induced by a specific stress. Some are localized to specific organelles and many family members have counterparts, referred to as heat shock cognates (HSCs) that are expressed under normal, non-stress conditions.

Mammalian HSPs have been classified mainly in four families according to their molecular weight: HSP90, HSP70, HSP60 and small HSPs (15–30 kDa) that include HSP27 (Jego et al. 2013).

In physiological conditions, the heat shock proteins are less than 2% but they reach the 20% in pathological conditions.

Moreover, abnormal Heat Shock Response (HSR) seems to play a critical role in neoplastic change and tumor development, since it protects from degradation proteins that are essential for tumorigenesis and cell proliferation (Calderwood et al. 2006). In many tumoral forms, the

constitutively activation of the HSR have an important clinical significance. For this reason, study of synthetic inhibitors targeting the major members of HSP family (hsp27, hsp72, hsp90) have recently emerged.

The two high molecular weight chaperones require ATP for their function and the ATP binding site has been considered for the design of molecules hindering the ATPase activity. A number of hsp72 and hsp90 inhibitors have been tested both on cultured cancer cells and in clinical trials (Braconi et al. 2009, Jegu et al. 2013). Recently, AUY922 (a third generation hsp90 inhibitor) was also studied in patients with HCC and showed therapeutic potential (Cheng et al. 2015). However, one of the effects observed during the treatment with this and other hsp90 inhibitors is a compensatory elevation of hsp72, which is finally expected to decrease the efficacy of the anticancer treatment (Jegu et al. 2013). For this reason, combined therapies using inhibitors of both the chaperones are currently under consideration.

On the other hand, the low molecular weight hsp27 does not display ATPase activity, but requires phosphorylation to exert its function, which makes it not amenable for inhibition by small molecules. The most studied hsp27 inhibitor is a second-generation antisense oligonucleotide (OGX-427) which reduces protein expression and is now under evaluation in clinical trials (Chi et al. 2016).

The HSPs expression is modulated by the Heat Shock Factors (HSFs), induced in cellular stress conditions, through the binding to the Heat Shock responsive Element (HSE). The major inducer of the HSPs is the HSF-1 (Jiang et al. 2015) also found to regulate glucose metabolism (Dai et al. 2007) and to increase the expression of the A isoform of the enzyme lactate dehydrogenase (LDH-A) (Zhao et al. 2009), suggesting a connection between the HSR and the Warburg effect.

These findings led our interest to study the impact of the LDH inhibition on heat shock response.

We focalized on the HSPs family members that are more connected to human malignancies (hsp27, hsp72 and hsp90).

As model of study, we chose the PLC/PRF/5 hepatocellular carcinoma cell line. The hepatocellular carcinoma (HCC) accounts for more than 80% of primary liver cancers and is generally characterized by poor prognosis (Wang et al. 2016). In hepatocellular carcinoma, constitutive activation of HSR was found to have high clinical significance. The three members of HSP family most commonly considered for the design of inhibitors (hsp27,

hsp72, hsp90) were repeatedly found to be over- expressed in HCC cells and to play a critical role in apoptosis inhibition and cell survival (Wang et al. 2016).

In our experiments, the relationship between HSR and LDH was investigated by hindering the enzyme activity with galloflavin (GF). Since the polyphenolic structure of this compound (see Fig. 4.23) does not allow to exclude additional, not LDH- related, biochemical activities, in all experiments we compared the effects observed with GF with those caused by oxamic acid (OXA).

RESULTS

First of all, we proceeded to evaluate the effects of the two LDH inhibitors on viability and lactate production on PLC/PRL/5 cell line. As showed in Fig. 4.23A, both OXA and GF cause a dose-dependent reduction of the lactate production in 6 hours. Instead, there is no significant effect on survival in 24 hours of treatment (Fig. 4.23B), the viability is still around the 75% with the highest doses of both compounds.

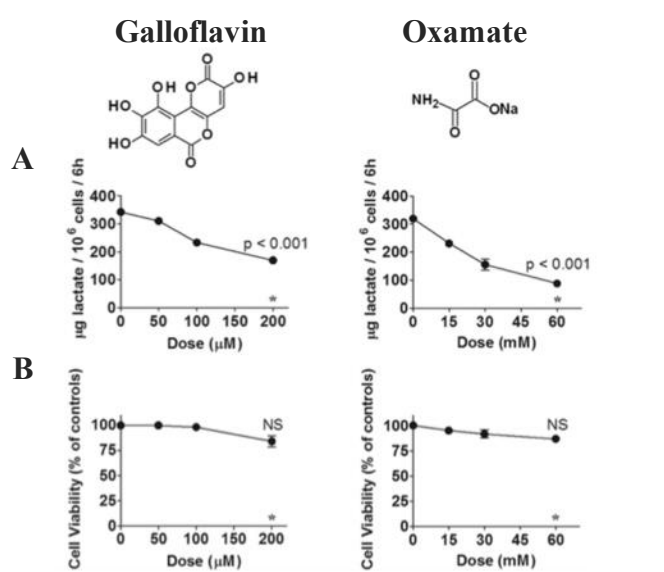


Figure 4.23. (A) Effect of GF and OXA on lactate production at 6 h. (B) Effect caused on PLC/PRF/5 cells viability at 24 h. Data of graphs (A) and (B) are mean values \pm SE from three determinations. Results were evaluated by ANOVA followed by Dunnet's post-test. The doses of inhibitors used for all the experiments have been marked with an asterisk. They caused statistically significant inhibition of LDH activity, but did not affect cell viability at 24 h.

The poor sensibility of PLC/PRF/5 cells to LDH inhibition indicate a good metabolic plasticity of this cell line, in agreement with previous experiments showing hepatocellular carcinoma cells viability to be significantly affected by OXA only after sustained treatments (Fiume et al. 2010).

This poor sensibility after short treatment is essential for the proceeding of the present study, since it allowed to exclude that all the observed effects could be linked to cell death induction. For the subsequent experiments of the study of HSPs, the selected doses of inhibitors used have been marked in the graphs of Fig. 4.23A and B with an asterisk; they are 200 μ M GF and 60 mM OXA.

As first step to characterise the HSPs, we analysed the expression of hsp27, hsp72, hsp90A and hsp90B under LDH inhibitor treatments.

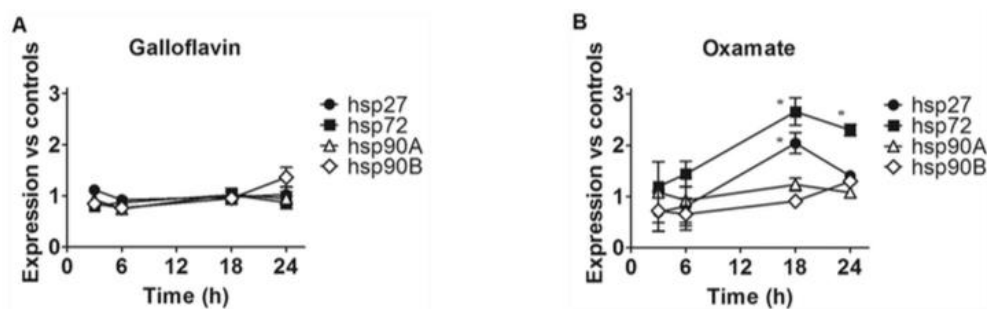


Figure 4.24. Expression of hsp27, hsp72 and hsp90 measured by real time PCR in PLC/PRF/5 cells exposed to GF (A) or OXA (B). A: GF did not affect the expression of the three HSPs. B: OXA caused increased hsp27 and hsp72 expression at 18 h, with a subsequent decline at 24 h. *, statistically significant difference compared to control cells, with $p < 0.05$.

There are no significant effects treating the cells 24 hours with galloflavin. Differently, in 18 hours OXA induces an increase of hsp27 and hsp72 expression which at 24 hours starts to drop again.

As explanation of the observed increase of both hsp72 and hsp27, literature reports that Hsp72 is activated in conditions of metabolic stress and reduced glucose, as in case of LDH inhibition, to favour oxidative metabolism (Drew et al. 2014). Moreover, LDH inhibition was found to generate oxidative stress in several tumor models (Le et al. 2010, Wang et al. 2012). In this context, hsp72 and hsp27 have been described as sensors of cellular redox changes and hsp27 was also found to protect cells from oxidative damage (Kalmar and Greensmith 2009, Toth et al. 2010).

To explain why galloflavin not induces the increase of the two chaperones, we hypothesized that, similarly to other phenolic compounds, GF could act as a free radical scavenger (Sureda et al. 2014).

To prove these hypothesis, we performed assays to evaluate the induction of oxidative stress in PLC/PRF/5 treated with OXA and GF.

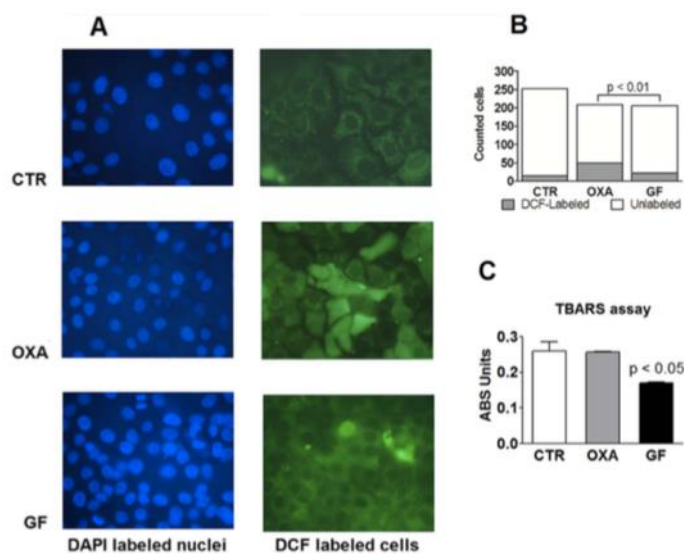


Figure 4.25. (A) Microscopic views of cells treated with OXA or GF and exposed to DCF-DA. In control and treated cultures, the fractions of DCF labeled cells (right panels) were calculated after counting a total 200–250 cells, evidenced by DAPI staining (left panels). They were plotted on graph (B). Data of (B) were analyzed by the χ^2 test, using the GraphPad Prism 5 software. (C) Results of TBARS colorimetric assay performed in PLC/PRF/5 cells treated with GF or OXA. Data were analyzed by ANOVA followed by Bonferroni post-test.

In Fig 4.25A has been measured the production of ROS (reactive oxygen species) by the DCFH-DA (dichloro-dihydro-fluorescein diacetate) assay. DCFH-DA is cell-permeable probe, when applied to intact cells, the probe crosses cell membranes and is enzymatically hydrolyzed by intracellular esterases to non-fluorescent dichlorofluorescein (DCFH). In the presence of ROS, DCFH is oxidized to highly fluorescent dichlorofluorescein (DCF), allowing the detection of ROS production in living cells. DCF-labeled cells can be counted under a fluorescence microscope. In control cells and in cells exposed to OXA or GF, the fraction of DCF labeled cells (right panels) was calculated counting a total 200–250 cells, evidenced by DAPI staining (left panels).

Fig. 3B reports the results of DCF-DA assay in graph showing that OXA significantly causes the increment of DCF-labeled PLC/PRF/5 cells, when compared to GF.

To support these data and to prove GF function as a free radical scavenger, we evaluate the ROS production by measuring the level of 2-thiobarbituric acid reactive substances (TBARS). They are naturally present molecules in biological specimens, their concentration usually increase as a response to oxidative stress (Armstrong and Browne 1994). TBARS include lipid hydroperoxides and aldehydes that react with 2-thiobarbituric acid, producing a chromophore. As shown in Fig. 4.25C, PLC/PRF/5 cells exposed to GF displayed significantly reduced TBARS staining when compared with control or OXA treated cultures.

Both assays confirmed the antioxidant potential of GF and explain why this compound can mitigate the oxidative stress associated with LDH inhibition, preventing the increase of the redox sensitive hsp27 and hsp72.

Afterwards, we proceeded by analysing the HSPs protein level by Western Blot exposing the PLC/PRF/5 to OXA and GF for 24 hours.

As showed in the next figure, OXA reduce the protein level of the three chaperones. This reduction interests especially the hsp27 that becomes difficult to detect.

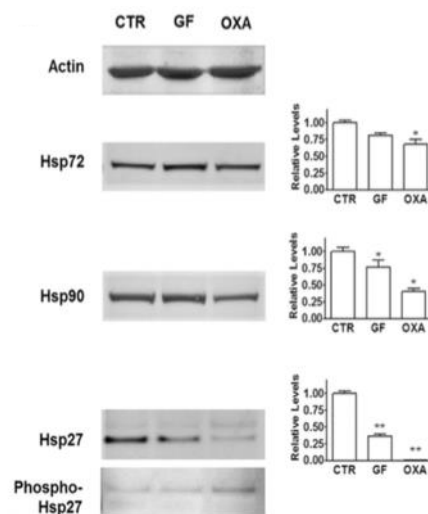


Figure 4.26. Effects of GF and OXA on HSPs protein level and function. Representative pictures of immunoblotting evaluations of hsp27, hsp72 and hsp90 after a 24 h exposure to OXA and GF. Bar graphs report the densitometric reading of the bands, normalized on actin level. Asterisks indicate a statistically significant difference of protein expression in comparison with cytokines treated cells. *, $p < 0.05$; **, $p < 0.01$. The not relevant detection of hsp27 phosphorylation (bottom) suggests lacking of activation.

The protein levels do not mimic the increased expression of hsp27 and hsp72 observed after 18 hours of exposure to OXA (Fig. 4.24B), in fact there is no increment of protein levels after 24 h. These evidences suggest an impairment of mRNA translation presumably linked to LDH inhibition. This hypothesis is in line with literature data showing LDH to be a mRNA binding protein, involved in post-transcriptional regulation of gene expression (Pioli et al. 2002).

As concerns the effect of galloflavin on HSPs protein level, also it reduces the protein levels of three chaperones but less marked compared to the reduction effects induced by OXA. This less effect can be explained by the slightly lower LDH inhibition power of the compound dose used for the present experiments (see Fig. 4.23A).

To understand well the impact of LDH inhibition on the HSPs, we analysed the functional status of the three chaperones.

The hsp27 is the easier one to verify, since it acts as chaperones in the phosphorylated form. The Fig. 4.26 shows a mild increase of the phosphorylated form only with OXA treatment, which, however, could not be reliably quantified by the densitometric reading of the band. These results suggest that LDH inhibition could markedly compromise the chaperone activity of this protein.

Differently to hsp27, hsp72 and hsp90 have an intrinsic ATPase activity. As reported in literature, the myricetin, a natural flavonoid with a molecular structure very similar to GF, inhibits the ATPase activity of hsp70 and related proteins (Chang et al. 2011). Molecular docking studies hypothesized the binding of myricetin to a site close to the nucleotide-binding cleft of hsp70, which could explain the loss of enzymatic activity. Flavonoids and related compounds were also found to inhibit the function of hsp90 (Davenport et al. 2014).

To evaluate the ATPase activity of the two chaperones, we developed an in vitro ATPase assay using human recombinant hsp72 and hsp90.

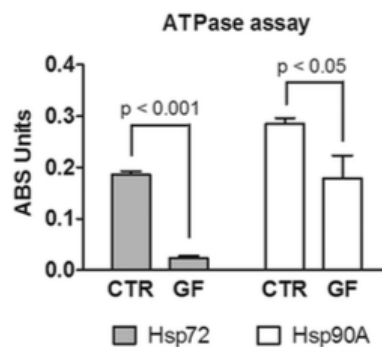


Figure 4.27. ATPase assay performed on human recombinant hsp72 and hsp90 exposed to GF. The enzymatic assay was performed by using the same level of substrate (ATP) and inhibitor (GF). Conditions have been detailed in Materials and Methods.

As the myricetin, GF can hinder the enzymatic activity of the two chaperones. The Fig. 4B showed for both HSPs a statistically significant reduction of ATPase function, which was almost completely abolished for hsp72.

To summarize, these results suggest that LDH inhibition can hinder the dysregulated HSR of hepatocellular carcinoma cells, since it significantly reduces the protein level of the major HSPs related to human cancers. Compared to OXA, more evident effects related to HSR inhibition can be expected by using GF because as the functional study of HSPs confirmed, GF can affect HSR not only through LDH inhibition, but also thanks to other properties of its molecular structure.

Then, to understand the consequences of the HSPs dysregulation in PLC/PRF/5 cells, as the chaperones most heavily affected by GF treatment (hsp27 and hsp72) have been described as critical factors in apoptosis resistance and replicative potential of cancer cells (Jego et al., 2013; Wang et al., 2016), we analysed the replicative capacity of PLC/PRF/5 cells evaluating the β -galactosidase activity.

The β -galactosidase activity at pH 6 is a known characteristic of senescent cells not found in pre-senescent, quiescent or immortal cells. So, we evaluated β -galactosidase activity by staining the treated cells with the chromogenic substrate 5-bromo-4-chloro-3-indolyl- β -D-galactopyranoside (X-gal).

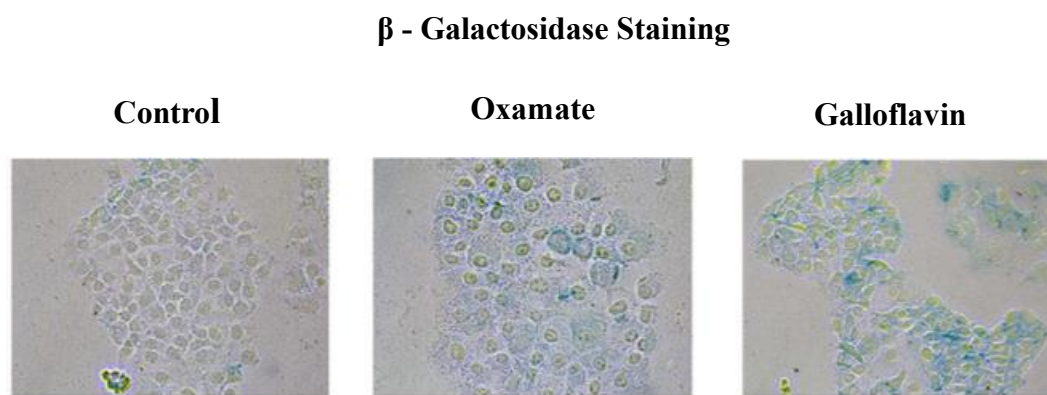


Figure 4.28. Microscopic views of PLC/PRF/5 cells exposed to OXA or GF and stained for the detection of β -galactosidase activity (global magnification 200 \times). The insoluble blue product of the enzymatic reaction is clearly visible in treated cells, showing particularly high intensity in cells exposed to GF.

Treating the cells with both LDH inhibitors and specially with GF leads the senescence induction as showed in Fig. 4.28 Compared to control cells, the presence of the blue product increases in the OXA treated cells and further in the GF treated cells. As this is not a quantitative method, we performed a clonogenicity assay which allow to quantify the single colonies.

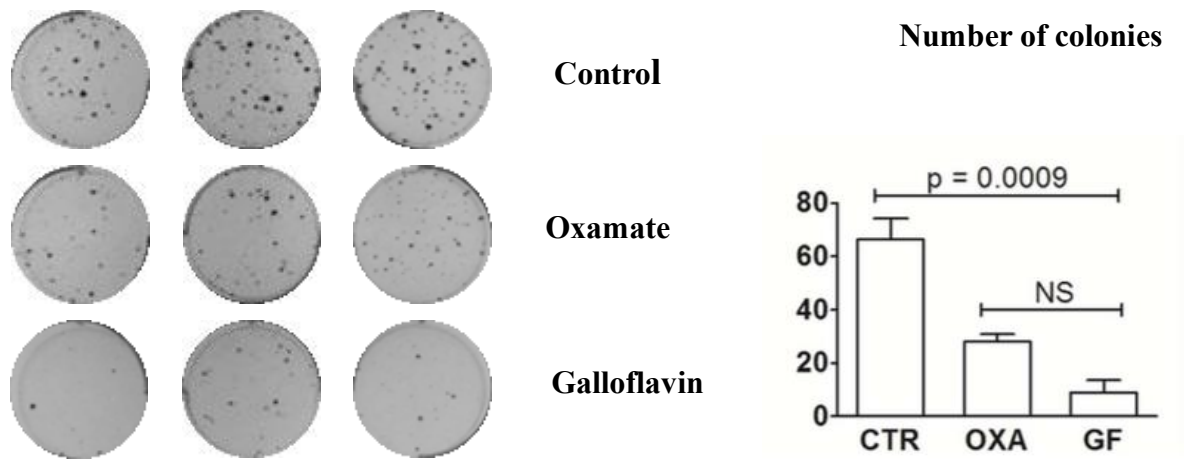


Figure 4.29. Colony formation assay. Pictures show the wells containing cell colonies stained with Crystal Violet. The number of colonies is reported on the bar graph aside. Results were evaluated by ANOVA followed by Bonferroni post-test.

The images of clonogenicity assay confirm the results previously obtained. The number of colonies were counted and plotted on the bar graph. ANOVA followed by Bonferroni post-test indicated a statistically significant difference between treated and control cells; also in this assay, GF apparently proved to be more efficient in reducing proliferative potential, although statistical evaluation indicated no significant difference in comparison with OXA.

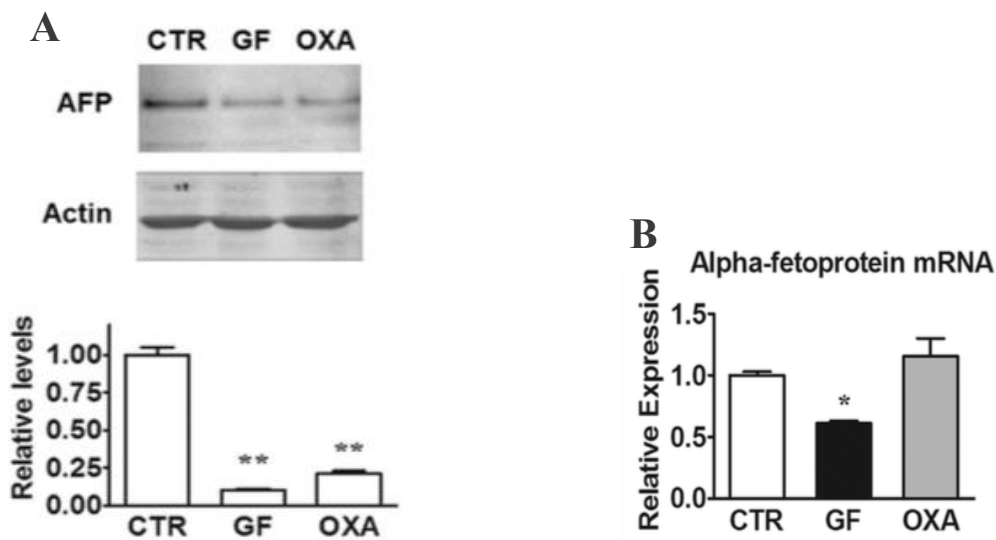


Figure 4.30. Effect of LDH inhibitors on alpha-fetoprotein expression and level. A: Both LDH inhibitors significantly reduced the protein level. **, $p < 0.01$ compared to control cells. B: Real time PCR evaluation of AFP expression after a 24 h exposure to OXA and GF. Contrary to OXA, GF significantly reduced AFP mRNA level. Asterisk indicates a statistically significant difference compared to control and OXA-treated cells, with $p < 0.05$.

In HCC cells, proliferative potential and resistance to apoptosis correlate with the level of alpha-fetoprotein (AFP), which was found to significantly decrease expression of the cyclin dependent kinase inhibitor p27 and to increase proliferating cell nuclear antigen (PCNA)

(Terentiev and Moldogazieva 2013). Moreover, Hsp72 was also found to regulate the level of AFP (Wang et al. 2013). On the basis of these evidences, we evaluated the expression and the protein level of AFP in PLC/PRF/5 cells. The results obtained are in line with the results of senescence assays (Fig. 4.28 and 4.29).

Both OXA and GF caused a marked reduction in AFP level compared to the control cells (Fig. 4.30A). Interestingly, while GF induces a sharp reduction of the AFP mRNA, OXA does not lead any statistically significant change, as showed in Fig. 4.30B. This finding suggests that the effects caused by OXA on AFP could be mediated by the impaired HSR, since they occur at protein but not at mRNA level. The data of Fig. 4.30A also confirm additional properties for GF, which amplify the effects of this molecule on HSR and cell senescence.

DISCUSSION

To summarize, HSR is important to restore the protein homeostasis and to allow the cells to survive by refolding the proteins or mediating their disintegration, but abnormal HSR seems to play a critical role in neoplastic change and tumor development (Calderwood et al. 2006).

For this reason, study of synthetic inhibitors targeting the major members of HSP family (hsp27, hsp72, hsp90) have recently emerged. During these treatments, using synthetic inhibitor targeting a single HSP, a common trend has been observed. These inhibitors induce a compensatory elevation of other HSPs, which decreases treatment efficacy.

The data of our experiments evidenced a connection between HSR and LDH-A, which is supported by the finding that HSF-1 (the master regulator of HSPs transcription) was also shown to induce the transcription of the LDH-A gene (Zhao et al. 2009). In the studied cellular model, LDH inhibition by OXA was found to impact on constitutively activated HSR by reducing the levels of the three examined HSPs, which resulted in cell senescence.

GF inhibits LDH activity but, similarly to other polyphenols (Colic and Pavelic 2000), possess multiple biochemical properties. Besides reproducing OXA effects, GF was also found to hinder the ATPase activity of hsp72 and hsp90 and to be a more efficient inducer of cell senescence.

In conclusion, our results suggest that LDH inhibition could be an efficient way to reduce the constitutively activated HSR in cancer cells, since differently from the currently available HSPs inhibitors, it can hinder at the same time the function of all the three major molecular chaperones involved in tumorigenesis. Moreover, the data obtained with GF suggest that, for its peculiar properties, the polyphenolic structure could be an appropriate molecular scaffold to design compounds joining LDH inhibitory activity with other anticancer effects. The

interesting pharmacological properties of polyphenols, combined with their good tolerability for normal cells, are now encouraging studies aimed at finding appropriate formulations to overcome the reduced solubility and bioavailability of these compounds (Gao and Hu 2010, Lewandowska et al. 2013).

Part B: The research of new LDH inhibitors

EXPERIMENTAL PART 1B: Identification of N-acylhydrazone derivatives as novel lactate dehydrogenase A inhibitors

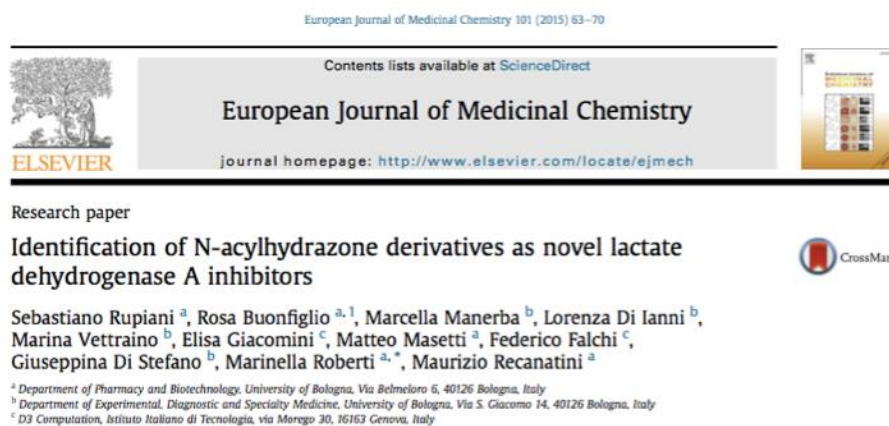


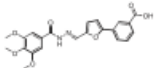

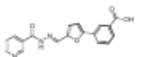
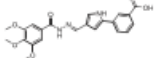
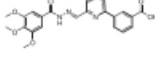
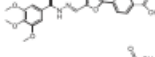
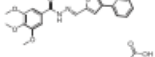
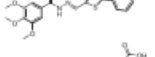
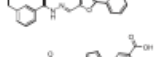
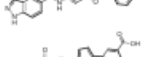
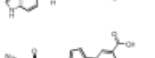
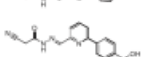
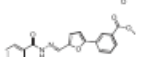
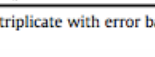
Figure 4.31. (Rupiani et al. 2015)

AIM OF THE STUDY

Since, both the poor solubility and chemical tractability of Galloflavin did not allow the consequent optimization, in this work it is described the identification of novel LDH-A inhibitors, which were selected by Virtual Screening and chemically manipulated for structure-activity relationship (SAR) studies.

RESULTS

An Ensemble-Based Virtual Screening was performed, aimed at including LDH-A flexibility in the screening campaign. Through this VS, based also on the commercial availability, 67 molecules were chosen for biological tests. The most frequent feature of these molecules was a carboxylic function, mimicking the same functional group of the endogenous substrate. Three of them (1-3, Table 4.4), showing a common N-acylhydrazone scaffold, were found to cause enzyme inhibition at micromolar level.

Compound		hLDH-A IC ₅₀ (μM) ^a	Lactate production IC ₅₀ (μM) ^a	Cell growth IC ₅₀ (μM) ^a
1		37 ± 5	42 ± 3	38 ± 7
2		37 ± 6	>200	n.d. ^b
3		43 ± 5	>200	>200
4		n.d. ^b	>200	80 ± 9
5		>200	n.d. ^b	n.d. ^b
6		125 ± 7	134 ± 27	100 ± 10
7		32 ± 6	52 ± 9	48 ± 14
8		41 ± 11	105 ± 17	95 ± 27
9		46 ± 6	>200	>200
10		41 ± 11	>200	45 ± 15
11		38 ± 10	100 ± 30	115 ± 14
12		48 ± 3	115 ± 3	64 ± 9
13		>200	n.d. ^b	n.d. ^b
15		>200	n.d. ^b	n.d. ^b

^a All points were tested in triplicate with error bars indicating the standard deviations.

^b Not determined.

Table 4.4. Activity of N-acylhydrazone analogues 1-13, 15 on purified human LDH-A and on lactic acid production and cell proliferation on Raji cells.

Initially all the compounds were evaluated for their inhibitory activity on purified human LDH-A. The compounds able to cause enzyme inhibition at micromolar level (1-3, 6-12) and 4 that was too fluorescent to be analyzed by fluorimetric method, were also investigated for their activity on lactic acid production and cell proliferation on Raji cell line. Further studies were performed on 1, the most active compound of the series.

In order to assess its mechanism of inhibition., competition assays with compound 1 were performed in the presence of scalar concentrations of pyruvate (0 – 2 mM) or NADH (20 – 150 μM). In the first case NADH in the reaction mix was maintained to 150 μM; in the second case pyruvate was 2 mM.

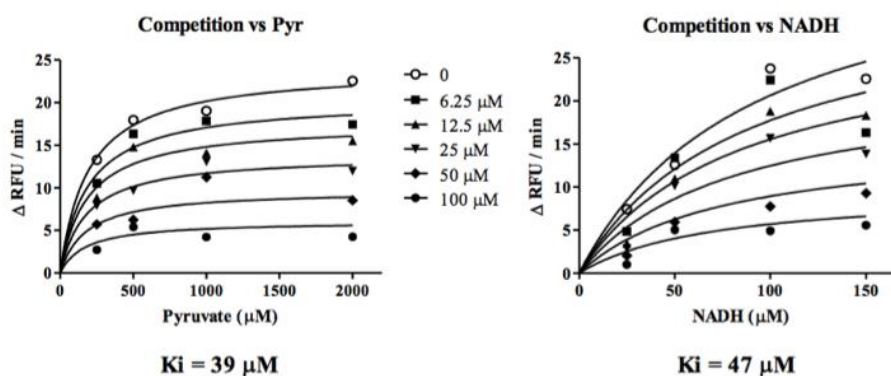


Figure 4.32. Competition LDH-A assay of compound 1 versus pyruvate and NADH. The enzymatic reaction was evaluated through the disappearance of NADH fluorescence, which is reported in the ordinate axis as Δ RFU/min. The two sets of experimental data were analyzed by applying the mixed model fit, using the Prism 5 GraphPad software.

LDH-A enzymatic assays (see in Materials and methods chapter) allowed to calculate the inhibition constants (K_i) vs pyruvate ($39 \mu\text{M}$) and NADH ($47 \mu\text{M}$) (Fig. 4.32).

Further experiments were addressed at verifying the occurrence of biological effects usually observed in cancer cells after LDH-A inhibition. These experiments were performed on Raji cells after 18 h exposure to compound 1 at $40 \mu\text{M}$. The dose was chosen on the basis of the data reported on Table 4.4 (50% inhibition on both lactate production and cell growth). As, the major function of LDH-A is to assure the rapid reoxidation of NADH, needed to sustain the glycolytic flux (Fiume et al. 2014), we analysed the NAD/NADH ratio in treated and control (untreated) cells.

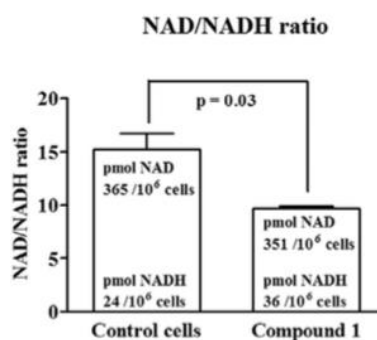


Figure 4.33. Evaluation of NAD/NADH balance measured in Raji cells 18 h after incubation with $40 \mu\text{M}$ of Compound 1.

In agreement with previous results obtained with small molecules LDH-A inhibitors (Le et al. 2010, Vettraino et al. 2013), treatment with compound 1 reduced NAD^+ regeneration and caused a statistically significant shifting of the redox balance in favour of the reduced form of the dinucleotide. The extent of the observed NADH increase (+50%) fits well with the effect caused by $40 \mu\text{M}$ compound 1 on lactate production in Raji cells (50% inhibition). Then, by

propidium iodide staining of the treated cells and subsequent flow cytometry analysis were studied the effects caused by compound 1 on cell cycle phases distribution.

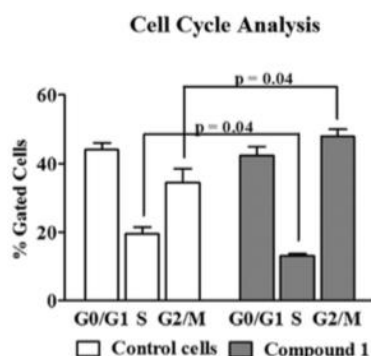


Figure 4.34. Analysis of cell cycle phases by flow cytometry using Propidium Iodide staining solution in Raji cells treated 18 h with 40 μ M of compound 1.

As showed in Fig. 4.34, after an 18 h treatment, compound 1 caused a small but statistically significant decrease of the cell fraction in S phase; on the contrary, cells in G2/M phase resulted significantly increased. This latter result is in agreement with published data obtained with the LDH inhibitor oxamate (Zhai et al. 2013, Madhok et al. 2010) and dichloroacetate (Madhok et al. 2010), a compound inhibiting glycolysis and lactate production. A recent investigation concerning the relationships between cell cycle progression and energy metabolism in cancer cells showed that the ATP requirement for G1 and S phases is largely satisfied by accelerated glycolysis, while the energetic needs for G2/M phase are mainly derived from mitochondrial oxidative phosphorylation. On the basis of the literature (Bao et al. 2013), our flow cytometry data, indicating a reduction of the cell population entering S phase and an increased fraction of G2/M cells, are compatible with effects exerted at the glycolytic level and can be a further evidence of the LDH-A inhibiting activity of compound 1. To assess whether the effect of compound 1 was not only limited to cell growth arrest, we measured by Western blot the expression of apoptosis markers.

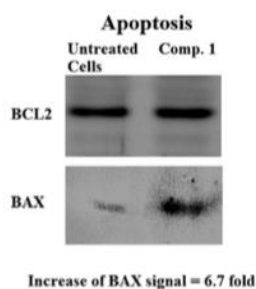


Figure 4.35. Apoptosis evaluation by measuring the differential expression of BAX and BCL2 proteins in Raji cells exposed to compound 1 (cell growth IC_{50} dose) for 18 h.

As apoptosis markers, we evaluated BAX and BCL2 proteins that are well studied regulators of the mitochondrial apoptosis pathway (Chalah and Khosravi-Far 2008). Moreover, increased BAX levels were already found in cancer cells treated with oxamate (Zhai et al. 2013) and other LDH inhibitors (Farabegoli et al. 2012). As shown in Fig. 4.35, an 18 h treatment with compound 1 did not substantially alter the level of BCL2 protein, but caused a 6.7-fold increase in BAX expression, denoting the induction of cell death signalling. Interestingly, contrary to oxamate, which was observed to trigger the mitochondrial apoptosis pathway in cells after a prolonged period of exposition (48 h) (Zhai et al. 2013), the effects caused by compound 1 on Raji cultures appeared to occur at earlier time.

A further experiment with compound 1 was aimed at evaluating its potential in combination tests with commonly used chemotherapeutic agents. Compound 1 (40 μ M) was tested on Raji cells in combination with four anticancer drugs usually employed in the therapy of haematological neoplasms. For each anticancer agent, the lowest dose causing a statistically significant effect on cell viability at 24 h (previously determined) was used. The doses were: 6 μ M cisplatin; 0.1 μ M daunomycin; 10 μ M sunitinib; 1 μ M etoposide. Each anticancer agent was subsequently tested in association with compound 1 to calculate the combination index, according to the procedure described in Materials and methods. A result ranging from 0.8 to 1.2 is indicative of additive effects.

Chemotherapeutic agent	Combination index ^a
Cisplatin	1.00 \pm 0.02
Daunomycin	0.88 \pm 0.15
Etoposide	0.86 \pm 0.01
Sunitinib	1.08 \pm 0.01

^a Association experiments were repeated twice. A result ranging from 0.8 to 1.2 is indicative of additive effects.

Table 4.5. Combination experiment of compound 1 with anticancer agents.

As already observed after LDH inhibition by oxamate or after LDH-A silencing (Zhou et al. 2010, Ahuja et al. 2010, Zhao et al. 2011), compound 1 showed the potential of increasing the therapeutic efficacy of commonly used chemotherapeutic agents. Finally, we compared the effects on cells viability caused by compound 1 on Raji cells and on normal lymphocytes, one of the cell populations more susceptible to the adverse effects of anticancer chemotherapy. The detailed experimental procedure is reported in Materials and methods chapter.

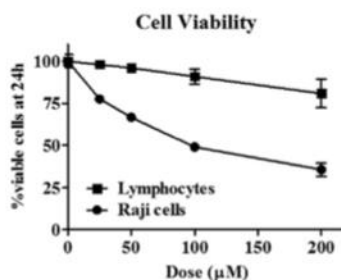


Figure 4.36. Effect of compound 1 on cell viability of Raji cultures and normal lymphocytes. 1×10^5 in 24-multiwell plates were exposed for 24h to 0-200 μM inhibitor. Normal lymphocytes viable cells were counted and compared to that measured after treatment of Raji cells.

No statistically significant (ANOVA) effect was found on normal cells viability even at the dose of 200 μM .

Although preliminary, all the obtained results were in support of the LDH inhibitory effect of compound 1; they also suggested a good tolerability of the molecule on normal lymphocytes and its capacity of improving the effects of commonly administered chemotherapy.

DISCUSSION

In continuation of our research for innovative antitumor lead candidates, through a VS campaign followed by SAR studies, we identified a new class of LDH-A inhibitors in a series of N-acylhydrazone derivatives. The new molecules were active at the micromolar range on purified LDH-A; notably the compound 1 showed a marked effect on lactate production in cells at the same concentration inhibiting purified LDH-A. A more detailed characterization of its biological properties confirmed 1 to be a suitable lead structure in the field of LDH-A inhibitors. Noteworthy, from a medicinal chemistry point of view, the N-acylhydrazone scaffold is a privileged structure, in which the biological relevance meets the synthetic accessibility, allowing to rapidly obtain variously substituted analogues, making the follow-up studies of the identified hits more efficient.

EXPERIMENTAL PART 2B: Synthesis of natural urolithin M6, a galloflavin mimetic, as a potential inhibitor of lactate dehydrogenase A



Cite this: *Org. Biomol. Chem.*, 2016, 14, 10981

Synthesis of natural urolithin M6, a galloflavin mimetic, as a potential inhibitor of lactate dehydrogenase A†

Sebastiano Rupiani,^a Laura Guidotti,^a Marcella Manerba,^b Lorenza Di Ianni,^b Elisa Giacomini,^c Federico Falchi,^c Giuseppina Di Stefano,^b Marinella Roberti*^a and Maurizio Recanatini^a

Figure 4.38. (Rupiani et al. 2016)

AIM OF THE STUDY

Since the key factors in Galloflavin activity are most the number and position of the hydrogen bonds (in green), they decided to develop new compounds mounted on a different scaffold, which could be a help to explore the SAR of GF without having to deal with its major limitations.

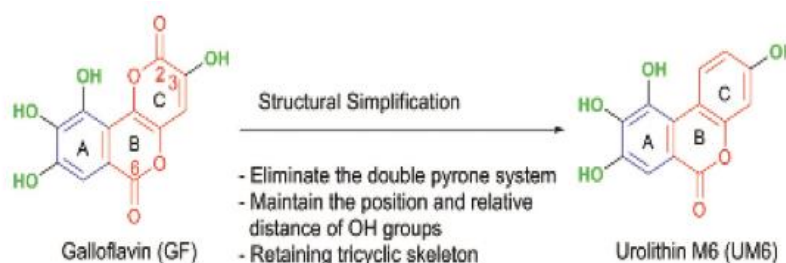


Figure 4.39. Illustration of the main concepts driving the structural simplification of GF.

Considering these features, they explored a chemical database of the existing molecules and identified a natural tetra-hydroxylated dibenzo-pyranone derivative compound known as urolithin M6 (UM6).

UM6 has been identified as a recurrent metabolite after the consumption of aliments rich in ellagitannins, such as berries, pomegranates, muscadine grapes, walnuts, almonds, and oak aged wines, among other foods. Upon hydrolysis in the gut, ellagitannins release ellagic acid (EA), which undergoes ring-opening and decarboxylation to pentahydroxy-urolithin M5.

From this, UM6 and several other urolithins (M7, A, B, C, D and E) are produced by the sequential removal of hydroxyl groups from different positions.

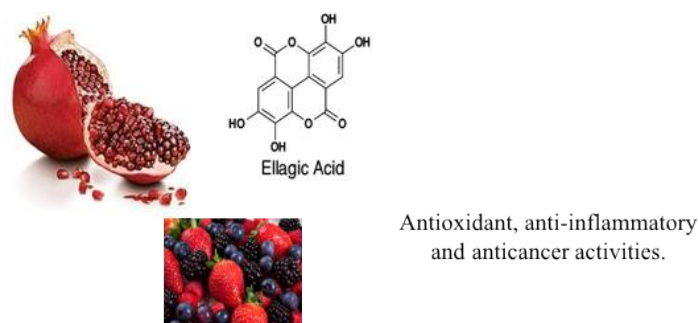


Figure 4.40. Ellagic acid molecular structure with examples of fruits containing it.

There is now a growing interest in the biological activities of urolithins; several studies carried out *in vitro* or in animal models suggest that urolithins have potential antioxidant (Bialonska et al. 2009, Ishimoto et al. 2011), anti-inflammatory (Ishimoto et al. 2011, Larrosa et al. 2010), anticancer (González-Sarrías et al. 2009, Adams et al. 2010) and antiglycation (Adams et al. 2010) activities.

UM6 was characterized for the first time as an ellagitannin metabolite in 2008 (Ito, Iguchi and Hatano 2008), and its production via a biotechnological method was described by (Tomás-Barberán et al. 2014). However, to the best of our knowledge, to date, neither biological study nor chemical synthesis has been reported for UM6. In this study, it is presented a fast and modular synthetic procedure that can be used to obtain UM6 (detailed in the full paper, (Rupiani et al. 2016) .

RESULTS

To validate the synthesized UM6 as a GF mimetic from a biological point of view, a preliminary study was undertaken to evaluate its inhibitory activity on purified human LDH-A.

Compound	hLDH-A IC ₅₀ ^a (μM)	Lactate production IC ₅₀ ^a (μM)	Cell growth IC ₅₀ ^a (μM)
GF	70 ± 10	62 ± 5	33 ± 4
UM6	77 ± 10	36 ± 3	25 ± 2

^a All points were tested in triplicate with error bars indicating the standard deviations.

Table 4.6. Activity of GF and UM6 on purified human LDH-A, lactic acid production and cell proliferation on Raji cells

As expected, the IC_{50} value of $77 \pm 10 \mu\text{M}$ was comparable to that of GF ($IC_{50} = 70 \pm 10 \mu\text{M}$). Consequently, UM6 was also investigated for its effect on lactic acid production and cell proliferation on Raji cell line. It exerted an evident effect on lactate production ($IC_{50} = 36 \pm 3 \mu\text{M}$) and inhibited the cell growth with an IC_{50} of $25 \pm 2 \mu\text{M}$ (see paragraphs 3.3, 3.4 and 3.5 in Materials and Methods chapter).

The results suggested that UM6 was a suitable hit structure in the field of LDH-A inhibitors. A more detailed characterization of its biological properties is ongoing and will be published elsewhere.

DISCUSSION

In summary, the natural urolithin M6 was identified as a possible chemical and biological Galloflavin mimetic. An efficient synthetic pathway was developed to synthesize UM6 in 5 steps with a 27% overall yield starting from the commercially available materials. In preliminary tests, the compound inhibited both the enzymatic activity of purified LDH-A and lactate production in cultured cells at a level that was comparable to GF, making it a suitable hit in the search for new LDH-A inhibitors.

Note that UM6 thus obtained could be used as an authentic compound for the identification of metabolites derived from gut microbial ellagic acid and for the evaluation of several possible biological effects of different parent urolithins.

4.2 Genetic approach to inhibit LDH enzyme activity

BACKGROUND AND AIM OF THE STUDY

The Jacques Pouyssegur research group, “Hypoxia signalling and cancer metabolism”, has genetically succeeded (use of ZFNs & CRISPR-Cas9) to reduce the rate of production and secretion of lactic acid in human and mouse tumor cell lines by specific knockouts of lactate/H⁺ symporter MCT1 or MCT4 or both. This gene disruption in lactic acid export showed a severe reduced tumor growth (but not cure) in immune incompetent mice (*nude*) (Marchiq et al. 2015). In addition, their collaborators have demonstrated that reduced lactic acid secretion in mouse melanoma B16, by shRNA-targeting LDH-A, induced a stronger immunosurveillance than with wild type melanoma cells exporting higher lactate levels (Brand et al. 2016).

On the basis of these evidences, they decided to work on the knockout (KO) of the Lactate Dehydrogenase A gene, to evaluate the effects not only of the reduction but of the complete elimination of LDH-A in cancer cell lines.

During the course of the experiments they have observed that a LDH-A KO in LS174 colon adenocarcinoma or in mouse B16 melanoma reduces the rate lactic acid secretion only moderately. Consequently, they hypothesized that the LDH-B isoform known to catalyse the reverse reaction (Lactate \gg Pyruvate) is capable to transform Pyruvate to Lactate in LDH-A KO cells. Therefore, they tried to isolate a LDH-B KO and a LDH-A/LDH-B double Knock-Out cells by using CRISPR/Cas9 technique.

The CRISPR-associated protein Cas9 is an endonuclease guided by small RNAs (sgRNAs) through Watson-Crick base pairing with target DNA, enabling Cas9 to introduce a site-specific double-strand break (DBS) in the DNA. The single guide RNA (sgRNA) engineered retains two critical features: a sequence at the 5' side that determines the DNA target site by Watson-Crick base-pairing and a duplex RNA structure at the 3' side that binds to Cas9. The target DNA sequence must immediately precede a 5'- NGG PAM (Protospacer Adjacent Motif) to mediate Cas9 cleavage at ~3 bp upstream of the PAM (each Cas9 orthologue has a unique PAM interacting site). This finding created a simple two-component system in which changes in the guide sequence of the sgRNA program Cas9 to target any DNA sequence of interest (Doudna and Charpentier 2014).

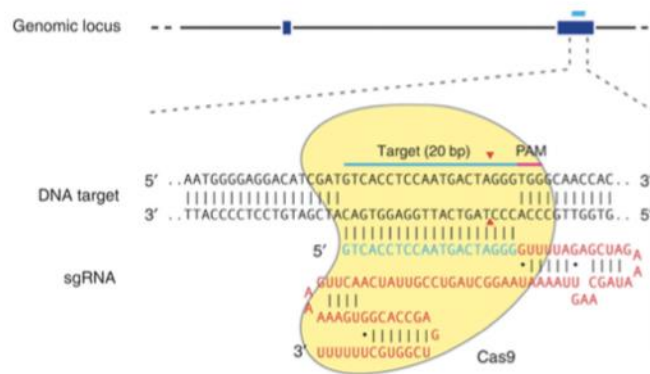


Figure 4.41. Schematic of the RNA-guided Cas9 nuclease. The Cas9 nuclease from *S. pyogenes* (in yellow) is targeted to genomic DNA (shown for example is the human *EMX1* locus) by an sgRNA consisting of a 20-nt guide sequence (blue) and a scaffold (red). The guide sequence pairs with the DNA target (blue bar on top strand), directly upstream of a requisite 5'-NGG adjacent motif (PAM; pink). Cas9 mediates a DSB ~3 bp upstream of the PAM (red triangle) (Ran et al. 2013).

In contrast to ZFN and TALEN methods, which use protein-DNA interactions for targeting, RNA-guided nucleases (RGNs) use simple, base-pairing rules between an engineered RNA and the target DNA site (Sander and Joung 2014). CRISPR/Cas9 represents a system markedly easier to design, highly specific, efficient and well-suited for high-throughput and multiplexed gene editing for a variety of cell types and organisms (Ran et al. 2013).

As for more than two years I worked on the pharmaceutical approach to inhibit the Lactate Dehydrogenase, for the period that I could spend abroad I chose to work on the genetic LDH inhibition in cancer cell lines and the characterization of the LDH KO cell lines obtained, together with the study in normoxia and hypoxia.

By the time I arrived in the laboratory of Dr. Jacques Pouyssegur, they have already obtained the LDH-A and LDH-B single and double KO in LS174T colon adenocarcinoma cells and at the same time in the collaborating German laboratory they got the same KOs in B16 mouse melanoma cells.

Consequently, in these months I had the possibility to work on the characterization of single LDH-A, LDH-B and double LDH-A/LDH-B KO clones of LS174T and B16 in normoxic and hypoxic conditions.

At the same time, I gained experience with the CRISPR/Cas9 technique, in an attempt to obtain the LDH-A/LDH-B KO in another cell line, U87 glioblastoma cells.

RESULTS

Gene Knock-Out by CRISPR/Cas9 technology

First of all, I checked the LDH-A, LDH-B and HIF-1 α protein levels in the selected cell line in normoxic and hypoxic conditions.

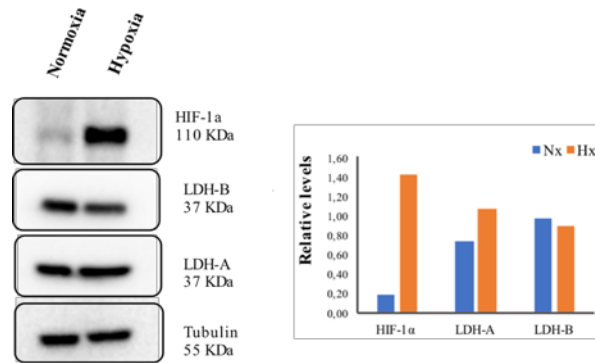


Figure 4.42. LDH-A, LDH-B and HIF-1 α protein levels in U87 cell lines after 24h of incubation in normoxia and hypoxia (O₂ 1%).

Hypoxia leads an increase of LDH-A isoform (the isoform basically linked to the enhanced lactate levels in neoplastic tissues) with a contemporary slightly decrease of the LDH-B isoform, and a high increment of HIF-1 α protein levels, confirming that hypoxic conditions may arise and stimulate HIF-1 to enhance glycolytic gene expression (Iyer et al. 1998).

Subsequently, I proceeded with the CRISPR/Cas9 plasmids transfection. To obtain the LDH-A and LDH-B KOs in LS174T and B16 cell lines, they performed two different transfections, one for each specific CRISPR/Cas9 plasmid. *LDH-A/LDH-B double-KO LS174T cell line* was obtained by transfecting *LDH-A-KO sub-clone* with LDH-B CRISPR/Cas9 plasmid.

In my case, I directly co-transfected U87 cells with both LDH-A and LDH-B CRISPR/Cas9 plasmids.

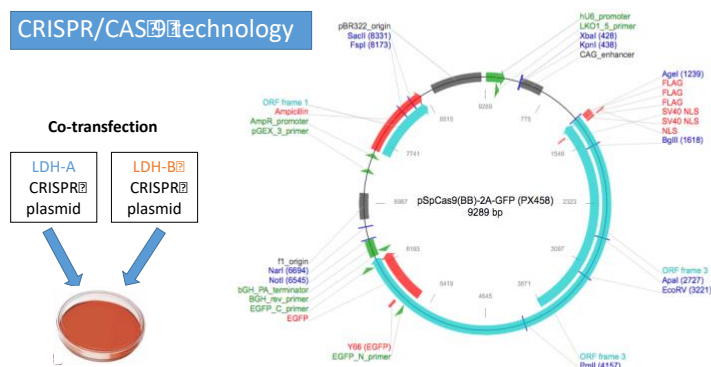


Figure 4.43. CRISPR/Cas9 plasmids specific for LDH-A and LDH-B genes to obtain the genetic Knock-Out in U87 cells.

By the BD FACSAria sorter it has been possible to select only the GFP positive cells, thus, those that successfully incorporated the plasmid. Subsequently, these cells were in part seeded singularly in 96 well plates, in part seeded at very low concentration to get single colonies.

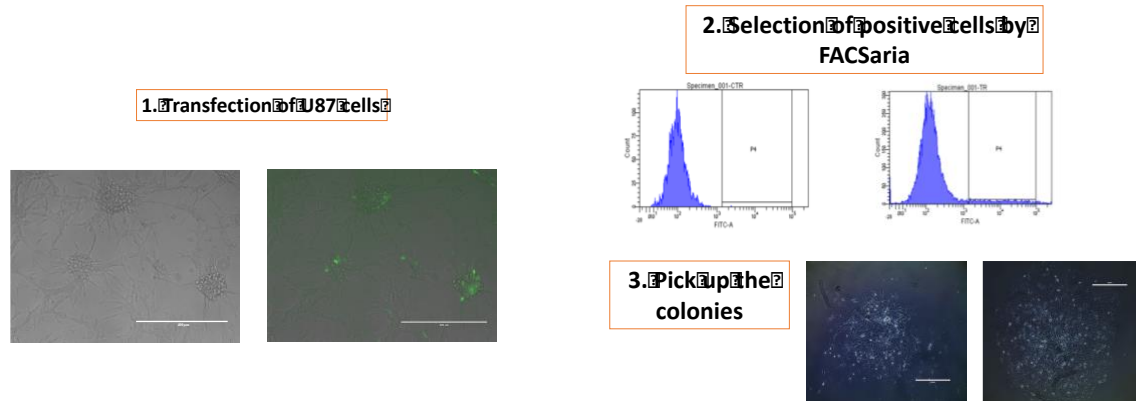


Figure 4.44. Steps after trasfection: CRISPR/Cas9 plasmids contain the GFP protein to verify the transfection efficiency (Step 1) and to select only the cells that have incorporate the plasmids (GFP positive cells), in this case by BD FACSaria sorter (Step 2). This sorter is also able to seed single cells in 96-well plate. To get single colonies also in 10 cm plates, the rest of the sorted cells have been seeded at very low concentration. Once obtained the single colonies, the step 3 consists in the pick up and expand them to can proceed at the selection of the right KO cells by screening.

The screening of the obtained clones has been done by Western Blot with LDH-A and LDH-B specific antibodies. After a preliminary screening of each clone, the clones showing single or double LDH-A/LDH-B KO have been screened again to can confirm the Knock-out.

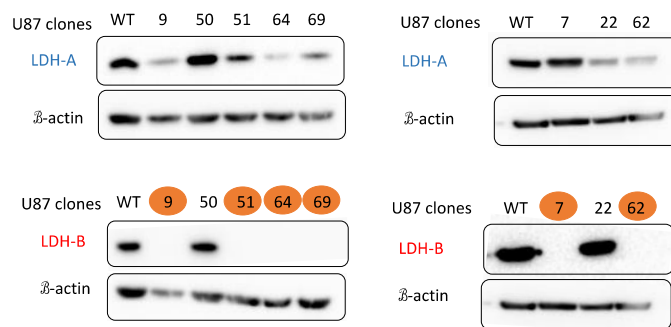


Figure 4.45. Western Blot to confirm the KO U87 clones using LDH-A and LDH-B specific antibodies. Antibody anti β -actin is used as loading control.

As result, six LDH-B KO clones have been confirmed. The evidences led us to conclude that, the LDH-B CRISPR/Cas9 plasmid seems to be much more efficient than the LDH-A CRISPR/Cas9 plasmid, confirming the past experiences.

Characterization of single and double LDH-A/LDH-B KO clones of LS174T and B16 cell lines

We have performed the characterization of the **LS174T** [*WT* (LDHA +/+LDHB +/+); *LDHA KO* (LDHA -/-); *LDHB KO* (LDHB -/-); *Heterozygote* (LDHA -/-LDHB +/-); *double KO* (LDHA -/-LDHB -/-)] and **B16** [*WT* (LDHA +/+LDHB +/+); *LDHA KO* (LDHA -/-); *LDHB KO* (LDHB -/-); *double KO* (LDHA -/-LDHB -/-)] clones.

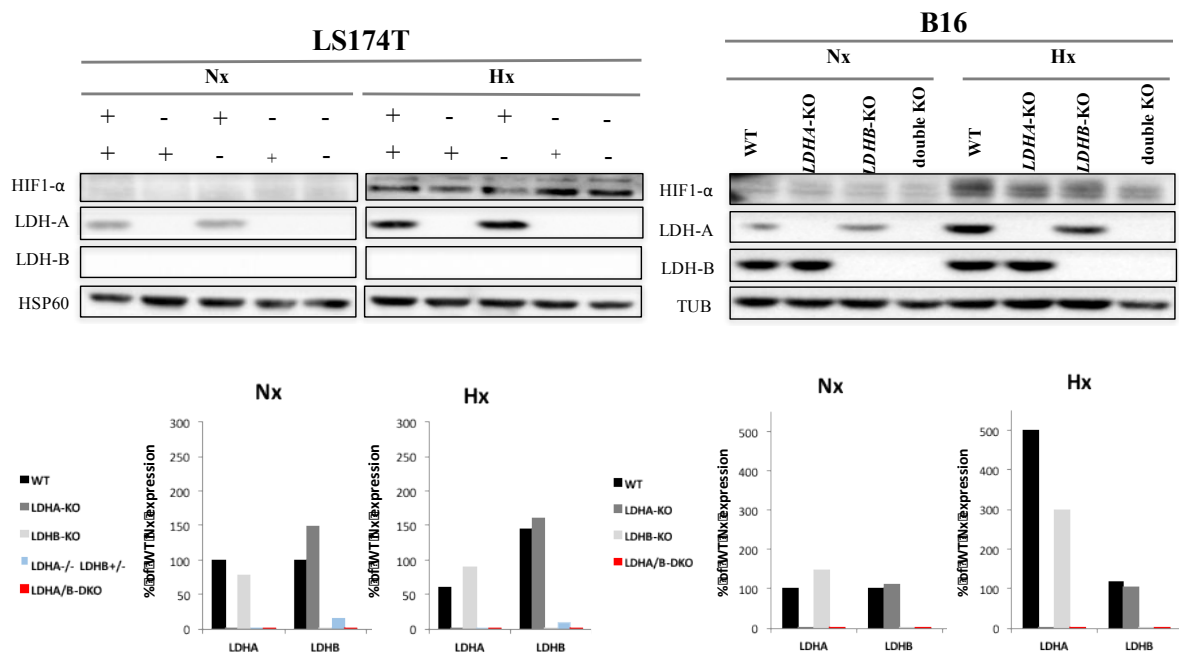


Figure 4.46. Western blot analysis of LS174T and B16 clones. Cells were seeded and after 24h of adhesion were left other 24h in normoxia or hypoxia (1% O₂) conditions. Antibody anti-HSP60 and anti-Tubulin are used as loading control.

The use of specific antibodies for the LDH-A and LDH-B allow us to discriminate between the two isoforms, confirming the LDH-A or/and LDH-B KOs. As showed in Fig. 4.46, LDH-A protein levels, present in WT and LDH-B KO clones, are increased in hypoxic conditions, in line with literature describing HIF-1 mediates hypoxia-induced LDH-A expression in cancer cells (Cui et al. 2017). Indeed, also HIF-1α levels rise in hypoxia, as expected. Instead, no significant variations emerged in LDH-B levels under hypoxic conditions.

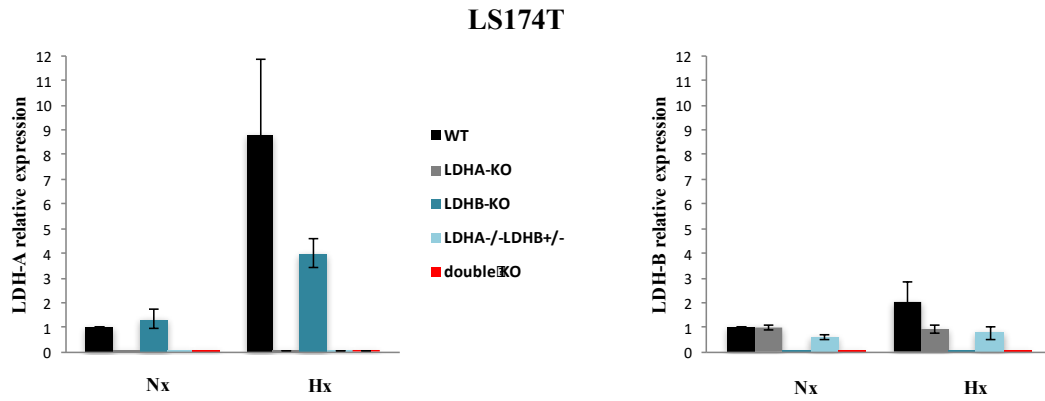


Figure 4.47. LDH-A and LDH-B mRNA levels in LS174T clones after 24h in normoxic and hypoxic (1% O₂) conditions.

The measure of the LDH-A and LDH-B mRNA levels confirmed the gene KOs and the trend of these two isoforms in hypoxic conditions. As the mRNA expression for mouse melanoma B16 clones had already been evaluated from the German group, in our laboratory, we analysed the LDH-A and LDH-B mRNA levels in human colon adenocarcinoma LS174T clones.

A further confirmation of the efficient LDH Knock-Out, has been done by determining LDH enzymatic activity. As known, LDH inter-converts pyruvate to lactate regenerating the cofactor NADH. As consequence of this, we proceeded by monitoring NADH oxidation in different condition of pH and substrates.

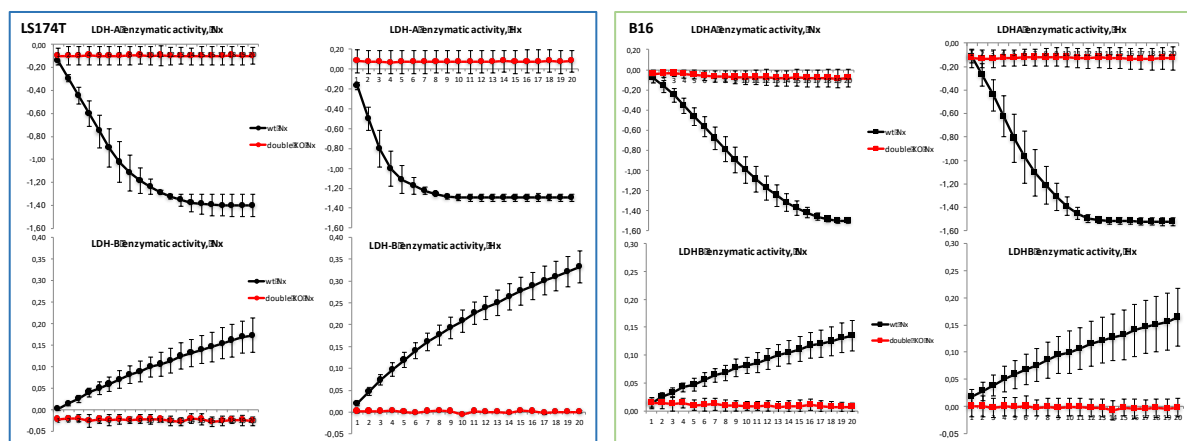


Figure 4.48. Evaluation of LDH enzymatic activity. The enzymatic conversion (pyruvate > lactate) is indicated with LDH-A activity, whereas the enzymatic conversion (lactate > pyruvate) is indicated as LDH-B activity. In the first panel are shown the results of LDH-A and LDH-B activity of LS174T clones; in the panel on the right those related to B16 clones. The black line corresponds to the LDH activity of WT clones; the red line indicates the LDHA/LDHB dKO clones (for technical details, see Materials and Methods).

The enzymatic conversion from pyruvate to lactate is indicated with LDH-A activity, as this isoform requires higher pyruvate concentrations to reach the maximum activity, contrary to LDH-B (see paragraph 1.2). Moreover, LDH-B, mainly expressed in heart muscle, favours the conversion of lactate into pyruvate (Draoui and Feron 2011). As consequence, the enzymatic conversion from lactate to pyruvate is indicated as LDH-B activity.

As clearly showed by the graphs (Fig. 4.48), in both cell lines, LDH enzymatic activity resulted impaired in the LDH double KO clones, in line with previous results.

Once confirmed the Knock-Out of the LDH enzyme in both cell lines, we proceeded with clones' characterization, starting by the evaluation of the gene KO's impact on proliferation rate.

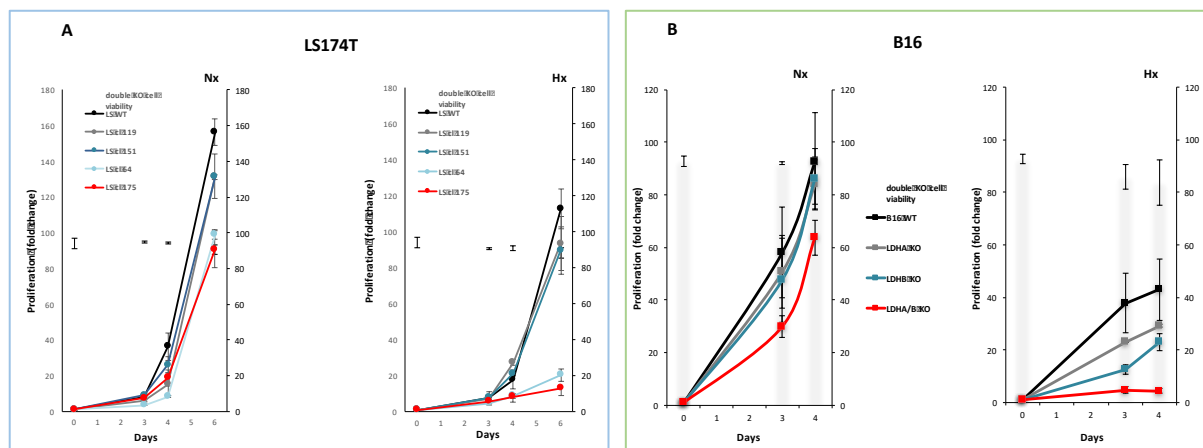


Figure 4.49. Proliferation (lines) and viability (columns) assay of LS174T (A) and B16 (B) clones after different days in normoxic and hypoxic (1% O₂) conditions. (A) Legend: WT, LDH-A KO (cl. 119), LDH-B KO (cl. 151), heterozygote (cl. 64), LDH-A/LDH-B dKO (cl. 175). See detailed procedure in Materials and Methods.

In Fig. 4.49A, evaluating the proliferation index, single LDH-A or LDH-B KO's lead slightly decrease in Nx and Hx compared to WT LS174T cells. Differently, the rate of growth undergoes a strong reduction in the case of heterozygote cells (clone 64) and of the LDH-A/LDH-B dKO (clone 175), especially in hypoxia. The cl. 175 does not reach the 20% of proliferation in hypoxic conditions, whereas its viability is not compromised in any of the two conditions, as shown by the columns of the graphs.

In the case of B16 clones (Fig. 4.49B), the trend is the same of the colon adenocarcinoma clones. Differently, all the clones show a lower rate of growth in hypoxia than normoxia. Moreover, the double KO's viability undergoes a slight reduction in hypoxic conditions.

Subsequently, extracellular acidification rates (ECAR) and oxygen consumption rates (OCR) of cells were analysed by Seahorse XF24 extracellular flux analyser.

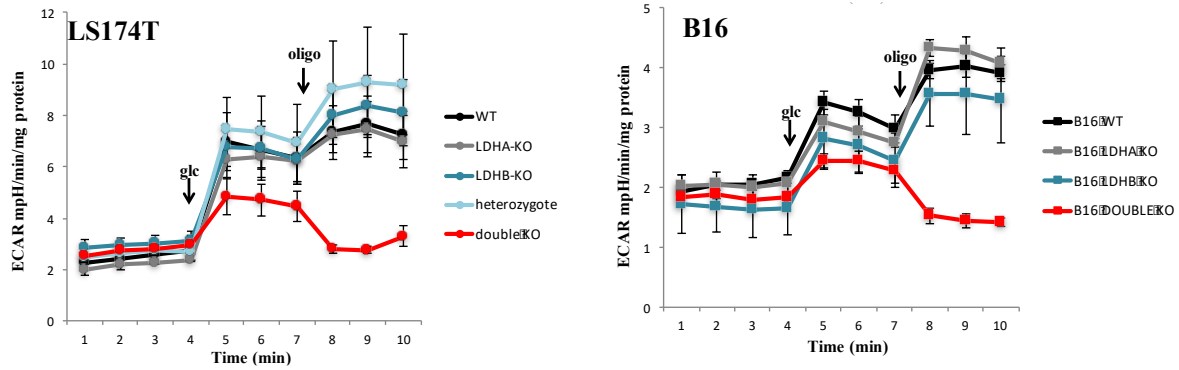


Figure 4.50. ECAR (extracellular acidification rates) analysis by Seahorse XF24 in LS174T and B16 clones. Glucose and oligomycin (complex V inhibitor) were added during the experiment.

As, lactate (via the enzymatic activity of LDH), is usually assumed to be the major mechanism responsible for tumour acidity (see the corresponding section of paragraph 1.1), from the ECAR measure, it is possible to evidence the impaired capacity of the double KO to produce lactate, contrary to the other clones.

When glucose is added, the ECAR rises also in the dKO; this increase is due to the CO₂ produced by enhancing the respiration rate, in fact, by adding oligomycin (a complex V inhibitor) the ECAR levels fall down, confirming the suppression of LDH activity in dKO clones.

In support of these data, we analysed also the production of lactate by extracellular lactate levels measurement.

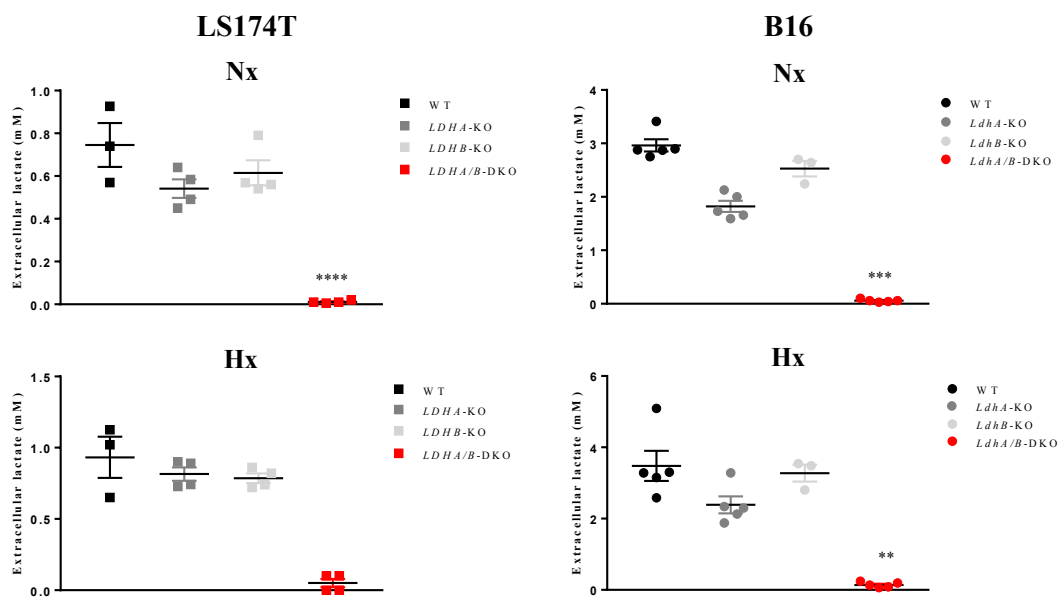


Figure 4.51. Extracellular lactate levels measurement of LS174T and B16 clones after 24h in normoxia or hypoxia (see paragraph 3.28).

By these last experiments, we confirmed that also LDH-B isoform (in LDH-A KO clones) are able to convert pyruvate to lactate.

In addition to the ECAR rates, the Seahorse XF24 machine, allows to determine at the same time the OCR (Oxygen Consumption Rates) of cells.

By the injection of sequential compounds, this machine allows to have an accurate measure of mitochondrial respiration by determining: basal respiration, ATP production, proton leak, maximal respiration, spare respiratory capacity, and non-mitochondrial respiration.

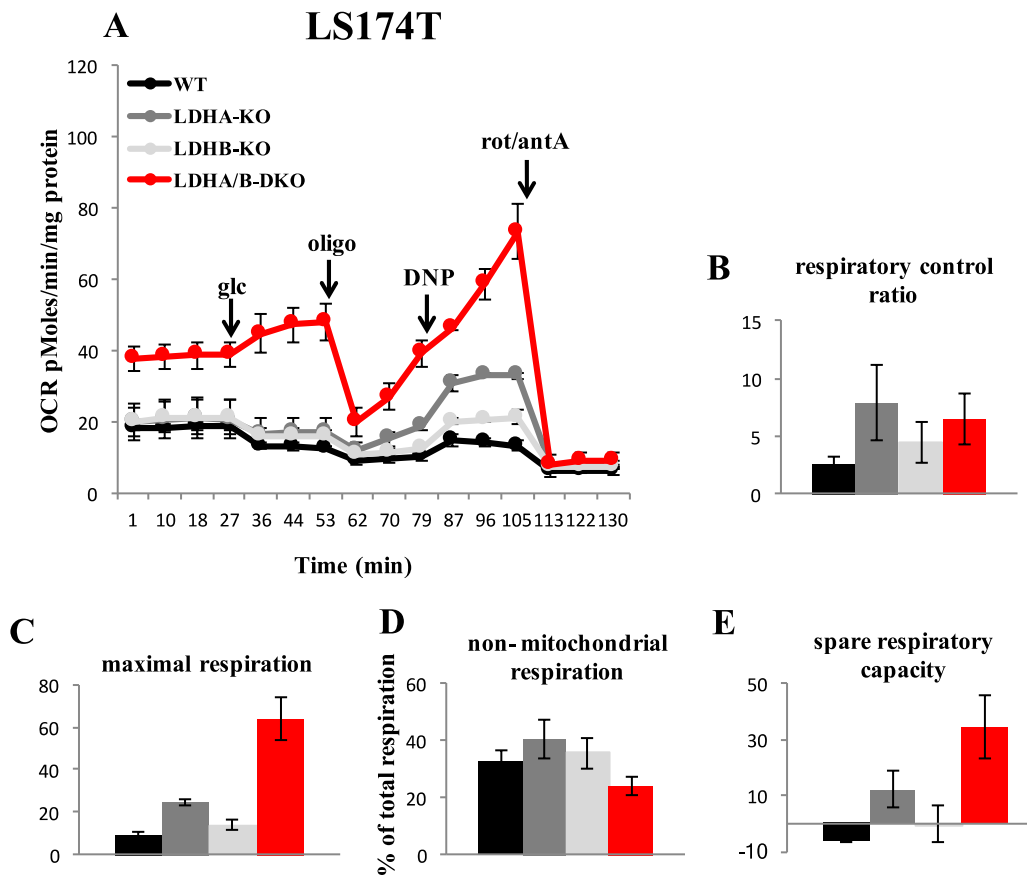


Figure 4.52. Oxygen consumption rate (OCR) analysis by Seahorse XF24 in LS174T clones. (A) OCR profiles by sequential compounds' addition (10 mM glucose, 1 μ M oligomycin, 100 μ M DNP, 1 μ M rotenone/1 μ M antimycinA), express as pMolesO₂/min/ μ g protein; (B) respiratory control ratio (maximal respiration / proton leak); (C) maximal respiration (in presence of DNP); (D) non-mitochondrial respiration; (E) spare respiratory capacity (maximal respiration / basal respiration) (Brand and Nicholls 2011).

By the analysis of OCR, it is possible to get important information about the cell respiratory control. The dKO clone shows a different profile than all the other clones. Indeed, differently to the others, the switch of dKO metabolism toward OXPHOS is proved by starting with higher levels (basal respiration), the consume of oxygen does not decrease after glucose addition, the dKO reaches the highest level after the addition of DNP (maximal respiration).

Indeed, also the spare respiratory capacity (difference between maximal and basal respiration) proves the major ability of double KO to respond to an increase in energy demand.

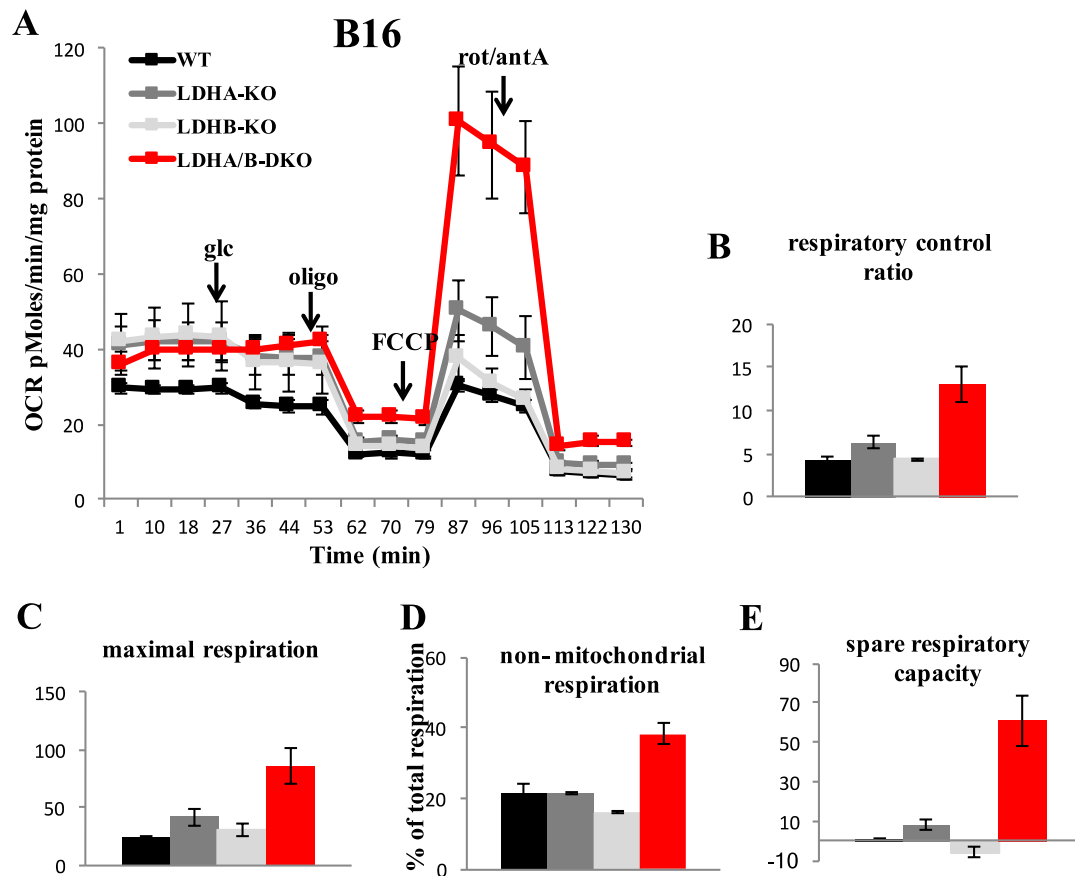


Figure 4.53. Oxygen consumption rate (OCR) analysis by Seahorse XF24 in B16 clones. (A) OCR profiles by sequential compounds' addition (10 mM glucose, 1 μ M oligomycin, 3 μ M FCCP, 1 μ M rotenone/1 μ M antimycinA), express as pMolesO₂/min/ μ g protein; (B) respiratory control ratio (maximal respiration / proton leak); (C) maximal respiration (in presence of FCCP); (D) non-mitochondrial respiration; (E) spare respiratory capacity (Brand and Nicholls 2011).

We obtained the same trend in the results of the OCR analysis in B16 clones.

From these data, we can appreciate that the elimination of A and B LDH isoforms leads a shift of metabolism from glycolysis to OXPHOS, which sensitise them to oxidative phosphorylation inhibitors, such as oligomycin (complex V inhibitor), as show below in the clonogenic assay images.

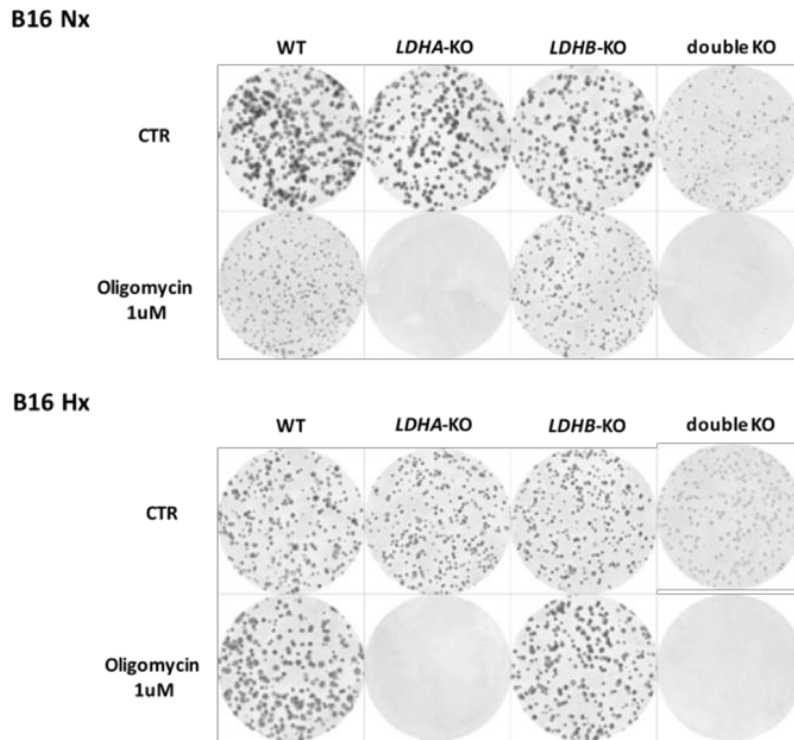


Figure 4.54. Clonogenic assay of B16 clones in normoxic and hypoxic (1 %O₂) conditions. Cells (1 x 10³) were plated into 60 mm² Ø dishes in 6 ml of RPMI, in triplicate. Oligomycin is added after 24h. Cell colonies were stained with Giemsa solution after 6-8 days.

LDHA-KO cells, differently to LDHB-KO cells, show high sensitivity to complex V inhibitor both in normal (20%) and in low (1%) oxygen levels. This effect suggests that LDHA-KO cells switch its metabolism from glycolysis to OXPHOS and its LDH-B isoform does not allow a rapid plasticity of adaptation to new conditions. Instead, in case of WT and LDHB-KO cells, the addition of oligomycin cause a slight decrease only in normoxic conditions, whereas no reduction effects are shown on colony formation in hypoxia.

Double KO cells show a lower rate of growth than the other clones in both oxygen conditions, their capacity to form colonies is completely abolished in presence of oligomycin, confirming their OXPHOS dependence.

Comparison of the effects of the LDH inhibitor compound with the genetic knockout of LDH

In reference to the pharmacological approach to inhibit LDH activity, as already described in the Introduction Chapter, GNE-140, of Genentech group, is actually the only inhibitor with nanomolar potency *in vitro* (Boudreau et al. 2016). Thus, it represents an interesting compound to evaluate the role of LDH in cancer cells and to compare the effects of the compound with the genetic knockout of LDH.

Dr. Jacques Pouyssegur has received this compound from the Genentech group to test it in the cell lines used in his laboratory. Therefore, I have performed clonogenic and fluxomics experiments (evaluating the cell metabolism by SeaHorse XF24) on B16 WT and LDH-A/LDH-B double KO cancer cells.

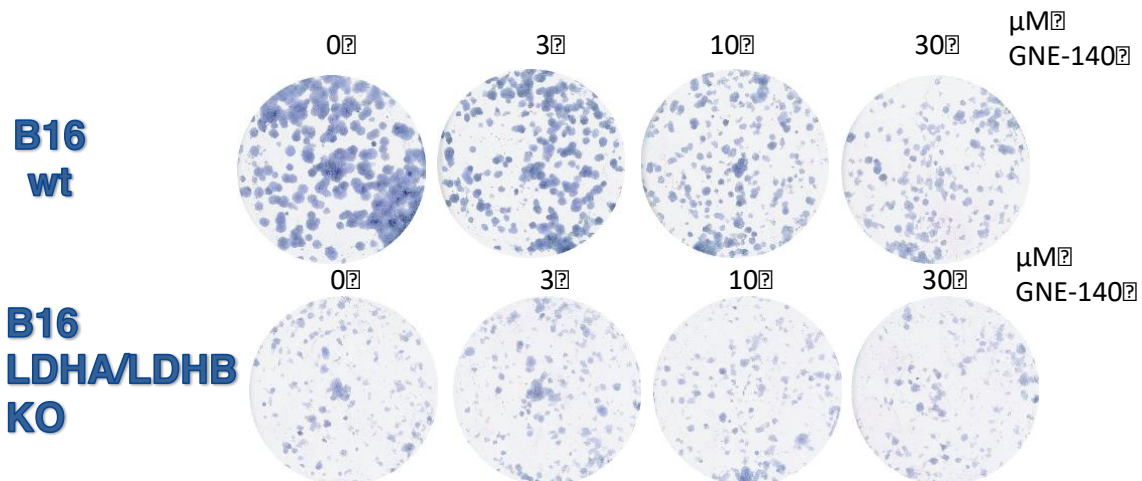


Figure 4.55. Clonogenic assay. Cells ($0,75 \times 10^3$) were plated into 12-well plates in 1,5 ml of RPMI, in duplicate for the different GNE-140 doses. GNE-140 is added after 24h. Cells were stained with 5% Giemsa solution after 7 days for colony visualization.

As it is shown in clonogenic assay (Fig. 4.55B), there is an inhibition of the capacity to form colonies for B16 WT in dose-dependent manner by using three doses of the compound, but not for the B16 LDH-A/LDH-B dKO.

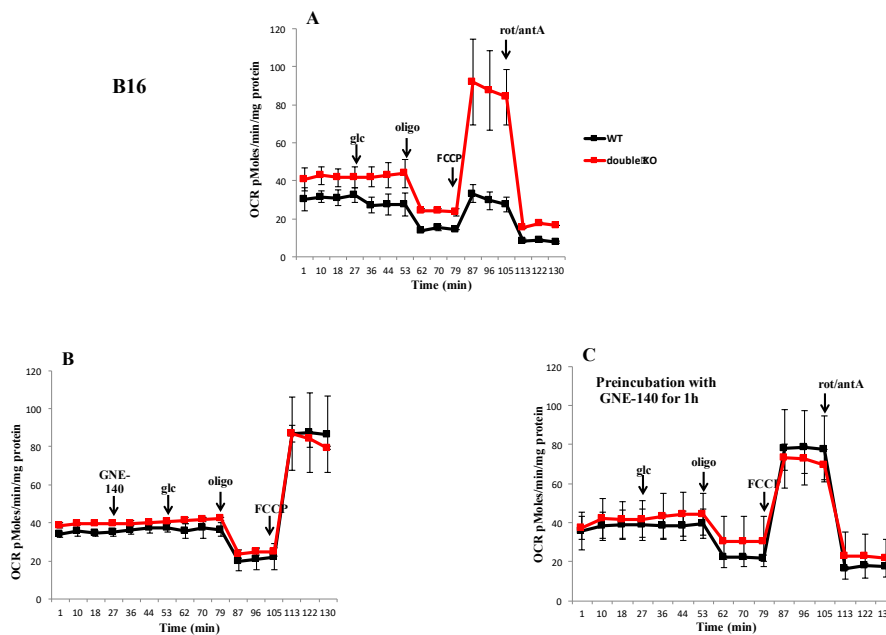


Figure 4.56 Oxygen consumption rate (OCR) analysis by Seahorse XF24 in B16 clones. (A) OCR profiles by sequential compounds' addition (10mM glucose, 1 μ M oligomycin, 3 μ M FCCP, 1 μ M rotenone/1 μ M antimycinA), express as pMolesO₂/min/ μ g protein; (B) OCR profiles by sequential compounds' addition (10 μ M GNE-140, 10 mM glucose, 1 μ M oligomycin, 3 μ M FCCP). (C) Pre-incubation with 10 μ M GNE-140 for 1 h; during the experiment, sequential compounds were added as in (A).

The analysis of OCR (Oxygen Consumption Rate) with a Seahorse XF24 analyser (Fig. 4.56) shows different response profiles to various compounds for the WT and the LDH-A/LDH-B dKO in absence of the compound GNE-140 (Fig. 4.56A). Instead, the treatment of both clones with GNE-140 (10 μ M) induces the WT to mimic the LDH-A/LDH-B dKO profile (Fig. 4.56 B-C).

In conclusion, from these experiments on B16 cells, by comparing genetic with the pharmacological inhibition of the enzyme Lactate Dehydrogenase, we can confirm the specificity of the target of GNE-140.

DISCUSSION

Because of the important role of Lactate Dehydrogenase in cancer metabolism, already discussed above, the attenuation or depletion of this enzyme results really fundamental to understand well the LDH role and its inhibition in the cure of cancer.

The LDH-A knockdown, already studied by others, resulted in the reprogramming of pyruvate metabolism and in the stimulation of mitochondrial respiration, leading to a compromised proliferation rate under hypoxia (Fantin et al. 2006) and a severe restriction of tumor growth, *in vivo* (Xie et al. 2014).

For a more complete understand of the LDH role, a total depletion of this enzyme was necessary. The innovative CRISPR/Cas9 technology allowed to obtain highly specific and efficient LDH gene knock-out in two cell lines. In LS174 colon adenocarcinoma and in mouse B16 melanoma, the Knock-Out of LDH-A (isoform overexpressed in many tumors) resulted in a reduction of lactic acid secretion only moderately. These findings led to work also on the KO of the LDH-B isoform, obtaining LDH-A and LDH-B single and double KO (Figures 4.46 - 4.47 - 4.48).

The LDH-B CRISPR-Cas9 plasmid emerged to be more efficient than the plasmid for LDH-A KO, allowing to obtain KO clones more easily and in less time, as confirmed also by my experiments on U87 glioblastoma cell line (Fig. 4.45).

By characterizing the LS174T and B16 LDH KO clones obtained, we can assert that the presence of LDH-A activity, in WT and LDHB-KO, makes the cells highly plastic to adapt to oxygen deficiency and to switch from OXPHOS to glycolysis, for survival and growth (Fig. 4.54). In addition, the LDH depletion (LDH-A/LDH-B double KO clones), impairing the lactic acid production (Figures 4.50 – 4.51), reduces the proliferation rate which results strongly affected in hypoxic conditions (Fig. 4.49). This higher sensitivity to hypoxic conditions is connected with metabolism switch from glycolysis to mitochondrial respiration of LDH dKO cells, as confirmed by Oxygen Consumption Rate (OCR) analysis (Figures 4.52 – 4.53) and the higher sensitivity to OXPHOS inhibitors (Fig. 4.54).

Over the utility of LDH dKO to understand well the LDH role in cancer cells, in the last part of the study, is underlined the usefulness of LDH dKO as control to compare the effects of LDH inhibitors (Figures 4.55 – 4.56), confirming the specificity of the target.

FINAL DISCUSSION

The reprogramming of energy metabolism represents one of the recently emerged hallmark of cancer as consequence of the alteration of oncogenes and oncosuppressors (Hanahan and Weinberg 2011). Otto Warburg was the first to observe that cancer cells can reprogram their glucose metabolism through the degradation of glucose to lactate even in the presence of oxygen (WARBURG 1956). This metabolic state, termed “aerobic glycolysis”, also provides the intermediates of the citric acid cycle as building block for cell growth and proliferation (DeBerardinis et al. 2008). Moreover, lactate seems to be the main cause of tumor acidity; in cancer cells, it is highly produced by the overexpressed LDH-A enzymatic isoform. Noteworthy, because LDH activity is not needed for pyruvate metabolism through the TCA cycle and for its position at the end of glycolytic pathway, LDH represents a significant therapeutic target. Unfortunately, the development of LDH inhibitors suitable for clinical use is proving a very difficult task, as established by our experience with the PRIN project and confirmed also by different studies involving multinational drug companies (Ward et al. 2012, Billiard et al. 2013, Fauber et al. 2014, Xie et al. 2014). As Galloflavin, the best compound found by our approach, due to its poor solubility, did not prove to be a practical starting point for structural modifications, the research of a more suitable hit in the search for new LDH-A inhibitors has been part of my thesis work. A new class of LDH-A inhibitors in a series of N-acylhy-drazone derivatives (Experimental Part 1B) and the natural urolithin M6 (Experimental Part 2B) were identified as possible chemical and biological galloflavin mimetics. Thus, they represent new starting points in the research of small molecule inhibitors.

Despite the difficulty to find LDH inhibitors suitable for clinical, the availability of in vitro active compounds allows at present a better understanding of the potentiality of LDH inhibition in anticancer treatments.

In Experimental Part 1A, we showed that two LDH inhibitors (oxamate and galloflavin) can increase the efficacy of cisplatin in cultured Burkitt's lymphoma cells (Loukes cells). This result has been demonstrated to be due to the induction of ROS production by LDH inhibition; ROS can be a further cause of DNA damage, which added to that produced by

cisplatin, leading to the failure of the response repair. Noteworthy, this potentiating effect is not exerted in proliferating normal lymphocytes.

In Experimental Part 2A, we illustrate that treatment of human colon adenocarcinoma cells (CaCo2 cells) with two pro-inflammatory cytokines, TNF- α and IL-17, modifies LDH activity, causing a shift toward the A isoform which results in increased lactate production. At the same time, the two cytokines appeared to induce features of epithelial-mesenchymal transition in the treated cells, such as reduction of E-cadherin levels and increased secretion of metalloproteinases. Notable, LDH activity inhibition with oxamate and galloflavin, were found to relieve the inflammation-induced effects.

In Experimental Part 3A, we explored the relationship between Heat Shock Response (HSR) and LDH-A. In cancer tissues, constitutive activation of HSR plays a major role in helping cell survival and proliferation. The transcription inducer of HSPs (Heat Shock Proteins), HSF-1, also activates glycolytic metabolism and increases the expression of LDH-A. So, by using two enzyme inhibitors (oxamate and galloflavin), in cultured hepatocellular carcinoma cells, we found that the reduction of LDH-A activity led to decreased level and function of the major HSPs involved in tumorigenesis. In addition, galloflavin (a polyphenol) also inhibited the ATPase activity of two of the examined HSPs. Finally, hindering HSR markedly lowered the alpha-fetoprotein cellular levels and induced senescence.

These studies leading us to assume LDH-A as common elements coordinating neoplastic proliferation, invasive growth and inflammation, suggesting for LDH inhibitor compounds a wider potential in anticancer treatment.

An important and fundamental way to understand well the LDH role in cancer cells is the Knock-Out of the LDH genes. This approach allows to study the effects of the LDH activity absence without taking into account the possible non-specific effects of the inhibitors.

This has been possible thank to the new innovative technology of CRISPR/Cas9. LDH-A and LDH-B single and double KO have been obtained in LS174T colon adenocarcinoma and in B16 mouse melanoma cells.

In both cell lines, LDHA-KO reduces the lactic acid secretion rate only moderately, indicating that also the B isoform of LDH enzyme can convert pyruvate to lactate in LDHA-KO cells. But, at the same time, cells without the A isoform show a higher sensitivity to OXPHOS inhibitors (Fig. 4.54).

The depletion of both A and B isoforms is necessary to impair completely the lactic acid production (Fig. 4.50 – 4.51) with consequent reduction of the proliferation rate, especially in hypoxic (1% O₂) conditions (Fig. 4.49).

In conclusion, the genetic KO of LDH enzyme allowed us to understand that LS174T and B16, as generally happen for cancer cells, prefer to use the “aerobic glycolysis” even if their OXPHOS mechanisms are not impaired, but in case of need, most of them are able to switch their metabolism from glycolysis to OXPHOS, even if their ability to grow and proliferate are limited. Indeed, LDHA/LDHB double KO cells show to have developed higher maximal respiration capacity (Fig 4.53C) and a corresponding high spare respiratory capacity (Fig 4.53C), to use when they need.

Moreover, the genetic KO of LDH enzyme allowed us to confirm the specificity of the target for the actually only inhibitor with nanomolar potency *in vitro*, GNE-140 (Figures 4.55 – 4.56). For future perspective, this genetic knock-out represents an important help in the search of LDH inhibitors suitable for clinical use that is proved to be a very difficult task (see paragraph 1.2).

LDH inhibitor compounds represent a wider potential in anticancer treatment that can be increased by combination therapy with other therapeutic agents.

REFERENCES

- Adams, L. S., Y. Zhang, N. P. Seeram, D. Heber & S. Chen (2010) Pomegranate ellagitannin-derived compounds exhibit antiproliferative and antiaromatase activity in breast cancer cells in vitro. *Cancer Prev Res (Phila)*, 3, 108-13.
- Ahuja, P., P. Zhao, E. Angelis, H. Ruan, P. Korge, A. Olson, Y. Wang, E. S. Jin, F. M. Jeffrey, M. Portman & W. R. Maclellan (2010) Myc controls transcriptional regulation of cardiac metabolism and mitochondrial biogenesis in response to pathological stress in mice. *J Clin Invest*, 120, 1494-505.
- Allison, S. J., J. R. Knight, C. Granchi, R. Rani, F. Minutolo, J. Milner & R. M. Phillips (2014) Identification of LDH-A as a therapeutic target for cancer cell killing via (i) p53/NAD(H)-dependent and (ii) p53-independent pathways. *Oncogenesis*, 3, e102.
- Armstrong, D. & R. Browne (1994) The analysis of free radicals, lipid peroxides, antioxidant enzymes and compounds related to oxidative stress as applied to the clinical chemistry laboratory. *Adv Exp Med Biol*, 366, 43-58.
- Bao, Y., K. Mukai, T. Hishiki, A. Kubo, M. Ohmura, Y. Sugiura, T. Matsuura, Y. Nagahata, N. Hayakawa, T. Yamamoto, R. Fukuda, H. Saya, M. Suematsu & Y. A. Minamishima (2013) Energy management by enhanced glycolysis in G1-phase in human colon cancer cells in vitro and in vivo. *Mol Cancer Res*, 11, 973-85.
- Barker SB, Summerson WH. The colorimetric determination of lactic acid in biological material. *J Biol Chem* 1941; 138:535-554.
- Barrallo-Gimeno, A. & M. A. Nieto (2005) The Snail genes as inducers of cell movement and survival: implications in development and cancer. *Development*, 132, 3151-61.
- Basak, N. P., A. Roy & S. Banerjee (2014) Alteration of mitochondrial proteome due to activation of Notch1 signaling pathway. *J Biol Chem*, 289, 7320-34.
- Baumann, F., P. Leukel, A. Doerfelt, C. P. Beier, K. Dettmer, P. J. Oefner, M. Kastenberger, M. Kreutz, T. Nickl-Jockschat, U. Bogdahn, A. K. Bosserhoff & P. Hau (2009) Lactate promotes glioma migration by TGF-beta2-dependent regulation of matrix metalloproteinase-2. *Neuro Oncol*, 11, 368-80.
- Beckert, S., F. Farrahi, R. S. Aslam, H. Scheuenstuhl, A. Königsrainer, M. Z. Hussain & T. K. Hunt (2006) Lactate stimulates endothelial cell migration. *Wound Repair Regen*, 14, 321-4.
- Ben-Neriah, Y. & M. Karin (2011) Inflammation meets cancer, with NF-κB as the matchmaker. *Nat Immunol*, 12, 715-23.
- Bialonska, D., S. G. Kasimsetty, S. I. Khan & D. Ferreira (2009) Urolithins, intestinal microbial metabolites of Pomegranate ellagitannins, exhibit potent antioxidant activity in a cell-based assay. *J Agric Food Chem*, 57, 10181-6.
- Billiard, J., J. B. Dennison, J. Briand, R. S. Annan, D. Chai, M. Colón, C. S. Dodson, S. A. Gilbert, J. Greshock, J. Jing, H. Lu, J. E. McSurdy-Freed, L. A. Orband-Miller, G. B. Mills, C. J. Quinn, J. L. Schneck, G. F. Scott, A. N. Shaw, G. M. Waitt, R. F. Wooster & K. J. Duffy (2013) Quinoline 3-sulfonamides inhibit lactate dehydrogenase A and reverse aerobic glycolysis in cancer cells. *Cancer Metab*, 1, 19.
- Bonuccelli, G., A. Tsigos, D. Whitaker-Menezes, S. Pavlides, R. G. Pestell, B. Chiavarina, P. G. Frank, N. Flomenberg, A. Howell, U. E. Martinez-Outschoorn, F. Sotgia & M. P. Lisanti (2010) Ketones and lactate "fuel" tumor growth and metastasis: Evidence that epithelial cancer cells use oxidative mitochondrial metabolism. *Cell Cycle*, 9, 3506-14.

- Boudreau, A., H. E. Purkey, A. Hitz, K. Robarge, D. Peterson, S. Labadie, M. Kwong, R. Hong, M. Gao, C. Del Nagro, R. Pusapati, S. Ma, L. Salphati, J. Pang, A. Zhou, T. Lai, Y. Li, Z. Chen, B. Wei, I. Yen, S. Sideris, M. McClelland, R. Firestein, L. Corson, A. Vanderbilt, S. Williams, A. Daemen, M. Belvin, C. Eigenbrot, P. K. Jackson, S. Malek, G. Hatzivassiliou, D. Sampath, M. Evangelista & T. O'Brien (2016) Metabolic plasticity underpins innate and acquired resistance to LDHA inhibition. *Nat Chem Biol*, 12, 779-86.
- Braconi, C., F. Meng, E. Swenson, L. Khrapenko, N. Huang & T. Patel (2009) Candidate therapeutic agents for hepatocellular cancer can be identified from phenotype-associated gene expression signatures. *Cancer*, 115, 3738-48.
- Brady, G., G. J. Macarthur & P. J. Farrell (2008) Epstein-Barr virus and Burkitt lymphoma. *Postgrad Med J*, 84, 372-7.
- Brand, A., K. Singer, G. E. Koehl, M. Kolitzus, G. Schoenhammer, A. Thiel, C. Matos, C. Bruss, S. Klobuch, K. Peter, M. Kastenberger, C. Bogdan, U. Schleicher, A. Mackensen, E. Ullrich, S. Fichtner-Feigl, R. Kesselring, M. Mack, U. Ritter, M. Schmid, C. Blank, K. Dettmer, P. J. Oefner, P. Hoffmann, S. Walenta, E. K. Geissler, J. Pouyssegur, A. Villunger, A. Steven, B. Seliger, S. Schreml, S. Haferkamp, E. Kohl, S. Karrer, M. Berneburg, W. Herr, W. Mueller-Klieser, K. Renner & M. Kreutz (2016) LDHA-Associated Lactic Acid Production Blunts Tumor Immunosurveillance by T and NK Cells. *Cell Metab*, 24, 657-671.
- Brand, M. D. & D. G. Nicholls (2011) Assessing mitochondrial dysfunction in cells. *Biochem J*, 435, 297-312.
- Breitinger, H.G., 2012. Drug Synergy – Mechanisms and Methods of Analysis. In: Acree, B., editor: Toxicity and Drug Testing, InTech. ISBN: 978-953-51-0004-1, <http://dx.doi.org/10.5772/30922>. <<http://www.intechopen.com/books/toxicity-and-drug-testing/drug-synergy-mechanisms-and-methods-of-analysis>>.
- Brizel, D. M., T. Schroeder, R. L. Scher, S. Walenta, R. W. Clough, M. W. Dewhirst & W. Mueller-Klieser (2001) Elevated tumor lactate concentrations predict for an increased risk of metastases in head-and-neck cancer. *Int J Radiat Oncol Biol Phys*, 51, 349-53.
- Burke, R. E., S. C. Harris & W. L. McGuire (1978) Lactate dehydrogenase in estrogen-responsive human breast cancer cells. *Cancer Res*, 38, 2773-6.
- Calderwood, S. K., M. A. Khaleque, D. B. Sawyer & D. R. Ciocca (2006) Heat shock proteins in cancer: chaperones of tumorigenesis. *Trends Biochem Sci*, 31, 164-72.
- Cantley, L. C. (2002) The phosphoinositide 3-kinase pathway. *Science*, 296, 1655-7.
- Chalah, A. & R. Khosravi-Far (2008) The mitochondrial death pathway. *Adv Exp Med Biol*, 615, 25-45.
- Chang, L., Y. Miyata, P. M. Ung, E. B. Bertelsen, T. J. McQuade, H. A. Carlson, E. R. Zuiderweg & J. E. Gestwicki (2011) Chemical screens against a reconstituted multiprotein complex: myricetin blocks DnaJ regulation of DnaK through an allosteric mechanism. *Chem Biol*, 18, 210-21.
- Chen, J. Q. & J. Russo (2012) Dysregulation of glucose transport, glycolysis, TCA cycle and glutaminolysis by oncogenes and tumor suppressors in cancer cells. *Biochim Biophys Acta*, 1826, 370-84.
- Cheng, W., A. Ainiwaer, L. Xiao, Q. Cao, G. Wu, Y. Yang, R. Mao & Y. Bao (2015) Role of the novel HSP90 inhibitor AUY922 in hepatocellular carcinoma: Potential for therapy. *Mol Med Rep*, 12, 2451-6.
- Cheung, E. C. & K. H. Vousden (2010) The role of p53 in glucose metabolism. *Curr Opin Cell Biol*, 22, 186-91.

- Chhabra, S., S. Jain, C. Wallace, F. Hong & B. Liu (2015) High expression of endoplasmic reticulum chaperone grp94 is a novel molecular hallmark of malignant plasma cells in multiple myeloma. *J Hematol Oncol*, 8, 77.
- Chi, K. N., E. Y. Yu, C. Jacobs, J. Bazov, C. Kollmannsberger, C. S. Higano, S. D. Mukherjee, M. E. Gleave, P. S. Stewart & S. J. Hotte (2016) A phase I dose-escalation study of apatorsen (OGX-427), an antisense inhibitor targeting heat shock protein 27 (Hsp27), in patients with castration-resistant prostate cancer and other advanced cancers. *Ann Oncol*, 27, 1116-22.
- Chomczynski, P. & N. Sacchi (1987) Single-step method of RNA isolation by acid guanidinium thiocyanate-phenol-chloroform extraction. *Anal Biochem*, 162, 156-9.
- Colic, M. & K. Pavelic (2000) Molecular mechanisms of anticancer activity of natural dietetic products. *J Mol Med (Berl)*, 78, 333-6.
- Cooke, M. S., M. D. Evans, M. Dizdaroglu & J. Lunec (2003) Oxidative DNA damage: mechanisms, mutation, and disease. *FASEB J*, 17, 1195-214.
- Cui, J., M. Shi, D. Xie, D. Wei, Z. Jia, S. Zheng, Y. Gao, S. Huang & K. Xie (2014) FOXM1 promotes the warburg effect and pancreatic cancer progression via transactivation of LDHA expression. *Clin Cancer Res*, 20, 2595-606.
- Cui, X. G., Z. T. Han, S. H. He, X. D. Wu, T. R. Chen, C. H. Shao, D. L. Chen, N. Su, Y. M. Chen, T. Wang, J. Wang, D. W. Song, W. J. Yan, X. H. Yang, T. Liu, H. F. Wei & J. Xiao (2017) HIF1/2 α mediates hypoxia-induced LDHA expression in human pancreatic cancer cells. *Oncotarget*, 8, 24840-24852.
- Dai, C., L. Whitesell, A. B. Rogers & S. Lindquist (2007) Heat shock factor 1 is a powerful multifaceted modifier of carcinogenesis. *Cell*, 130, 1005-18.
- Dai, R. P., F. X. Yu, S. R. Goh, H. W. Chng, Y. L. Tan, J. L. Fu, L. Zheng & Y. Luo (2008) Histone 2B (H2B) expression is confined to a proper NAD⁺/NADH redox status. *J Biol Chem*, 283, 26894-901.
- Davenport, J., M. Balch, L. Galam, A. Girgis, J. Hall, B. S. Blagg & R. L. Matts (2014) High-throughput screen of natural product libraries for hsp90 inhibitors. *Biology (Basel)*, 3, 101-38.
- De Simone, V., F. Pallone, G. Monteleone & C. Stolfi (2013) Role of TH17 cytokines in the control of colorectal cancer. *Oncoimmunology*, 2, e26617.
- Debacq-Chainiaux, F., J. D. Erusalimsky, J. Campisi & O. Toussaint (2009) Protocols to detect senescence-associated beta-galactosidase (SA-beta-gal) activity, a biomarker of senescent cells in culture and in vivo. *Nat Protoc*, 4, 1798-806.
- DeBerardinis, R. J., J. J. Lum, G. Hatzivassiliou & C. B. Thompson (2008) The biology of cancer: metabolic reprogramming fuels cell growth and proliferation. *Cell Metab*, 7, 11-20.
- Deng, H., J. Zheng, A. Clarke, J. J. Holbrook, R. Callender & J. W. Burgner (1994) Source of catalysis in the lactate dehydrogenase system. Ground-state interactions in the enzyme-substrate complex. *Biochemistry*, 33, 2297-305.
- Di Meo, F., V. Lemaire, J. Cornil, R. Lazzaroni, J. L. Duroux, Y. Olivier & P. Trouillas (2013) Free radical scavenging by natural polyphenols: atom versus electron transfer. *J Phys Chem A*, 117, 2082-92.
- Di Stefano, G., M. Manerba & M. Vettraino (2013) NAD metabolism and functions: a common therapeutic target for neoplastic, metabolic and neurodegenerative diseases. *Curr Top Med Chem*, 13, 2918-29.
- Ding, J., Z. H. Miao, L. H. Meng & M. Y. Geng (2006) Emerging cancer therapeutic opportunities target DNA-repair systems. *Trends Pharmacol Sci*, 27, 338-44.
- Dodou, K., R. J. Anderson, D. A. Small & P. W. Groundwater (2005) Investigations on gossypol: past and present developments. *Expert Opin Investig Drugs*, 14, 1419-34.

- Dorward, A. M. & G. Singh (1996) Energetic characteristics of cisplatin resistant ovarian carcinoma cells. *Anticancer Res*, 16, 443-7.
- Dos Santos Ferreira, A. C., R. A. Fernandes, J. K. Kwee & C. E. Klumb (2012) Histone deacetylase inhibitor potentiates chemotherapy-induced apoptosis through Bim upregulation in Burkitt's lymphoma cells. *J Cancer Res Clin Oncol*, 138, 317-25.
- Doudna, J. A. & E. Charpentier (2014) Genome editing. The new frontier of genome engineering with CRISPR-Cas9. *Science*, 346, 1258096.
- Draoui, N. & O. Feron (2011) Lactate shuttles at a glance: from physiological paradigms to anti-cancer treatments. *Dis Model Mech*, 4, 727-32.
- Drew, B. G., V. Ribas, J. A. Le, D. C. Henstridge, J. Phun, Z. Zhou, T. Soleymani, P. Daraei, D. Sitz, L. Vergnes, J. Wanagat, K. Reue, M. A. Febbraio & A. L. Hevener (2014) HSP72 is a mitochondrial stress sensor critical for Parkin action, oxidative metabolism, and insulin sensitivity in skeletal muscle. *Diabetes*, 63, 1488-505.
- Dworak, H.F., 1986. Tumors: wounds that do not heal, similarities between tumor stroma generation and wound healing. *N. Engl. J. Med.* 315, 1650–1659.
- Eszes, C. M., R. B. Sessions, A. R. Clarke, K. M. Moreton & J. J. Holbrook (1996) Removal of substrate inhibition in a lactate dehydrogenase from human muscle by a single residue change. *FEBS Lett*, 399, 193-7.
- Fan, J., T. Hitosugi, T. W. Chung, J. Xie, Q. Ge, T. L. Gu, R. D. Polakiewicz, G. Z. Chen, T. J. Boggon, S. Lonial, F. R. Khuri, S. Kang & J. Chen (2011) Tyrosine phosphorylation of lactate dehydrogenase A is important for NADH/NAD(+) redox homeostasis in cancer cells. *Mol Cell Biol*, 31, 4938-50.
- Fantin, V. R., J. St-Pierre & P. Leder (2006) Attenuation of LDH-A expression uncovers a link between glycolysis, mitochondrial physiology, and tumor maintenance. *Cancer Cell*, 9, 425-34.
- Farabegoli, F., M. Vettrai, M. Manerba, L. Fiume, M. Roberti & G. Di Stefano (2012) Galloflavin, a new lactate dehydrogenase inhibitor, induces the death of human breast cancer cells with different glycolytic attitude by affecting distinct signaling pathways. *Eur J Pharm Sci*, 47, 729-38.
- Farahani, E., H. K. Patra, J. R. Jangamreddy, I. Rashedi, M. Kawalec, R. K. Rao Pariti, P. Batakis & E. Wiechec (2014) Cell adhesion molecules and their relation to (cancer) cell stemness. *Carcinogenesis*, 35, 747-59.
- Fauber, B. P., P. S. Dragovich, J. Chen, L. B. Corson, C. Z. Ding, C. Eigenbrot, S. Labadie, S. Malek, D. Peterson, H. E. Purkey, K. Robarge, S. Sideris, M. Ultsch, B. Wei, I. Yen, Q. Yue & A. Zhou (2014) Identification of 3,6-disubstituted dihydropyrones as inhibitors of human lactate dehydrogenase. *Bioorg Med Chem Lett*, 24, 5683-5687.
- Ferruzza, S., C. Rossi, M. L. Scarino & Y. Sambuy (2012) A protocol for in situ enzyme assays to assess the differentiation of human intestinal Caco-2 cells. *Toxicol In Vitro*, 26, 1247-51.
- Firth, J. D., B. L. Ebert & P. J. Ratcliffe (1995) Hypoxic regulation of lactate dehydrogenase A. Interaction between hypoxia-inducible factor 1 and cAMP response elements. *J Biol Chem*, 270, 21021-7.
- Fiume, L., M. Manerba, M. Vettrai & G. Di Stefano (2010) Impairment of aerobic glycolysis by inhibitors of lactic dehydrogenase hinders the growth of human hepatocellular carcinoma cell lines. *Pharmacology*, 86, 157-62.
- (2014) Inhibition of lactate dehydrogenase activity as an approach to cancer therapy. *Future Med Chem*, 6, 429-45.
- Formby, B. & R. Stern (2003) Lactate-sensitive response elements in genes involved in hyaluronan catabolism. *Biochem Biophys Res Commun*, 305, 203-8.

- Gao, S. & M. Hu (2010) Bioavailability challenges associated with development of anti-cancer phenolics. *Mini Rev Med Chem*, 10, 550-67.
- Gillies, R. J., I. Robey & R. A. Gatenby (2008) Causes and consequences of increased glucose metabolism of cancers. *J Nucl Med*, 49 Suppl 2, 24S-42S.
- GOLDMAN, R. D., N. O. KAPLAN & T. C. HALL (1964) LACTIC DEHYDROGENASE IN HUMAN NEOPLASTIC TISSUES. *Cancer Res*, 24, 389-99.
- González-Sarriás, A., J. C. Espín, F. A. Tomás-Barberán & M. T. García-Conesa (2009) Gene expression, cell cycle arrest and MAPK signalling regulation in Caco-2 cells exposed to ellagic acid and its metabolites, urolithins. *Mol Nutr Food Res*, 53, 686-98.
- Granchi, C., S. Bertini, M. Macchia & F. Minutolo (2010) Inhibitors of lactate dehydrogenase isoforms and their therapeutic potentials. *Curr Med Chem*, 17, 672-97.
- Granja, S., I. Marchiq, R. Le Floch, C. S. Moura, F. Baltazar & J. Pouyssegur (2015) Disruption of BASIGIN decreases lactic acid export and sensitizes non-small cell lung cancer to biguanides independently of the LKB1 status. *Oncotarget*, 6, 6708-21.
- Grivennikov, S. I., F. R. Greten & M. Karin (2010) Immunity, inflammation, and cancer. *Cell*, 140, 883-99.
- Halestrap, A. P. (2012) The monocarboxylate transporter family--Structure and functional characterization. *IUBMB Life*, 64, 1-9.
- (2013) Monocarboxylic acid transport. *Compr Physiol*, 3, 1611-43.
- Halestrap, A. P. & R. M. Denton (1974) Specific inhibition of pyruvate transport in rat liver mitochondria and human erythrocytes by alpha-cyano-4-hydroxycinnamate. *Biochem J*, 138, 313-6.
- Hanahan, D. & R. A. Weinberg (2011) Hallmarks of cancer: the next generation. *Cell*, 144, 646-74.
- He, H., M. C. Lee, L. L. Zheng, L. Zheng & Y. Luo (2013) Integration of the metabolic/redox state, histone gene switching, DNA replication and S-phase progression by moonlighting metabolic enzymes. *Biosci Rep*, 33, e00018.
- Hernlund, E., L. S. Ihlund, O. Khan, Y. O. Ates, S. Linder, T. Panaretakis & M. C. Shoshan (2008) Potentiation of chemotherapeutic drugs by energy metabolism inhibitors 2-deoxyglucose and etomoxir. *Int J Cancer*, 123, 476-483.
- Heussen, C. & E. B. Dowdle (1980) Electrophoretic analysis of plasminogen activators in polyacrylamide gels containing sodium dodecyl sulfate and copolymerized substrates. *Anal Biochem*, 102, 196-202.
- Hewitt, C. O., C. M. Eszes, R. B. Sessions, K. M. Moreton, T. R. Dafforn, J. Takei, C. E. Dempsey, A. R. Clarke & J. J. Holbrook (1999) A general method for relieving substrate inhibition in lactate dehydrogenases. *Protein Eng*, 12, 491-6.
- Ihlund, L. S., E. Hernlund, O. Khan & M. C. Shoshan (2008) 3-Bromopyruvate as inhibitor of tumour cell energy metabolism and chemopotentiator of platinum drugs. *Mol Oncol*, 2, 94-101.
- Ishimoto, H., M. Shibata, Y. Myojin, H. Ito, Y. Sugimoto, A. Tai & T. Hatano (2011) In vivo anti-inflammatory and antioxidant properties of ellagitannin metabolite urolithin A. *Bioorg Med Chem Lett*, 21, 5901-4.
- Ito, H., A. Iguchi & T. Hatano (2008) Identification of urinary and intestinal bacterial metabolites of ellagitannin geraniin in rats. *J Agric Food Chem*, 56, 393-400.
- Iyer, N. V., L. E. Kotch, F. Agani, S. W. Leung, E. Laughner, R. H. Wenger, M. Gassmann, J. D. Gearhart, A. M. Lawler, A. Y. Yu & G. L. Semenza (1998) Cellular and developmental control of O₂ homeostasis by hypoxia-inducible factor 1 alpha. *Genes Dev*, 12, 149-62.
- Jamieson, E. R. & S. J. Lippard (1999) Structure, Recognition, and Processing of Cisplatin-DNA Adducts. *Chem Rev*, 99, 2467-98.

- Jego, G., A. Hazoumé, R. Seigneuric & C. Garrido (2013) Targeting heat shock proteins in cancer. *Cancer Lett*, 332, 275-85.
- Jiang, B. H., F. Agani, A. Passaniti & G. L. Semenza (1997) V-SRC induces expression of hypoxia-inducible factor 1 (HIF-1) and transcription of genes encoding vascular endothelial growth factor and enolase 1: involvement of HIF-1 in tumor progression. *Cancer Res*, 57, 5328-35.
- Jiang, S., K. Tu, Q. Fu, D. C. Schmitt, L. Zhou, N. Lu & Y. Zhao (2015) Multifaceted roles of HSF1 in cancer. *Tumour Biol*, 36, 4923-31.
- Jones, R. G. & C. B. Thompson (2009) Tumor suppressors and cell metabolism: a recipe for cancer growth. *Genes Dev*, 23, 537-48.
- Kalmar, B. & L. Greensmith (2009) Induction of heat shock proteins for protection against oxidative stress. *Adv Drug Deliv Rev*, 61, 310-8.
- Kanno, T., K. Sudo, M. Kitamura, S. Miwa, A. Ichiyama & Y. Nishimura (1983) Lactate dehydrogenase A-subunit and B-subunit deficiencies: comparison of the physiological roles of LDH isozymes. *Isozymes Curr Top Biol Med Res*, 7, 131-50.
- Kanno, T., K. Sudo, M. Maekawa, Y. Nishimura, M. Ukita & K. Fukutake (1988) Lactate dehydrogenase M-subunit deficiency: a new type of hereditary exertional myopathy. *Clin Chim Acta*, 173, 89-98.
- Kartalou, M. & J. M. Essigmann (2001) Mechanisms of resistance to cisplatin. *Mutat Res*, 478, 23-43.
- Kato, Y., S. Ozawa, C. Miyamoto, Y. Maehata, A. Suzuki, T. Maeda & Y. Baba (2013) Acidic extracellular microenvironment and cancer. *Cancer Cell Int*, 13, 89.
- Klein, H. L. (2008) The consequences of Rad51 overexpression for normal and tumor cells. *DNA Repair (Amst)*, 7, 686-93.
- Kohlmann, A., S. G. Zech, F. Li, T. Zhou, R. M. Squillace, L. Commodore, M. T. Greenfield, X. Lu, D. P. Miller, W. S. Huang, J. Qi, R. M. Thomas, Y. Wang, S. Zhang, R. Dodd, S. Liu, R. Xu, Y. Xu, J. J. Miret, V. Rivera, T. Clackson, W. C. Shakespeare, X. Zhu & D. C. Dalgarno (2013) Fragment growing and linking lead to novel nanomolar lactate dehydrogenase inhibitors. *J Med Chem*, 56, 1023-40.
- Koukourakis, M. I., A. Giatromanolaki, E. Sivridis, G. Bougioukas, V. Didilis, K. C. Gatter, A. L. Harris & T. a. A. R. Group (2003a) Lactate dehydrogenase-5 (LDH-5) overexpression in non-small-cell lung cancer tissues is linked to tumour hypoxia, angiogenic factor production and poor prognosis. *Br J Cancer*, 89, 877-85.
- Koukourakis, M. I., A. Giatromanolaki, E. Sivridis & T. a. A. R. Group (2003b) Lactate dehydrogenase isoenzymes 1 and 5: differential expression by neoplastic and stromal cells in non-small cell lung cancer and other epithelial malignant tumors. *Tumour Biol*, 24, 199-202.
- Kraus, S. & N. Arber (2009) Inflammation and colorectal cancer. *Curr Opin Pharmacol*, 9, 405-10.
- Kroemer, G. & J. Pouyssegur (2008) Tumor cell metabolism: cancer's Achilles' heel. *Cancer Cell*, 13, 472-82.
- Kumar, S., T. R. Donti, N. Agnihotri & K. Mehta (2014) Transglutaminase 2 reprogramming of glucose metabolism in mammary epithelial cells via activation of inflammatory signaling pathways. *Int J Cancer*, 134, 2798-807.
- Larrosa, M., A. González-Sarrías, M. J. Yáñez-Gascón, M. V. Selma, M. Azorín-Ortuño, S. Toti, F. Tomás-Barberán, P. Dolara & J. C. Espín (2010) Anti-inflammatory properties of a pomegranate extract and its metabolite urolithin-A in a colitis rat model and the effect of colon inflammation on phenolic metabolism. *J Nutr Biochem*, 21, 717-25.

- Lauten, M., C. Beger, K. Gerdes, G. Asgedom, C. Kardinal, K. Welte & M. Schrappe (2003) Expression of heat-shock protein 90 in glucocorticoid-sensitive and -resistant childhood acute lymphoblastic leukaemia. *Leukemia*, 17, 1551-6.
- Le, A., C. R. Cooper, A. M. Gouw, R. Dinavahi, A. Maitra, L. M. Deck, R. E. Royer, D. L. Vander Jagt, G. L. Semenza & C. V. Dang (2010) Inhibition of lactate dehydrogenase A induces oxidative stress and inhibits tumor progression. *Proc Natl Acad Sci U S A*, 107, 2037-42.
- Lee, C. Y., Y. S. Moon, J. H. Yuan & A. F. Chen (1982) Enzyme inactivation and inhibition by gossypol. *Mol Cell Biochem*, 47, 65-70.
- Lee, J. W., P. Wang, M. G. Kattah, S. Youssef, L. Steinman, K. DeFea & D. S. Straus (2008) Differential regulation of chemokines by IL-17 in colonic epithelial cells. *J Immunol*, 181, 6536-45.
- Leidgens, V., C. Seliger, B. Jachnik, T. Welz, P. Leukel, A. Vollmann-Zwerenz, U. Bogdahn, M. Kreutz, O. M. Grauer & P. Hau (2015) Ibuprofen and Diclofenac Restrict Migration and Proliferation of Human Glioma Cells by Distinct Molecular Mechanisms. *PLoS One*, 10, e0140613.
- Leung, E. Y., J. E. Kim, M. Askarian-Amiri, W. R. Joseph, M. J. McKeage & B. C. Baguley (2014) Hormone Resistance in Two MCF-7 Breast Cancer Cell Lines is Associated with Reduced mTOR Signaling, Decreased Glycolysis, and Increased Sensitivity to Cytotoxic Drugs. *Front Oncol*, 4, 221.
- Levine, A. J. & A. M. Puzio-Kuter (2010) The control of the metabolic switch in cancers by oncogenes and tumor suppressor genes. *Science*, 330, 1340-4.
- Lewandowska, U., K. Szewczyk, E. Hrabec, A. Janecka & S. Gorkach (2013) Overview of metabolism and bioavailability enhancement of polyphenols. *J Agric Food Chem*, 61, 12183-99.
- Lewis, B. C., H. Shim, Q. Li, C. S. Wu, L. A. Lee, A. Maity & C. V. Dang (1997) Identification of putative c-Myc-responsive genes: characterization of rcl, a novel growth-related gene. *Mol Cell Biol*, 17, 4967-78.
- Liu, T., Y. Zhou, K. S. Ko & H. Yang (2015) Interactions between Myc and Mediators of Inflammation in Chronic Liver Diseases. *Mediators Inflamm*, 2015, 276850.
- Loar, P., H. Wahl, M. Kshirsagar, G. Gossner, K. Griffith & J. R. Liu (2010) Inhibition of glycolysis enhances cisplatin-induced apoptosis in ovarian cancer cells. *Am J Obstet Gynecol*, 202, 371.e1-8.
- Longley, D. B. & P. G. Johnston (2005) Molecular mechanisms of drug resistance. *J Pathol*, 205, 275-92.
- Lu, H., C. L. Dalgard, A. Mohyeldin, T. McFate, A. S. Tait & A. Verma (2005) Reversible inactivation of HIF-1 prolyl hydroxylases allows cell metabolism to control basal HIF-1. *J Biol Chem*, 280, 41928-39.
- Lu, J., M. Tan & Q. Cai (2015) The Warburg effect in tumor progression: mitochondrial oxidative metabolism as an anti-metastasis mechanism. *Cancer Lett*, 356, 156-64.
- Madhok, B. M., S. Yeluri, S. L. Perry, T. A. Hughes & D. G. Jayne (2010) Dichloroacetate induces apoptosis and cell-cycle arrest in colorectal cancer cells. *Br J Cancer*, 102, 1746-52.
- Majumder, P. K. & W. R. Sellers (2005) Akt-regulated pathways in prostate cancer. *Oncogene*, 24, 7465-74.
- Maltepe, E., J. V. Schmidt, D. Baunoch, C. A. Bradfield & M. C. Simon (1997) Abnormal angiogenesis and responses to glucose and oxygen deprivation in mice lacking the protein ARNT. *Nature*, 386, 403-7.
- Manerba, M., L. Di Ianni, L. Fiume, M. Roberti, M. Recanatini & G. Di Stefano (2015) Lactate dehydrogenase inhibitors sensitize lymphoma cells to cisplatin without

- enhancing the drug effects on immortalized normal lymphocytes. *Eur J Pharm Sci*, 74, 95-102.
- Manerba, M., L. Di Ianni, M. Govoni, M. Roberti, M. Recanatini & G. Di Stefano (2017a) Lactate dehydrogenase inhibitors can reverse inflammation induced changes in colon cancer cells. *Eur J Pharm Sci*, 96, 37-44.
- (2017b) LDH inhibition impacts on heat shock response and induces senescence of hepatocellular carcinoma cells. *Eur J Pharm Sci*, 105, 91-98.
- Manerba, M., M. Vettraino, L. Fiume, G. Di Stefano, A. Sartini, E. Giacomini, R. Buonfiglio, M. Roberti & M. Recanatini (2012) Galloflavin (CAS 568-80-9): a novel inhibitor of lactate dehydrogenase. *ChemMedChem*, 7, 311-7.
- Marchini, A., R. Longnecker & E. Kieff (1992) Epstein-Barr virus (EBV)-negative B-lymphoma cell lines for clonal isolation and replication of EBV recombinants. *J Virol*, 66, 4972-81.
- Marchiq, I., R. Le Floch, D. Roux, M. P. Simon & J. Pouyssegur (2015) Genetic disruption of lactate/H⁺ symporters (MCTs) and their subunit CD147/BASIGIN sensitizes glycolytic tumor cells to phenformin. *Cancer Res*, 75, 171-80.
- Markert, C. L., J. B. Shaklee & G. S. Whitt (1975) Evolution of a gene. Multiple genes for LDH isozymes provide a model of the evolution of gene structure, function and regulation. *Science*, 189, 102-14.
- Marullo, R., E. Werner, N. Degtyareva, B. Moore, G. Altavilla, S. S. Ramalingam & P. W. Doetsch (2013) Cisplatin induces a mitochondrial-ROS response that contributes to cytotoxicity depending on mitochondrial redox status and bioenergetic functions. *PLoS One*, 8, e81162.
- Maxwell, P. H., G. U. Dachs, J. M. Gleadle, L. G. Nicholls, A. L. Harris, I. J. Stratford, O. Hankinson, C. W. Pugh & P. J. Ratcliffe (1997) Hypoxia-inducible factor-1 modulates gene expression in solid tumors and influences both angiogenesis and tumor growth. *Proc Natl Acad Sci U S A*, 94, 8104-9.
- McFate, T., A. Mohyeldin, H. Lu, J. Thakar, J. Henriques, N. D. Halim, H. Wu, M. J. Schell, T. M. Tsang, O. Teahan, S. Zhou, J. A. Califano, N. H. Jeung, R. A. Harris & A. Verma (2008) Pyruvate dehydrogenase complex activity controls metabolic and malignant phenotype in cancer cells. *J Biol Chem*, 283, 22700-8.
- Meijer, T. W., O. C. Schuurbijs, J. H. Kaanders, M. G. Looijen-Salamon, L. F. de Geus-Oei, A. F. Verhagen, J. Lok, H. F. van der Heijden, S. E. Rademakers, P. N. Span & J. Bussink (2012) Differences in metabolism between adeno- and squamous cell non-small cell lung carcinomas: spatial distribution and prognostic value of GLUT1 and MCT4. *Lung Cancer*, 76, 316-23.
- Miles, M. F., P. Hung & R. A. Jungmann (1981) Cyclic AMP regulation of lactate dehydrogenase. Quantitation of lactate dehydrogenase M-subunit messenger RNA in isoproterenol- and N⁶,O^{2'}-dibutyryl cyclic AMP-stimulated rat C6 glioma cells by hybridization analysis using a cloned cDNA probe. *J Biol Chem*, 256, 12545-52.
- Min, C., S. F. Eddy, D. H. Sherr & G. E. Sonenshein (2008) NF-kappaB and epithelial to mesenchymal transition of cancer. *J Cell Biochem*, 104, 733-44.
- Miyajima, H., Y. Takahashi, M. Suzuki, T. Shimizu & E. Kaneko (1993) Molecular characterization of gene expression in human lactate dehydrogenase-A deficiency. *Neurology*, 43, 1414-9.
- Moran, J. H. & R. G. Schnellmann (1996) A rapid beta-NADH-linked fluorescence assay for lactate dehydrogenase in cellular death. *J Pharmacol Toxicol Methods*, 36, 41-4.
- Moretti, M., J. Bennett, L. Tornatore, A. K. Thotakura & G. Franzoso (2012) Cancer: NF-kB regulates energy metabolism. *Int J Biochem Cell Biol*, 44, 2238-43.

- Morimoto, R. I. (1993) Cells in stress: transcriptional activation of heat shock genes. *Science*, 259, 1409-10.
- O'Rourke, J. F., C. W. Pugh, S. M. Bartlett & P. J. Ratcliffe (1996) Identification of hypoxically inducible mRNAs in HeLa cells using differential-display PCR. Role of hypoxia-inducible factor-1. *Eur J Biochem*, 241, 403-10.
- Olaussen, K. A., J. Adam, E. Vanhecke, P. Vielh, R. Pirker, L. Friboulet, H. Popper, A. Robin, F. Commo, J. Thomale, L. Kayitalire, M. Filipits, T. Le Chevalier, F. André, E. Brambilla & J. C. Soria (2013) PARP1 impact on DNA repair of platinum adducts: preclinical and clinical read-outs. *Lung Cancer*, 80, 216-22.
- Osthus, R. C., H. Shim, S. Kim, Q. Li, R. Reddy, M. Mukherjee, Y. Xu, D. Wonsey, L. A. Lee & C. V. Dang (2000) Deregulation of glucose transporter 1 and glycolytic gene expression by c-Myc. *J Biol Chem*, 275, 21797-800.
- PAPACONSTANTINO, J. & S. P. COLOWICK (1961) The role of glycolysis in the growth of tumor cells. I. Effects of oxamic acid on the metabolism of Ehrlich ascites tumor cells in vitro. *J Biol Chem*, 236, 278-84.
- Pavlidis, S., D. Whitaker-Menezes, R. Castello-Cros, N. Flomenberg, A. K. Witkiewicz, P. G. Frank, M. C. Casimiro, C. Wang, P. Fortina, S. Addya, R. G. Pestell, U. E. Martinez-Outschoorn, F. Sotgia & M. P. Lisanti (2009) The reverse Warburg effect: aerobic glycolysis in cancer associated fibroblasts and the tumor stroma. *Cell Cycle*, 8, 3984-4001.
- Peng, G. & Y. Liu (2015) Hypoxia-inducible factors in cancer stem cells and inflammation. *Trends Pharmacol Sci*, 36, 374-83.
- Perl, A. K., P. Wilgenbus, U. Dahl, H. Semb & G. Christofori (1998) A causal role for E-cadherin in the transition from adenoma to carcinoma. *Nature*, 392, 190-3.
- Petrelli, F., M. Cabiddu, A. Coinu, K. Borgonovo, M. Ghilardi, V. Lonati & S. Barni (2015) Prognostic role of lactate dehydrogenase in solid tumors: a systematic review and meta-analysis of 76 studies. *Acta Oncol*, 54, 961-70.
- Pinheiro, C., A. Longatto-Filho, J. Azevedo-Silva, M. Casal, F. C. Schmitt & F. Baltazar (2012) Role of monocarboxylate transporters in human cancers: state of the art. *J Bioenerg Biomembr*, 44, 127-39.
- Pioli, P. A., B. J. Hamilton, J. E. Connolly, G. Brewer & W. F. Rigby (2002) Lactate dehydrogenase is an AU-rich element-binding protein that directly interacts with AUF1. *J Biol Chem*, 277, 35738-45.
- Poole, R. C. & A. P. Halestrap (1993) Transport of lactate and other monocarboxylates across mammalian plasma membranes. *Am J Physiol*, 264, C761-82.
- Rademakers, S. E., J. Lok, A. J. van der Kogel, J. Bussink & J. H. Kaanders (2011) Metabolic markers in relation to hypoxia; staining patterns and colocalization of pimonidazole, HIF-1 α , CAIX, LDH-5, GLUT-1, MCT1 and MCT4. *BMC Cancer*, 11, 167.
- Ran, F. A., P. D. Hsu, J. Wright, V. Agarwala, D. A. Scott & F. Zhang (2013) Genome engineering using the CRISPR-Cas9 system. *Nat Protoc*, 8, 2281-2308.
- Read, J. A., V. J. Winter, C. M. Eszes, R. B. Sessions & R. L. Brady (2001) Structural basis for altered activity of M- and H-isozyme forms of human lactate dehydrogenase. *Proteins*, 43, 175-85.
- Rupiani, S., R. Buonfiglio, M. Manerba, L. Di Ianni, M. Vettrano, E. Giacomini, M. Masetti, F. Falchi, G. Di Stefano, M. Roberti & M. Recanatini (2015) Identification of N-acylhydrazone derivatives as novel lactate dehydrogenase A inhibitors. *Eur J Med Chem*, 101, 63-70.
- Rupiani, S., L. Guidotti, M. Manerba, L. D. Ianni, E. Giacomini, F. Falchi, G. Di Stefano, M. Roberti & M. Recanatini (2016) Synthesis of natural urolithin M6, a galloflavin

- mimetic, as a potential inhibitor of lactate dehydrogenase A. *Org Biomol Chem*, 14, 10981-10987.
- Ryan, H. E., J. Lo & R. S. Johnson (1998) HIF-1 alpha is required for solid tumor formation and embryonic vascularization. *EMBO J*, 17, 3005-15.
- Saigusa, S., K. Tanaka, Y. Toiyama, T. Yokoe, Y. Okugawa, Y. Ioue, C. Miki & M. Kusunoki (2009) Correlation of CD133, OCT4, and SOX2 in rectal cancer and their association with distant recurrence after chemoradiotherapy. *Ann Surg Oncol*, 16, 3488-98.
- Sambuy, Y., I. De Angelis, G. Ranaldi, M. L. Scarino, A. Stammati & F. Zucco (2005) The Caco-2 cell line as a model of the intestinal barrier: influence of cell and culture-related factors on Caco-2 cell functional characteristics. *Cell Biol Toxicol*, 21, 1-26.
- Sander, J. D. & J. K. Joung (2014) CRISPR-Cas systems for editing, regulating and targeting genomes. *Nat Biotechnol*, 32, 347-55.
- Schlesinger, M. J. (1990) Heat shock proteins. *J Biol Chem*, 265, 12111-4.
- Semenza, G. L. (2010a) Defining the role of hypoxia-inducible factor 1 in cancer biology and therapeutics. *Oncogene*, 29, 625-34.
- (2010b) HIF-1: upstream and downstream of cancer metabolism. *Curr Opin Genet Dev*, 20, 51-6.
- Semenza, G. L., B. H. Jiang, S. W. Leung, R. Passantino, J. P. Concordet, P. Maire & A. Giallongo (1996) Hypoxia response elements in the aldolase A, enolase 1, and lactate dehydrogenase A gene promoters contain essential binding sites for hypoxia-inducible factor 1. *J Biol Chem*, 271, 32529-37.
- Sharief, F. S., S. H. Wilson & S. S. Li (1986) Identification of the mouse low-salt-eluting single-stranded DNA-binding protein as a mammalian lactate dehydrogenase-A isoenzyme. *Biochem J*, 233, 913-6.
- Sharma, A., K. Singh & A. Almasan (2012) Histone H2AX phosphorylation: a marker for DNA damage. *Methods Mol Biol*, 920, 613-26.
- Sheng, S. L., J. J. Liu, Y. H. Dai, X. G. Sun, X. P. Xiong & G. Huang (2012) Knockdown of lactate dehydrogenase A suppresses tumor growth and metastasis of human hepatocellular carcinoma. *FEBS J*, 279, 3898-910.
- Shi, M., J. Cui, J. Du, D. Wei, Z. Jia, J. Zhang, Z. Zhu, Y. Gao & K. Xie (2014) A novel KLF4/LDHA signaling pathway regulates aerobic glycolysis in and progression of pancreatic cancer. *Clin Cancer Res*, 20, 4370-80.
- Shim, H., C. Dolde, B. C. Lewis, C. S. Wu, G. Dang, R. A. Jungmann, R. Dalla-Favera & C. V. Dang (1997) c-Myc transactivation of LDH-A: implications for tumor metabolism and growth. *Proc Natl Acad Sci U S A*, 94, 6658-63.
- Song, Y. D., K. F. Zhang, D. Liu, Y. Q. Guo, D. Y. Wang, M. Y. Cui, G. Li, Y. X. Sun, J. H. Shen, X. G. Li, L. Zhang & F. J. Shi (2014) Inhibition of EGFR-induced glucose metabolism sensitizes chondrosarcoma cells to cisplatin. *Tumour Biol*, 35, 7017-24.
- Sonveaux, P., T. Copetti, C. J. De Saedeleer, F. Végran, J. Verrax, K. M. Kennedy, E. J. Moon, S. Dhup, P. Danhier, F. Frérart, B. Gallez, A. Ribeiro, C. Michiels, M. W. Dewhirst & O. Feron (2012) Targeting the lactate transporter MCT1 in endothelial cells inhibits lactate-induced HIF-1 activation and tumor angiogenesis. *PLoS One*, 7, e33418.
- Straus, D. S. (2013) TNF α and IL-17 cooperatively stimulate glucose metabolism and growth factor production in human colorectal cancer cells. *Mol Cancer*, 12, 78.
- Sugden, M. C. & M. J. Holness (2003) Recent advances in mechanisms regulating glucose oxidation at the level of the pyruvate dehydrogenase complex by PDKs. *Am J Physiol Endocrinol Metab*, 284, E855-62.

- Sullivan, E. J., M. Kurtoglu, R. Brenneman, H. Liu & T. J. Lampidis (2014) Targeting cisplatin-resistant human tumor cells with metabolic inhibitors. *Cancer Chemother Pharmacol*, 73, 417-27.
- Sureda, A., S. Tejada, M. e. M. Bibiloni, J. A. Tur & A. Pons (2014) Polyphenols: well beyond the antioxidant capacity: polyphenol supplementation and exercise-induced oxidative stress and inflammation. *Curr Pharm Biotechnol*, 15, 373-9.
- Swygert, S. G. & C. L. Peterson (2014) Chromatin dynamics: interplay between remodeling enzymes and histone modifications. *Biochim Biophys Acta*, 1839, 728-36.
- Terentiev, A. A. & N. T. Moldogazieva (2013) Alpha-fetoprotein: a renaissance. *Tumour Biol*, 34, 2075-91.
- Terzić, J., S. Grivennikov, E. Karin & M. Karin (2010) Inflammation and colon cancer. *Gastroenterology*, 138, 2101-2114.e5.
- Tomás-Barberán, F. A., R. García-Villalba, A. González-Sarriás, M. V. Selma & J. C. Espín (2014) Ellagic acid metabolism by human gut microbiota: consistent observation of three urolithin phenotypes in intervention trials, independent of food source, age, and health status. *J Agric Food Chem*, 62, 6535-8.
- Tong, X., F. Zhao & C. B. Thompson (2009) The molecular determinants of de novo nucleotide biosynthesis in cancer cells. *Curr Opin Genet Dev*, 19, 32-7.
- Toth, M. E., S. Gonda, L. Vigh & M. Santha (2010) Neuroprotective effect of small heat shock protein, Hsp27, after acute and chronic alcohol administration. *Cell Stress Chaperones*, 15, 807-17.
- Tourtas, T., M. T. Birke, F. E. Kruse, U. C. Welge-Lüssen & K. Birke (2012) Preventive effects of omega-3 and omega-6 Fatty acids on peroxide mediated oxidative stress responses in primary human trabecular meshwork cells. *PLoS One*, 7, e31340.
- Trachootham, D., J. Alexandre & P. Huang (2009) Targeting cancer cells by ROS-mediated mechanisms: a radical therapeutic approach? *Nat Rev Drug Discov*, 8, 579-91.
- Usman, M. W., F. Luo, H. Cheng, J. J. Zhao & P. Liu (2015) Chemopreventive effects of aspirin at a glance. *Biochim Biophys Acta*, 1855, 254-63.
- Valvona, C. J., H. L. Fillmore, P. B. Nunn & G. J. Pilkington (2016) The Regulation and Function of Lactate Dehydrogenase A: Therapeutic Potential in Brain Tumor. *Brain Pathol*, 26, 3-17.
- Vander Heiden, M. G., L. C. Cantley & C. B. Thompson (2009) Understanding the Warburg effect: the metabolic requirements of cell proliferation. *Science*, 324, 1029-33.
- Vaughan, R. A., R. Garcia-Smith, J. Dorsey, J. K. Griffith, M. Bisoffi & K. A. Trujillo (2013) Tumor necrosis factor alpha induces Warburg-like metabolism and is reversed by anti-inflammatory curcumin in breast epithelial cells. *Int J Cancer*, 133, 2504-10.
- Vettraino, M., M. Manerba, M. Govoni & G. Di Stefano (2013) Galloflavin suppresses lactate dehydrogenase activity and causes MYC downregulation in Burkitt lymphoma cells through NAD/NADH-dependent inhibition of sirtuin-1. *Anticancer Drugs*, 24, 862-70.
- Végran, F., R. Boidot, C. Michiels, P. Sonveaux & O. Feron (2011) Lactate influx through the endothelial cell monocarboxylate transporter MCT1 supports an NF- κ B/IL-8 pathway that drives tumor angiogenesis. *Cancer Res*, 71, 2550-60.
- Walsh, R. C., I. Koukoulas, A. Garnham, P. L. Moseley, M. Hargreaves & M. A. Febbraio (2001) Exercise increases serum Hsp72 in humans. *Cell Stress Chaperones*, 6, 386-93.
- Wang, C., Y. Zhang, K. Guo, N. Wang, H. Jin, Y. Liu & W. Qin (2016) Heat shock proteins in hepatocellular carcinoma: Molecular mechanism and therapeutic potential. *Int J Cancer*, 138, 1824-34.
- Wang, X., Q. Wang, H. Lin, S. Li, L. Sun & Y. Yang (2013) HSP72 and gp96 in gastroenterological cancers. *Clin Chim Acta*, 417, 73-9.

- Wang, X. C., L. Jiang & H. M. Zhou (1997) Minimal functional unit of lactate dehydrogenase. *J Protein Chem*, 16, 227-31.
- Wang, Z. Y., T. Y. Loo, J. G. Shen, N. Wang, D. M. Wang, D. P. Yang, S. L. Mo, X. Y. Guan & J. P. Chen (2012) LDH-A silencing suppresses breast cancer tumorigenicity through induction of oxidative stress mediated mitochondrial pathway apoptosis. *Breast Cancer Res Treat*, 131, 791-800.
- WARBURG, O. (1956) On respiratory impairment in cancer cells. *Science*, 124, 269-70.
- Ward, R. A., C. Brassington, A. L. Breeze, A. Caputo, S. Critchlow, G. Davies, L. Goodwin, G. Hassall, R. Greenwood, G. A. Holdgate, M. Mrosek, R. A. Norman, S. Pearson, J. Tart, J. A. Tucker, M. Vogtherr, D. Whittaker, J. Wingfield, J. Winter & K. Hudson (2012) Design and synthesis of novel lactate dehydrogenase A inhibitors by fragment-based lead generation. *J Med Chem*, 55, 3285-306.
- Whitaker-Menezes, D., U. E. Martinez-Outschoorn, Z. Lin, A. Ertel, N. Flomenberg, A. K. Witkiewicz, R. C. Birbe, A. Howell, S. Pavlides, R. Gandara, R. G. Pestell, F. Sotgia, N. J. Philp & M. P. Lisanti (2011) Evidence for a stromal-epithelial "lactate shuttle" in human tumors: MCT4 is a marker of oxidative stress in cancer-associated fibroblasts. *Cell Cycle*, 10, 1772-83.
- Witkiewicz, A. K., D. Whitaker-Menezes, A. Dasgupta, N. J. Philp, Z. Lin, R. Gandara, S. Sneddon, U. E. Martinez-Outschoorn, F. Sotgia & M. P. Lisanti (2012) Using the "reverse Warburg effect" to identify high-risk breast cancer patients: stromal MCT4 predicts poor clinical outcome in triple-negative breast cancers. *Cell Cycle*, 11, 1108-17.
- Xie, H., J. Hanai, J. G. Ren, L. Kats, K. Burgess, P. Bhargava, S. Signoretti, J. Billiard, K. J. Duffy, A. Grant, X. Wang, P. K. Lorkiewicz, S. Schatzman, M. Bousamra, A. N. Lane, R. M. Higashi, T. W. Fan, P. P. Pandolfi, V. P. Sukhatme & P. Seth (2014) Targeting lactate dehydrogenase--a inhibits tumorigenesis and tumor progression in mouse models of lung cancer and impacts tumor-initiating cells. *Cell Metab*, 19, 795-809.
- Xie, H., V. A. Valera, M. J. Merino, A. M. Amato, S. Signoretti, W. M. Linehan, V. P. Sukhatme & P. Seth (2009) LDH-A inhibition, a therapeutic strategy for treatment of hereditary leiomyomatosis and renal cell cancer. *Mol Cancer Ther*, 8, 626-35.
- Xie, J., B. S. Wang, D. H. Yu, Q. Lu, J. Ma, H. Qi, C. Fang & H. Z. Chen (2011) Dichloroacetate shifts the metabolism from glycolysis to glucose oxidation and exhibits synergistic growth inhibition with cisplatin in HeLa cells. *Int J Oncol*, 38, 409-17.
- Yun, J., C. Rago, I. Cheong, R. Pagliarini, P. Angenendt, H. Rajagopalan, K. Schmidt, J. K. Willson, S. Markowitz, S. Zhou, L. A. Diaz, V. E. Velculescu, C. Lengauer, K. W. Kinzler, B. Vogelstein & N. Papadopoulos (2009) Glucose deprivation contributes to the development of KRAS pathway mutations in tumor cells. *Science*, 325, 1555-9.
- Zhai, X., Y. Yang, J. Wan, R. Zhu & Y. Wu (2013) Inhibition of LDH-A by oxamate induces G2/M arrest, apoptosis and increases radiosensitivity in nasopharyngeal carcinoma cells. *Oncol Rep*, 30, 2983-91.
- Zhang, F. & R. L. Aft (2009) Chemosensitizing and cytotoxic effects of 2-deoxy-D-glucose on breast cancer cells. *J Cancer Res Ther*, 5 Suppl 1, S41-3.
- Zhang, Y., X. Zhang, X. Wang, L. Gan, G. Yu, Y. Chen, K. Liu, P. Li, J. Pan, J. Wang & S. Qin (2012) Inhibition of LDH-A by lentivirus-mediated small interfering RNA suppresses intestinal-type gastric cancer tumorigenicity through the downregulation of Oct4. *Cancer Lett*, 321, 45-54.

- Zhang, Y. N., P. C. Lie & X. Wei (2009) Differentiation of mesenchymal stromal cells derived from umbilical cord Wharton's jelly into hepatocyte-like cells. *Cytotherapy*, 11, 548-58.
- Zhao, D., S. W. Zou, Y. Liu, X. Zhou, Y. Mo, P. Wang, Y. H. Xu, B. Dong, Y. Xiong, Q. Y. Lei & K. L. Guan (2013a) Lysine-5 acetylation negatively regulates lactate dehydrogenase A and is decreased in pancreatic cancer. *Cancer Cell*, 23, 464-76.
- Zhao, J. G., K. M. Ren & J. Tang (2014) Overcoming 5-Fu resistance in human non-small cell lung cancer cells by the combination of 5-Fu and cisplatin through the inhibition of glucose metabolism. *Tumour Biol*, 35, 12305-15.
- Zhao, X., T. Lwin, X. Zhang, A. Huang, J. Wang, V. E. Marquez, S. Chen-Kiang, W. S. Dalton, E. Sotomayor & J. Tao (2013b) Disruption of the MYC-miRNA-EZH2 loop to suppress aggressive B-cell lymphoma survival and clonogenicity. *Leukemia*, 27, 2341-50.
- Zhao, Y., E. B. Butler & M. Tan (2013c) Targeting cellular metabolism to improve cancer therapeutics. *Cell Death Dis*, 4, e532.
- Zhao, Y., H. Liu, Z. Liu, Y. Ding, S. P. Ledoux, G. L. Wilson, R. Voellmy, Y. Lin, W. Lin, R. Nahta, B. Liu, O. Fodstad, J. Chen, Y. Wu, J. E. Price & M. Tan (2011) Overcoming trastuzumab resistance in breast cancer by targeting dysregulated glucose metabolism. *Cancer Res*, 71, 4585-97.
- Zhao, Y. H., M. Zhou, H. Liu, Y. Ding, H. T. Khong, D. Yu, O. Fodstad & M. Tan (2009) Upregulation of lactate dehydrogenase A by ErbB2 through heat shock factor 1 promotes breast cancer cell glycolysis and growth. *Oncogene*, 28, 3689-701.
- Zhong, X. H. & B. D. Howard (1990) Phosphotyrosine-containing lactate dehydrogenase is restricted to the nuclei of PC12 pheochromocytoma cells. *Mol Cell Biol*, 10, 770-6.
- Zhou, M., Y. Zhao, Y. Ding, H. Liu, Z. Liu, O. Fodstad, A. I. Riker, S. Kamarajugadda, J. Lu, L. B. Owen, S. P. Ledoux & M. Tan (2010) Warburg effect in chemosensitivity: targeting lactate dehydrogenase-A re-sensitizes taxol-resistant cancer cells to taxol. *Mol Cancer*, 9, 33.